ADDIS ABABA UNIVERSITY

ETHIOPIAN INSTITUTE OF WATER RESOURCES

SPECTRAL UNMIXING -AND INTEGRATED HYDROLOGIC MODEL FOR SEDIMENT ESTIMATION, EVALUATION OF CLIMATE CHANGE IMPACT AND MANAGEMENT TYPES:

THE CASE OF THE UPPER TEKEZE RIVER BASIN, ETHIOPIA

HAGOS GEBRESLASSIE GEBRU

PhD. Degree

August 2020

Addis Ababa, ETHIOPIA

ADDIS ABABA UNIVERSITY
ETHIOPIAN INSTITUTE OF WATER RESOURCES

SPECTRAL UNMIXING -AND INTEGRATED HYDROLOGIC MODEL FOR SEDIMENT ESTIMATION, EVALUATION OF CLIMATE CHANGE IMPACT AND MANAGEMENT TYPES:

THE CASE OF THE UPPER TEKEZE BASIN, ETHIOPIA

HAGOS GEBRESLASSIE GEBRU

A Dissertation Submitted to the School of Graduate Studies of Addis Ababa University in Partial Fulfilment of the Requirements for the Doctor of Philosophy of Degree (PhD) in Water resources Engineering and Management

RESEARCH SUPERVISORS

Main Advisor:

Assefa M. Melesse (PhD, Professor), Department of Earth and Environment, Florida International University, USA

Co-Advisors:

Kiven Bishop (PhD, Professor), Department of Aquatic Science and assessment, Swedish University of Agricultural Science, Sweden

Azage Gebreyohannes Gebremariam (PhD. Asisistant Professor), Ethiopian Institute of Water Resources, Addis Ababa University, Ethiopia

August 2020
Addis Ababa, ETHIOPIA

APPROVAL SHEET

SPECTRAL UNMIXING-AND INTEGRATED HYDROLOGIC MODEL FOR SEDIMENT ESTIMATION, EVALUATION OF CLIMATE CHANGE IMPACT AND MANAGEMENT TYPES: The Case of the Upper Tekeze Basin, Ethiopia

Researcher's Declaration:

I certify that I am responsible for the work submitted in this PhD research project, and that the original work is my own. I have not submitted this work to any other institution for the award of a degree of Doctor of Philosophy. All information (including diagrams and tables) or other information, which is cited from, or based on, the work of others, has its source clearly acknowledged and referenced in the document at the place where it appears.

Hagos Gebreslassie Gebru	_____	Sep.6, 2020
Name	Signature	date

DISSERTATION APPROVAL

ADDIS ABABA UNIVERSITY

SCHOOL OF GRADUATE STUDIES

This is to certify that the dissertation prepared by Hagos Gebreslassie Gebru entitled: "***Spectral Unmixing -and Integrated Hydrologic Model for Sediment Estimation, Evaluation of Climate Change Impact and Management Types: The Case of the Upper Tekeze Basin, Ethiopia",*** submitted in fulfillments for the requirements for the Degree of Doctor of Philosophy (Water Resource Engineering and management) complies with the regulations of the University and meets the accepted standards with respect to originality and quality.

Signed by the examining committee

Dr. Taye Alemayehu		08/09/2020
Chair person, examiner committee	Signature	Date
Dr. Adane Abebe		07/09/20202
External examiner	Signature	Date
Dr. Tena Alamirew		08/09/2020
Internal examiner	Signature	Date
Dr. Michael Mehari		17/09/2020
Internal examiner	Signature	Date
Prof. Assefa M. Melesse		Sep. 06, 2020
Main Advisor	Signature	Date
Prof. Kevin Bishop		7 Sep. 2020
Co-Advisor	Signature	Date
Dr. Azage G. Gebremariam		20 Sep.2020
Co-Advisor	Signature	Date

ACKNOWLEDGEMENT

I would like to acknowledge and express my sincere thanks and gratitude to all individuals who, in one or another way, helped me to finalize my PhD study. First, I would like to thank my supervisors whose contributions were instrumental from the beginning. I am greatly indebted to Prof. Dr. Assefa M. Melesse for the willingness he shown me to provide scientific support with a very short email. His continuous support and guidance were valuable during the whole process of this dessertation. Moreover, I would like to acknowledge and extend my heartfelt gratitude to my co-promoters Prof. Dr. Kevin Bishop and Dr. Azage Gebreyohannes for their continuous scientific support and very helpful comments and suggestions. I will never forget the experience I shared from the Swedish University Agricultural Science (SLU, Sweden) which become real with continuous follow up of Prof. Kevin and Dr. Azage. I want to convey my aknowlodgement to staffs in SLU, especially to Dr. Faruk for the heartfelt humbleness he has shown, and scientific support given tome.

It gives me a great pleasure to acknowledge Addis Ababa University, Ethiopia, for providing facility and financial support for this research. I also interested to extend my acknowledgement to ASD Inc., a PANalytical company, USA, for the provision of the handheld Spectroradiometer instrument with full transport costs covered. It was unthinkable to complete this research without the instrument support from the ASD Inc., a PANalytical company. Special thank goes to the staffs in the company Suzan Park and Betsy K. who facilitated and make this instrument support program real.

I would like to thank to the Abergele Woreda Office, Amhara Regional State, and the respective district offices and guards in Tsirare and Tekeze Rivers sites for their kind cooperation in facilitating the field data collection campaign. I also thank the Ethiopian Minster of Water, Energy, and Irrigation for providing necessary flow and sediment data. I am grateful to all EiWR staff and students for the good times we had together in the University of Addis Ababa, Akaki campus. My PhD studentship mate Mr Alemayo Fola has shown real friendship and support during the hard times and deserves special thanks. The time we have passed with and the scientific comments provided from Dr. Zenebe Girmay were unforgettable. I would like to extend my gratitude to the College of Agriclture and Environmentand all my colleagues from Adigrat University, Ethiopia. A lot of motivating courages had been fllowing from them to perservere and succeed in my PhD. work.

I am very grateful tomy beloved wife Tsegakiros Embafrash, my son Sofonyas Hagos and parentswhowith their patience and unreserved help brought me up to this stage. They relentlessly supported me throughout my life and encouraged me to succeed in my academics from the beginning. I got all the necessary support and love from my family; I am so grateful for all their support.

DEDICATION

I dedicate this work with a great love and respect to my wife Tsegakiros Embafrash from whom I have got to learn how love is and my first son Sefonyas Hagos by whom I have gotten refreshed after work. The dedication also extends to my father Gebreslassie Gebru from whom I have got to learn how kindness is,my mother Atsibiha Gebretekle, from whom I have got to learn how life hardship has to pass and to my youngest sister Kibeten Gebreslassie from whom I have gotten to know how God's blessing is.

BIOGRAPHICAL SKETCH

Hagos Gebreslasie Gebru was born on August 18, 1983 in a village called *Ahirag*, Hawzen, Eastern zone of Tigray Regional State, Ethiopia, to his father Gebreslassie Gebru and his mother Atsibaha G\tekle. He started modern education in a rural area in 1992 and attended elementary school in *Megab*, and secondary school at the nearby town, Hawzen. He attended preparatory school in Adigrat and Mekelle cities, Tigray Regional State, Ethiopia.

He entered at Jimma University in 2004 and graduated with a B.Sc. degree in Natural Resources Management in 2006. Soon after his graduation, he was employed as a graduate assitintant in Wollega University, Ethiopia. After serving for two years in this University he joined the M.Sc. program at Wondo Genet College of Forestry and Natural Resource, Hawassa University in April 2009 in the program of Watershed Management (Soil and Water Conservation). His research was on "Gully and land use dynamics using remote sensing".

After his post-graduate education, Hagos returned to Wollega University and served one year. After a year he has transferred to Adgrat University, Northern Ethiopia. As a lecturer, he taught undergraduate courses such as Hydrology, Irrigation, land use planing, watershed management and Water harvesting technology. Besides this, he has been involved in various research and community services undertaken with in the university. He also served as Assistant Registrar and academic quality assurance office of collegesin the University. Part of his MSc thesis and other researcheshave been published in internationally peer reviewed journals.

In November 2015, Hagos joined EiWR as a Ph.D. student in Addis Ababa University under the program of Water resources engineering and management. He studied the application of spectral unmixing and integrated hydrologic model for sediment estimation, climate and management change evaluation in Tekeze basin, Ethiopia. From the present work, he published two articles and another two arein the peer review process of international journals. The articles are attached at the back of this thesis for further reference. Moreover, Hagos has presented and participated in many international and national conferences. In his academic career, Hagos is interested in teaching and researching on issues related to Remote sensing hydrology, sedimentology, hydroclimatology, ecohydrology, and other issues related to water resources management.

LIST PUBLISHED AND UNDERREVIEW PAPERS

The original works of this Doctor of Philosophy research study produced the following two published on reputable international journals and two more under review/under development scientific articles. Moreover

Published papers

1. **Gebreslassie, H.G., Melesse, A.M., Bishop, K. and Gebremariam, A.G., 2020.** Linear spectral unmixing algorithm for modelling suspended sediment concentration of flash floods, upper Tekeze River, Ethiopia. *International Journal of Sediment Research*.35/1, 79-90.
   https://www.sciencedirect.com/journal/international-journal-of-sediment-research/vol/35/issue/1
2. **Gebreslassie, H.G., Melesse, A.M. and Gebremariam, A.G., 2019**. Double-stage linear spectral unmixing analysis for improving accuracy of sediment concentration estimation from MODIS data: the case of Tekeze River, Ethiopia. *Modeling Earth Systems and Environment*, pp.1-10.
   https://link.springer.com/journal/40808/onlineFirst/page/2

Under review and on development

3. Sediment management modeling using spectral unmixing remote sensing integrated SWAT, the case of upper Tekeze basin, Ethiopia: Submited to International Soil and Water Conservation Research
4. Integrating linear spectral unmixing analysis and hydrologic model for enhancing sediment yield prediction: The case of the upper Tekeze basin, under development

Conference participation and proceedings

Some parts of the findings in this research research were accepted for scientific workshop presentations in different international and national conferences and published in different proceedings.

1. 18th international symposium on sustainable water resource development held at Arbaminch University, Ethiopia
2. Tekeze-Atbara regional conference, Sudan
3. 3rd National conference on integrated geographical and environmental researches for sustainable development, Mekelle University, Ethiopia

ABSTRACT

Remote sensing is a less costly and reasonably accurate technology for monitoring and modelling river systems. However, the coarseness of remote sensing data together with the dynamic inherent optical properties of the variables constrained its application. Thus, the overall purpose of this research was to propose the spectral unmixing approach for building remote sensing model and parametrizing the physically distributed hydrologic model, soil and water assessment tool (SWAT), for estimating sediment concentration and evaluating impact of climate and sediment management changes.

Laboratory, time series in-situ and space remote sensing data analyses were triangulated to construct linear spectral unmixing analysis (LSUA) and compared with the conventional (empirical) remote sensing models. The models were constructed in laboratory experiments using sediment types sampled from the Tekeze and Tsirare Riverbeds deposited sediments and then tested to estimate the daily SSCs from in-situ and space remote sensing data and evaluated against the observed SSCs in the Rivers. To enhance the LSUA model accuracy into the mixed pixels of the moderate-resolution imaging spectroradiometer (MODIS) images, a new approach called Double-stage-LSUA (DLSUA) was proposed. In this case, LSUA was applied at two stages that LSUA in the first stage was used to unmix the pixels' reflectance into respective macro endmembers' (rock\bare-land and turbid water) reflectance and the LSUA in the next stage was used to determine spectral mixing coefficients (SMCs) of the constituents in the turbid water (micro components including pure water and sediment) was proposed. Finally, the SSCs of the Rivers were simulated by inserting the computed SMCs into the LSUA model generated in the laboratory. The LSUA approach was also tested to monitor the spatial variability of a vegetation parameter of soil erosion and sediment (C-factor) which is the required parameter in most sediment estimating hydrologic models. The spatial minimum C-factor of the upper Tekeze River basin was first mapped using the LSUA technique from the Landsat images and tested its accuracy using time series field monitoring. Average C-factor was integrated into hydrological response units (HRUs) of SWAT. This differs from the conventional approach where the C-factors have been integrated into land-use type units of SWAT. The LSUA integrated SWAT was demonstrated in evaluating climate and sediment management change scenarios on sediment yield. The goodness-of-fit indices including Nash-Sutcliffe coefficient (NSE), Coefficient of determination (R^2), Root Mean Square of Error (RMSE), Root mean Square of error- observations standard deviation Ratio (RSR) and Percent Bias (PBIAS) were used to evaluate the performance of the model outputs.

The application of LSUA approach to finer (ground) and coarser (MODIS) resolutions remote sensing data for modelling variability of SSCs of the Tekeze Rivers were performed averagely at R^2 = 0.92 with RMSE = ±0.75g/l and R^2 = 0.83 with RMSE ±9.96, respectively. These performances were relatively good compared to the simulations using the conventional empirical regression remote sensing model performed at R^2=0.78 with

RMSE = ±6.76g/l and R^2 = 0.74 with RMSE ±16.2, respectively. The success of applying the LSUA approach was not only for the direct estimation of SSCs, but it was also successful for determining the spatial variation of C-factor values within and among land-use types. The demonstration in the upper Tekeze basin showed that the use of the minimum C-factor map produced using LSUA and integrating it into HRUs of SWAT improved the fit between the predicted and the measured sediment yield. The coefficients including NSE, PBIAS, RSR and R^2 for sediment yield were 0.72, 0.39, 34.2 & 0.68, respectively, when the C-factor values were for the land-use type units of SWAT. When the C-factor was for the HRUs in SWAT, the corresponding values were 0.84, 0.23, 10, & 0.89. The average rainfall and temperature over the basin experienced neither significant increasing nor decreasing trends in the time scales. In contrast, trend analyses of different variables on the simulated sediment yield from the upper Tekeze basin have shown a significant increasing trend. Moreover, the sediment concentration simulation using the LSUA-SWAT shows that applying filter strips, stone bunds, and reforestation or integration of these scenarios reduced the current sediment yields by different rates (Ave. 9-38%).

The LSUA approach has found to be effective in generating relatively accurate and universal models working with both ground-based (finer-resolution), and space-based (coarser-resolution) remote sensing data from river systems. LSUA was also effective in determining the variability of C-factor among and within landuse types. The successful integration of the C-factor values into HRUs enhances the sensitivity of SWAT to the spatial variability of C-factor and then sediment yield. Therefore, the current study implied that prior studying and considering the inherent optical properties of endmembers during analysis is important to enhance remote sensing technology for modelling and monitoring sediment concentrations. The continuous and significant increasing trend of sediment concentration in the basin irrespective of the insignificant and non trending changes of climate variables has implied that the changes in catchment characteristics over time including changes in land use and/or land cover in the basin are the governing factors. Moreover, the sediment yield in the basin varies with the changes in sediment management type. Hence, though further calibration and validation are needed, the LUSA and its integration to hydrologic models (eg. SWAT) approach can support decision-making concerning the SSCs variability and impacts of climate change and management alternatives at the river basin scale better than the conventional approaches.

Keywords: C-factor, Empirical remote sensing, Linear unmixing, Sediment monitoring, Sediment type, Spectral mixing coefficient, suspended sediment concentration, Tekeze River basin

TABLE OF CONTENTS

LIST OF FIGURES

LIST OF TABLES

LIST OF APPENDICES

ACRONYMS AND ABBREVIATIONS

AGNPS	Agricultural Non-Point Source
AOP	Apparent Optical Property
DEM	Digital Elevation Model
DLSUA	Double stage Linear Spectral Unmixing analysis
DN	Digital Number
DNG	Digital Number of Green Band
DNNIR	Digital Number of Near Infrared Band
EMoWEI	Ethiopian Ministry of Water, Energy and Irrigation
ERTS	Earth Resources Technology Satellite
HRU	Hydrologic Responsive Units
ICOLD	International Commission on Large Dams
IOP	Inherent Optical Propertyt
IPCC	Inter-Governmental Panel for Climate Change
LSU	Linear Spectral Un-mixing
LSUA	Linear Spectral Unmixing analysis
MIWRs	Ministry of Irrigation and Water Resources for Sudan
MNDWI	Modified Normalized Difference Water Index
MODIS	Moderate-Resolution Imaging Spectroradiometer
MSE	Mean Square Error
NDVI	Normalized Deviation Vegetation Index
NIR	Near Infrared Band
NSE	Nash–Sutcliffe Efficiency
PBIAS	Percent Biase

PPM	Particle Per Million
R/MUSLE	Revised or Modified Universal Soil Loss Equation
R2	Coefficient of determination
RMSE	Relative Mean Square Error
RS	Remote Sensing
RSR	Ration of square root error to the standard deviation of measured data)
SSC	Suspended Sediment Concentration
SU	Spectral Unmixing
SWAT	Soil and Water Assessment Tool
SW-NIR	Short Wave Near Infrared
TSS	Total Suspended Solids
USLE	Universal Soil Loss Equation
WEPP	water erosion prediction project

WORKING DEFINITIONS FOR TERMINOLOGIES

C-factor: Defined as the ratio of soil loss from a field with a cover and management to that of a soil with out any cover (Wischmeier and Smith, 1978).

Climate change: A change in the state of the climate that can be identified (e.g., by using statistical tests) by changes in the mean and/or the variability of its properties and that persists for an extended period, typically decades or longerdue to natural internal processes or external forcings, or to persistent anthropogenic changes in the composition of the atmosphere or in land use (IPCC. 2012).

Hydrologic model: is a simplification of a real-world system (e.g., surface water, soil water, wetland, groundwater, and estuary) that aids in understanding, predicting, and managing both the flow and quality of water.

Linear spectral unmixing: is a technique to determine the relative abundance of materials that are depicted in linearly mixed reflectance based on the materials' spectral characteristics. The macroscopically pure components are assumed to be homogeneously distributed in separate patches within the field of view.

Mixed pixel: A pixel that has a digital number which represents the average energy emitted or reflected from several different surfaces occurring within that area represented by the pixel.

Nonlinear spectral unmixing:is a technique to determine the relative abundance of materials that are depicted in mixed reflectance based on the materials' spectral characteristics. The macroscopically pure components are intimately mixed inside the pixel.

Pure pixel: A pixel that has a digital number which represents energy emitted or reflected from a single surface occurring within that area represented by the pixel

Remote sensing: is the acquisition of information about an object or phenomenon withoutmaking physical contact with the object and thus in contrast to on-site sampling.

Sediment: A naturally occurring material that is broken down by processes of weathering and erosion, and is subsequently transported by the action of water, or by the force of gravity acting on the particles.

Spectral unmixing: consists in the identification of the spectrally pure signatures of the materials present in the scene (called endmembers) and the estimation of the fractional abundances for each pixel associated with the endmembers or, in other words, the contribution of each endmember on each mixed pixel.

Suspended sediment concentration refers to the sediment that is supported by the upward components of turbulent currents and stays in suspension for an appreciable length of time.

CHAPTER ONE:

INTRODUCTION

This chapter briefly introduces the research background, statement of the problem, research questions and objectives. Firstly, the parameters of sediment transport and deposition that vary in space and time are reviewed. Secondly, a brief introduction to the importance, types and drawbacks of different sediment monitoring and modelling techniques are presented. Thirdly, then the potential of remote sensing technology to overcome the discussed drawbacks and options of remote sensing are described. The research gaps in relation to applying remote sensing for sediment concentration monitoring and modelling are discussed. In the end, based on these discussions, the objectives and research questions as well as the outline of this thesis are formulated, discussed and presented.

1.1 Background of the study

Sediment transportation and deposition cause visible impacts on a range of environmental, economic and social issues. The changes in sediment transportation rate and pattern are causing important pressures on physical (Walling and Fang, 2003; Siyam et al., 2005; Haregeweyn, et al., 2012) and biochemical processes (Li et al., 2008; Shen et al., 2013; Pan et al., 2016) in rivers and reservoirs. Reducing the storage capacity and water quality of reservoirs, river flow dynamics and burring agricultural and non-agricultural resources in downstream areas are the prominent effects making sediment transportation and deposition a global concern (ICOLD, 2009; Walling and Fang, 2003). Apart from these offsite impacts, soil erosion and sedimentation have multiple onsite impacts including depletion of

green water (El-Swaify and Hurni, 1996) and environmental degradations (Pimentel et al., 1995; Pimentel, 2006). Hence, sedimentation has irreversible impacts on irrigation, hydroelectric and water supply infrastructures of the riparian countries. At the same time, there are investigations indicating sediment transport and sedimentation can be an opportunity for having fertile soil in downstream countries (Takeda and Fukushima, 2004) and for facilitating aquatic ecosystems through nutrient replenishment and creation of benthic habitat and spawning areas. Moreover, lack of sediment transport and deposition can cause physical changes to the terrain of river systems. Thus, though the excess sediment is the most common concern, deficiency of sediment transport can also be an important environmental and socio-economic concern.

Sediment transportation varies spatiotemporally based on the ratings (lower to extreme), the source areas (wash load and bed material load), the way it transports (suspension and bedload) and the composition (grain size distribution, nutrients, organic matter etc.) it holds. Studies have also indicated that these variations will continue worsening in the future under the projected climate and land-use change scenarios (Ward et al., 2009; Mango et al., 2011a; Moore et al., 2015; Adem et al., 2016; Azari et al., 2016; Romano et al., 2018; Wang et al., 2018). These variations have their own respective implications to the alteration of impacts, monitoring\modelling and controlling mechanisms. Because of the subsistent nature of the livelihood, higher dependence on natural resources and lack of sustainable management strategies, the rate and impacts of sedimentation on human welfare are worser in developing countries than in developed countries (Vanmaercke et al., 2011; 2014).

Sediment transport is the general term used for the transport of material (clay, silt, sand, gravels, and boulders) in rivers and streams. A distinction is made between bedload and suspended-load sediment. The bedload characterizes grains rolling, sliding and saltating along the riverbed. The suspended sediment concentration (SSC) refers to the sediment that is supported by the upward components of turbulent currents and stays in suspension for an appreciable length of time. The suspended load mainly includes the fine soil particles brought into suspension from the catchment area rather than from the streambed material and is called the washload. Monitoring and modelling the variabilities of SSCs is critically important to study the causing factors, effects on the environment and socioeconomic, as well as for designing effective adaptation and mitigation strategies.

As a result, despite the variability of accuracy and investment cost, there are multiple in-situ sampling tools (Wren et al., 2000), turbidity measuring and laser diffractometers (Felix et al. 2013) and acoustic techniques (Costa et al. 2012; Felix et al. 2013) that have been used for monitoring and modelling the SSCs. The basic drawbacks in one or more of these techniques are time and labour consuming for a field-laboratory analysis and are less potential to provide spatiotemporal information.This high cost of facility and maintenance discourage the implementation of hydrological monitoring networks to provide long-term, large scale, and uninterrupted observations, which are critically important for soil erosion and sedimentation studies under the increasing natural and anthropogenic changes over the world. The researches by GEMS, (2003) and Villar et al., (2012) have remarked that the construction of in-situ sediment gauging stations and maintenance is too costly that three quarters of the world cannot afford a full-scale monitoring infrastructure and will not be

able to construct this infrastructure in the near future. Even, there are researchers arguing that most of the sediment related effects would have been minimized and\or mitigated if river systems were with accurate and adequate sediment monitoring and modelling campaigns (Wren et al., 2000; Babic Mladenovicet al., 2015).

Recently researchers are shifting toward less costly and reasonable accurate remote sensing-/integrated hydrologic models. Recent advances in satellite technology, sensory, image acquisition and processing, and data accessibility have drawn much attention in using remote sensing approach in determining SSC, especially in highly turbid inland waters. Remote sensing has been found potential in sediment concentrations quantification (Ouillon et al., 1998; Villar et al., 2013; Zhan et al., 2017), grain size distribution (Carbonneau et al., 2005; Zhang et al., 2015), and deposition pattern (Choubey, 1994; Condé et al., 2019) assessments.

Apart from the above direct applications of remote sensing on sediments studies, remote sensing is also potential in parametrizing empirical, conceptual and physics-based computer based hydrologic models important for modelling sediment yield in River systems. The hydrologic engineering centre river analysis system (HEC-RAS; HEC, 1995), water erosion prediction technology (WEPP, Nearing et al., 1989), agricultural non-point source pollution (AGNPS; Young et al., 1989), soil and water assessment tool (SWAT; Arnold et al., 1998), and artificial neural network (ANN; Willis et al., 1996) are some of the hydrologic models unthinkable unless the remote sensing technology exists. Remote sensing can be used to parametrize the land use (e.g.Goodwin et al., 2005; Soenen et al., 2010;Bewket and Abebe, 2013; Hagos, 2014; Birhane et al., 2019), soil (eg.Mulder et al., 2011; Forkuor et al., 2017),

topography (eg.Mulder et al., 2011; Krishna et al., 2019) and climatevariables (e.g. Ohring et al., 2002; Sultanaand Nasrollahi, 2018).Remote sensing can also be used to estimate rainfall (e.g. Marra et al., 2017) and surface runoff (Jayakody et al., 2010; Rao et al., 2010).

Despite the above direct and indirect application potential of remote sensing for monitoring and modelling sediment transportation, challenges have kept the potentials underexploited. The potential of remotely sensed data analysis for monitoring processes on the earth surface especially for monitoring and modelling sediment transport is not still fully exploited. The challenges are related to the coarseness of the remote sensing data compared to the finesse of the environmental variables. The spatial and temporal resolutions of most sensors especially the publicly accessed remote sensing data are coarser compared to the sediment related variables. They provide mixed pixels or reflectance values, i.e. discrete elements of the two dimensions (2D) ground space. Since no pixel/ reflectance value, however finer it might be, represents complete homogeneous characteristics, the measured signal by the sensor always results from the interactions of electromagnetic radiation with multiple constituents within each pixel.The mixed nature of the spectral information considerably constrains the accuracy remote sensing application (Heinz & Chang, 2001; Keshava & Mustard, 2002; Song, 2005). Even in the future, it seems very difficult to get sensors which capture finer environmental processes and objects at a pure pixel level. The mixed nature of reflectance may not be only due to the coarseness of the sensors, it can also result in intimate mixtures.

Thus, subpixel analysis is required to enhance the accuracy of remote sensing to capture the variability of finer variables. Obtaining subpixel information requires the use of an

analytical approach called spectral unmixing analysis (SUA). The subpixel analysis approach, non\linearspectral unmixing analysis (N\LSUA), effective in analysing coarser remote sensing data has been extensively applied to characterize surface objects and processes. It has been used in monitoring urban environments (Phinn et al., 2002; Small, 2002), vegetation dynamics (Elmore et al., 2000; Riano et al., 2002) and mapping land degradation (Metternicht and Fermont, 1998; Haboudane et al., 2002). Apart from the earth, it has been also used for the characterization of objects on the Moon and Mars (Adams et al., 1986; Bell et al., 2002). But this approach has not been exploited in the area of hydrologic processes including in the sedimentology.

1.2 Statement of problems

Monitoring sediment transportation and deposition pattern is very difficult and costly, especially at larger scales. The sediment measurements in the globe are inadequate and usually carried at restricted temporal and spatial scales. The decline in the number of stations, data quality and changes in the data holding policy have made sediment data less reliable for users to understand the spatiotemporal variability of sediment, the relation with driving factors, and response to different management interventions. This problem is more immense especially in developing countries due to inadequate and non-continuous monitoring, lack of funding, and differences in processing and data quality control (Lewandowski et al., 2002). The rapid and early phasing out of dams and reservoirs constructed after huge investment are mainly associated with ineffective planning of the reservoirs during the design phase, which in turn attributed to lack of sediment data and lack of appropriate methodologies to predict sediment yield. In general, the factor which

kept sediment transportation and deposition more immense problem throughout the globe is due to limited information drived from less accurate and indequate sediment data.

Since the start of launching the Earth Resources Technology Satellite (ERTS-1) in the 1970s, remote sensing has become versatile technology to characterise, map, analyse and model hydrological variables with reasonable cost and accuracy. The application of remote sensing in water resources related studies mainly laid either on direct estimation of the hydrological variables and/or indirectly for modelling parameters which determine the hydrological processes. Sediment transportation in river systems is one of the hydrologic processes that remote sensing has been applied directly and indirectly. In the direct application of remote sensing, SSCs in River systems have been monitored using the various visible and NIR bands of satellite imageries directly. The reflectance of solar radiation from the water surface has been linked directly to the amount and type of sediments existed in the flowing water (Doxaran et al., 2002; Chen et al., 2004). Hence, different site-specific semi-/empirical models have been developed to measuere SSCs (Jiang et al., 2009, Nechad et al., 2010). Apart from this direct application, remote sensing can also be used for mapping and modelling input parameters of different sediment simulating hydrologic models. Vegetation parameter of soil erosion and sediment yield (C-factor) is one of the required parameter in multiple hydrologic models (eg. SWAT) used for predicting sediment yield (Arnold et al., 1998). The C-factor is place and time-specific parameter difficult to estimate over broad geographic areas. Conventionally, it has been determined using in-situ experimentation (Wischmeier and Smith, 1978). Different vegetation index (Bonn et al., 1997; Baret and Guyot., 1991), direct linear regression

analysis (Stephens and Cihlar, 1982; Cihlar, 1987), and joint sequential co-simulation with Landsat TM images with the C-factor from point values (Gertner et al., 2002; Wang et al., 2003) are the remote sensing techniques that have been used for computing C-factor values.

These might present general knowledge about the targeted variable. But, they may not yield any further insight into the variables. Most models have relied upon the empirical relationships between the variables. Such models are affected by the variability of spectral property of sediment types or vegetation and then are less capable in their universal application and may not extend to the full range of conditions present in the river systems (Whitlock et al., 1981; Ritchie et al., 2003). This problem is more complex when one used coarser remote sensing data. Constructing physically based models which can be used for predicting the SSCs or vegetation parameter which could be applied across a range of rivers, a range of sediment types and transporting conditions and over multiple bands of imagery is therefore important.

Consequently, the desires to extract the constituents' optical property from a spectral mixture, as well as the proportions in which they appear are important to numerous tactical scenarios in which sub-pixel detail is valuable. The spectral unmixing (SU), decomposing remote sensed electromagnetic spectra into a combination of spectrally pure (endmembers) signatures, is becoming promising technique (e.g. Adams et al., 1986; Ustin et al., 1993). The SU can be used for analysing multi spectral data collected from space, air and ground plated sensors. It provides a comprehensive and quantitative mapping of the elementary materials that are present in the acquired data. More precisely, SU can identify the spectral signatures of these materials (usually called endmembers) and can estimate their relative

contributions (or abundances) to the measured spectra. Both linear and nonlinear approach can be applied for unmixing the reflectance signature of surface objects. Unlike the nonlinear one, the linear spectral unmixing (LSUA) approach is the quick and easy way of analysing coarser remote sensing data. The LSUA which consider a given pixel/reflectance value as a linear combination of primary components (endmembers) is advantageous for maximizing the use of remote sensing for modelling and monitoring environmental variables (Oyama et al., 2007).

Even though LSUA is found to be effective in enhancing the analysis of coarser remote sensing data, the potential has not been exploited in the area of sediment transportation. Extracting the level of sediment concentrations of turbid water from land features has not been considered. In the highly erosion risk river basins, an extremely turbid flash flood having confused optical properties distributed sparsely in a subpixel-scale size. In such pixels, both reflectance from macroscopically (E.g. land features and turbid water) and microscopicall (E.g. water, sediment, organic matter etc.) pure components are mixed. Consequently, the obvious water extraction remote sensing methods often fail to distinguish the narrow rivers with turbid water and estimate sediment concentration in the turbid water. The wider surface areas having low albedo surfaces and terain shadows, which are easily confused with the water bodies in a mountainous river basin (E.g. Tekeze basin), also bring a big challenge to apply it. The approach is not studied adequately in arid and semi-arid areas consist of complex spectral properties due to different mosaics of vegetation, intensive land use pressures, sensitivity to climate fluctuations, dynamic soils' spectral property (colour change, mineralogy, textures, presence of sand and rocks), surface

roughness and various other factors. Consequently, the application principles are not well developed in the area of monitoring and modelling sediment transport for such river systems.

Thus, the main hypothesis of this dissertation is *spectral unmixing (sub-pixel) analysis approach can enhance the potential of coarser remote sensing data for monitoring the SSCs and improve the sensitivity of hydrologic models to model the response of sediment transport to the climate and management scenarios*. The upper Tekeze basin where the Tekeze hydroelectric dam (Tk5) has constructed to collect about $9*10^9 m^3$ of water from 30,390 km^2 drainage area for generating 300MW was targeted in this study.

1.3 Research Questions

i. Can application of linear spectral unmixing algorithm to finer and coarser remote sensing data enhance estimation of suspended sediment concentration of River?

ii. Can linear spectral unmixing remote sensing algorithm enhance and be an option for mapping the spatial variability of vegetation parameter of soil erosion and sediment yield (C-factor)?

iii. Can integrating linear spectral unmixing remote sensing algorithm-based vegetation parameter of soil erosion and sediment yield (C-factor) into SWAT improve performance in modelling the spatiotemporal variability of sediment yield?

iv. How are the trends of climate (precipitation and temperature) and sediment yield in the upper Tekeze basin and the relationship in between?

v. How is the efficiency variation of land management options for mnmizing sediment yield in large scale basins?

1.4 Objectives

1.4.1 General objective

The overall objective of this research was to evaluate potentials of spectral unmixing remote sensing and integrated hydrologic model for modelling sediment concentration, climate and management changes impact in the upper Tekeze River systems.

1.4.2 Specific Objectives

i. Constructing and evaluating a linear spectral unmixing remote sensing model determining suspended sediment concentrations of Rivers from ground and space remote sensing data
ii. Evaluating potential of linear spectral unmixing remote sensing analysis approach in determining vegetation parameter of soil erosion and sediment yield (C-factor)
iii. Integrating the spatial vegetation parameter of soil erosion and sediment yield (C-factor) from linear spectral analysis into SWAT for enhancing accuracy of spatiotemporal sediment yield
iv. Evaluation of trend of climate change, sediment yield and the relationship in between of the upper Tekeze River basin and using LSUA integrated SWAT
v. Evaluating the effectiveness of land management scenarios in reducing sediment yield to the Tekeze hydroelectric dam using LSUA integrated SWAT

1.5 Conceptual framework of thes study

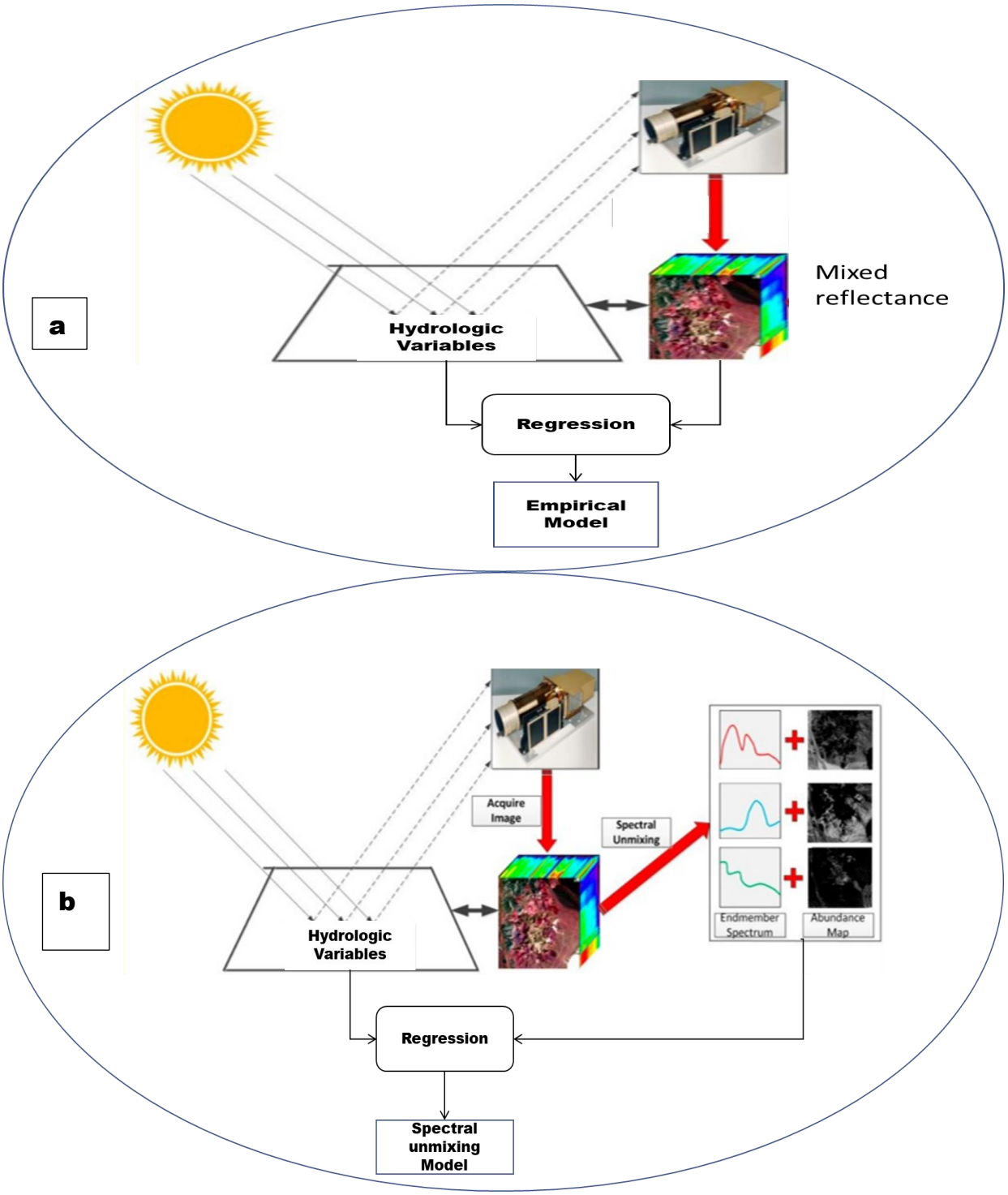

Fig. 1: Conceptual framework of in previous studies (a) and current study (b)

The above framework is presented to show that this research is conducted based on the new approach as indicated above (Fig. 1). The reflectance values of water resources systems at sensors are the combined effect of the reflectance of different objects or constituents in and\or around our entity. So, we have two approaches for analysing the variability of our concerns. The first approach which is commonly applied\conventional one is to use the lumped reflectance and regressing it with the variable we concerned. The second option which can be considered as an emerging approach is first to build detail knowledge about the optical property of the components in the mixture. So, we proposed spectral unmix remote sensing analysis technique to estimate the abundance of the components in the mixed pixels.

1.6 Significance of the research

Most river systems of the world carries a significant amount of sediment transported by runoff from contributing watersheds and river beds. It is impossible to think about a river system without sediment. The only options we have are either to design adaptation strategies to live with it and/or to plan mitigating strategies to minimize it into less affecting status. Unfortunately, both require accurate documentation of information related to rate and pattern of the sediment transport at finer spatial and temporal scales. The information related to the root causes, types and rates of sediment transport in place and time-wise is important to understand how the sediment transport responds to the natural and anthropogenic perturbations in basins, Rivers, and reservoirs and then this helps for designing effective mitigation and adaptation strategies.

Hence, the absence of continuous sediment monitoring coupled with the limited methodology of estimating sediment in ungauged watersheds will pose a major challenge in understanding the spatiotemporal sediment dynamics. Consequently, the status of sediment transportation, the interaction between sediment transportation and the driving calamities (land use and climate) and the response of sediment transportation to different mitigation strategies have been inadequately modeled. Therefore this research was proposed to develop and evaluate alternative remote sensing sediment monitoring techniques, parametrizing hydrologic models, evaluating trend-based relations between sediment yield and climate change and identify the best sediment management scenarios.

1.7 Benefit and beneficiaries of the research

The study presents up-to-date theory, knowledge, dataset and information on spectral unmixing - and integrated hydrologic model for sediment estimation and evaluation of climate impacts and management changes in the upper Tekeze basin, Ethiopia. The findings of the study can be utilised by researchers, sceintific communities, research institutions, and local stockholders. Some of the benefits and beneficiaries of the research are:

Enhanced knowlodge (Scientific Articles): In advancing new knowlde in the areas of remote sensing and sediment issues, scientific publication listed at the beginning of the document which allow researchers to keep up-to-date knowledge and with the new developments of spectral unmixing- and integrated SWAT for sediment estimation, evaluation of climate change impacts on sediment and sediment management options. Different valuable articles published in international journals that can be used for development and research purposes are producing. This work

inevitably helps in decision making in water resource management, particularly in reducing the sediment risk of the Tekeze hydroelectric dam.

Monitoring and modelling Frameworks: There are different monitoring and modelling tools outputs delivered during and after the research. The new LSUA model used for determining the suspended sediment concentration, the LSUA integrated SWAT with enhanced sensitivity to the vegetation parameter of soil erosion and then sediment yield, the sensitivity of LSUA integrated SWAT for climate and sediment trend & interaction with sediment yield, and sediment management options are some of the outputs from this research.

Scientific data/information: the primary sediment and reflectance data generated during the research, the new thematic map of C-factor and land-use, sediment risk map, and prioritized sediment management options are some of the outputs from this research.

1.8 Structure of the dissertation

The dissertation document is organized in six chapters, and the relevant appendices supported by a list of references. The arrangement of the dissertation is as follows:

Chapter 1: Provides general background information, justifications key questions to be answered, objectives and key outputs of the research.

Chapter 2: Presents a review of literature relevant to the various components of the research and the corresponding theoretical background is presented in this section.

Chapter 3: This chapter describes the study area, research design, procedures and methodologies used in this research for each research component.

Chapter 4: Presents the results of the overall research activity and analysis of each research component separately.

Chapter 5: Provides a discussion of the results in an integrated manner, showing complementary of results and their degree of importance in four major sub-topics including:

i. Spectral profile characterizing and modelling the sediment concentration in flash floods (high sediment concentration) using the spectral unmixing technique at laboratory, field and MODIS images.

ii. Applying spectral unmixing analysis for mapping and monitoring the vegetation parameter of soil erosion and sediment (C-factor) for enhancing the performance of SWAT in modelling the spatiotemporal variability of sediment yield in large River basins

iii. Determining the trend of climate change (precipitation and temperature) and the response of sediment yield in the study area

iv. Evaluating d/t sediment management options using LSUA integrated SWAT

Chapter 6: summary of the key findings and conclusions of the research and recommendations

CHAPTER TWO:

LITERATURE REVIEW

This chapter briefly reviewed the status of sediment transportation and deposition at different scales and highlights of the impacts are given. Different sediment monitoring and modelling techniques with their respective drawbacks are summarised. The current status of applying remote sensing technology and its pros and cons for sediment monitoring and modelling are critically reviewed. Summary of current developments in using remote sensing technology in quantifying SSC for inland waters, focusing on the theoretical considerations and application potentials of this emerging method are presented. A brief review of what are the opportunities and delimitations applying spectral unmixing analysis for understanding sediment transportation and implications for effective sediment mitigation and adaptation strategies are reviewed.

2.1 Spatiotemporal sediment variability, impacts and monitoring techniques

A higher and worsening trend of sediment transport and deposition rate has been reported. Recent anthropogenic pressures on the Earth's surface, including population growth, wide-ranging disturbance of the land surface by land-use activities, infrastructure development and mineral exploitation, and modification of the hydrological cycle caused by water resource exploitation, have resulted significant changes to the sediment loads of some of the world's rivers. Despite a decreasing trend in some rivers, an increasing trend in many of the studied rivers has been reported. According to the review by Walling and Webb, (1996) the total suspended sediment transport to the oceans in 1950s through the 1980s was

estimated to be about 15 - 20 billion tons annually. In 2000s, the sediment transport increased to 24-30 billion tons annually (Walling, 2008; Sumi and Hirose, 2009).

The sediment transport and deposition rates vary regionally, nationally and at field scale. The soil erosion and sedimentation in developing countries are more severe compared to the developed world and then the impacts are worst in such countries. Higher sediment yield values up to 15,699 $tkm^{-2}\ y^{-1}$ in African River basins were reported by Vanmaercke et al., (2014) compared to the 40-200 $tkm^{-2}\ y^{-1}$ in Europe by Vanmaercke et al., (2011). More specifically Ethiopia is described as a leading country with extreme sediment yield (Beyene, 2011) with recorded annual soil loss ranging 1,600 – 30,000 $tkm^{-2}\ y^{-1}$. Sediment transportation in Ethiopian River systems is even more severe compared to other nearby River systems (Siyam et al., 2005). The Blue Nile and Tekeze River systems originated from the Ethiopian highlands are for instance the major sources (72% and 25% respectively) of sediment loads in the Nile basin (Tarek, 2009). Like the rate of sediment transportation, the rate of sediment deposition and its impact on dams and reservoirs varies regionally and from country to country. The dams and reservoirs' reduction percentage due to sedimentation for developed/ing countries data that were obtained from different sources and methods are compiled (Fig. 2).

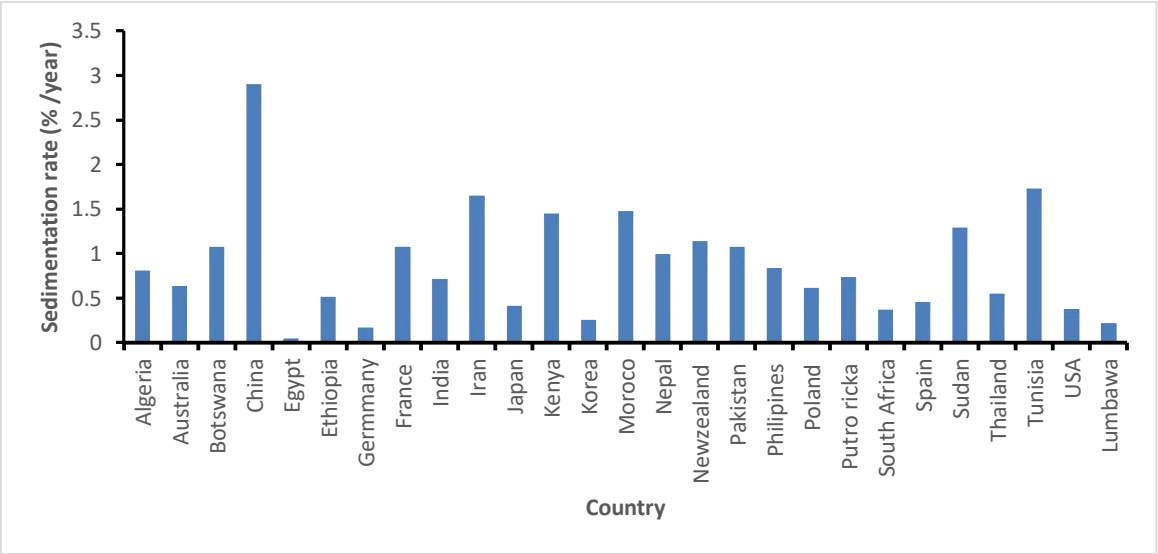

Fig. 2: Volume reduction of dams and reservoirs in different countries due to sedimentation (ICOLD, 2009)

Though the quantification of sedimentation vs country in Fig. 2 might be affected by the spatiotemporal distribution of the studies considered, it can provide a general representation of the sedimentation rate in the countries. The rates of reservoirs volume loss due to sedimentation are well below 1.0 % in each year for most of the countries; however, there are countries such as Tanzania and China that have sedimentation rates well above 2.0 % loss in a year (Fig. 2). The average sedimentation rate in Africa, Asia, Europe and North America can be summarised to be 1.20, 1.44, 0.58 and 0.38 %, respectively (Fig 2).

The fluvial processes and sediment loads (Syvitskiet al., 2005) as well as the availability of sediment to be transported, vary spatially and temporally as a response of inconsistent hydrologic variables. Many investigations have shown that hydroclimate change could significantly affect soil erosion patterns (Pruski and Nearing, 2002; Michael et al., 2005) and sediment flux (Xu, 2003; Syvitski et al., 2005; Zhu et al., 2008). The drastic increase of sediment flux from Gilgel Gibe basin, Ethiopia, was as a response to climate change in the

River basin (Demssie et al., 2007). Gebremicael et al., (2013) has reported a significant increasing change of sediment yield as a response to climate change in the upper Blue Nile. Anwar et al., (2016) has also found doubling progress of sediment flux in Gilgel Abay, upper Blue Nile, as a response of the climate change in the basin. Hence, climate variability is among the critical factors for spatial and temporal variability of sediment transportation.

Moreover land-use change (Hurni et al., 2005; Amsalu et al., 2007) and geomorphologies extremes (Tamene et al.,2006a; Nyssen et al., 2007) could also be an important factor of sediment transportation. The rapid population increases in the globe is causing rapid transition of erosion-resistant land-use types (e.g. forest land, shrubland) to erosion vulnerable types of land uses (e.g. crop, grazing and open land). The rapid population growth in Ethiopia (counted over 85 million in 2012 that is double of 1982 and expected to double by 2050) coupled with traditional farming system resulted rapid deforestation and intensification of land cultivation (Hurni et al., 2005; Amsalu et al., 2007; Balthazar et al., 2013). Consequently, Ethiopian River basins are not only experiencing accelerated sediment transportation but are also experiencing very dynamic sediment transportation. The abundant, worsening trend and spatiotemporal variable nature of sediment transportation need well planned and designed intervening measures. Accurate characterizing (concentration, size distribution, velocity, deposition pattern) of long-term sediment yield is important to predict the reservoirs' sediment deposition pattern and rate, evaluate its consequences on the water resource systems, identify appropriate reservoir sediment management strategy and specify feasible design. Moreover, identifying the root causes and source of sediment have paramount importance in designing effective mitigation

and adaptation strategies. Therefore, a model and/ or monitoring technique that capture the place specific and time-continuous nature of the processes is valuable.

2.2 Sediment monitoring and modelling techniques

The spatiotemporal variability of the sediment in amount, source of origin (wash load and bed material load), the way it transports (suspension and bedload) and the composition (grain size distribution, nutrients, organic matter etc.) it holds have their own respective implications to the alteration of the impacts, monitoring\ modelling and controlling mechanisms. The monitoring and modelling techniques must be developed in a way that can be suit to the above variabilities (WMO, 2000; Wren et al., 2000). Especially the diversity and technologic advancement of the techniques used to acquire for the sediment information are continuously growing.

Despite of the variability of accuracy and investment cost, there are different in-situ monitoring (Wren et al., 2000), Turbidimeters and Laser Diffractometers (Felix et al., 2013) and Acoustic techniques (Costa et al., 2012; Felix et al., 2013; Gruber et al., 2916) have been used for monitoring the suspended loads. Bedload transport can also be monitored either directly by collecting moving particles and using tracer particles or indirectly by active and passive sensors (Gottesfeld and Tunnicliffe, 2003; Møen et al., 2010). The detail of the sediment monitoring techniques is given below (table 1)

Table 1: Comparison of techniques for suspended sediment monitoring (Wren et al., 2000).

Technology	Operation	Advantage	Disadvantage
Bottle sampling	Water - sediment sample is taken isokinetically by submerging container in stream and is later analyzed	Accepted, time - tested technique, allows determination of concentration and size distribution, most other techniques are calibrated against bottle samplers	Poor temporal resolution, flow in-trusive, requires laboratory analysis to extract data, requires on - site personnel.
Pump sampling	Water - sediment sample is pumped from stream and later analyzed.	Accepted, time - tested technique, allows determination of concentration and size distribution.	Poor temporal resolution, flow intrusive, requires laboratory analy-sis, does not usually sample isokinetically.
Acoustic	Sound backscattered from sediment is used to determine size distribution and concentration.	Good spatial and temporal resolution, measures over wide vertical range, nonintrusive.	Backscattered acoustic signal is difficult to translate, signal attenuation at high particle concentration.
Focused beam reflectance	Time of reflection of laser incident on sediment particles is measured.	No particle size dependency, wide particle size and concentration measuring range.	Expensive, flow intrusive, point measurement only.
Laser diffraction	Refraction angle of laser incident on sediment particles is measured.	No particle - size dependency	Unreliable, expensive, flow intrusive, point measurement only, limited particle - size range.
Nuclear	Backscatter or transmission of gamma or X - rays through water - sediment samples is measured.	Low power consumption, wide particle size and concentration measuring range.	Low sensitivity, radioactive source decay, regulations, flow intrusive, point measurement only.
Optical	Backscatter or transmission of visible or infrared light through water - sediment sample is measured.	Simple, good temporal resolution, allows remote deployment and data logging, relatively inexpensive.	Exhibits strong particle - size dependency, flow intrusive, point measurement only, instrument fouling.
Remote spectral reflectance	Light reflected and scattered from body of water is remotely measured.	Able to measure over broad areas.	Poor resolution, poor applicability in fluvial environment, particle - size dependency

The drawbacks in one or more of these techniques are time and labor consuming for a field - laboratory analysis and having poor spatial and temporal resolution data. The need for continuous instrument validation and calibration due to their sensitivity to color, size and composition variability is also another additional burden on such techniques.

2.2.1 Remote sensing for monitoring and modeling sedimenttransport

Globally, the very common method of sediment load monitoring is in-situ sampling followed by laboratory analysis (Wren et al., 2000). As this method involves with site selection, water sampling, transportation of the samples, laboratory processing (drying and weighing), and post-analysis procedures, it is labour and time intensive. Especially for

remote stations, the cost could not be affordable to many developing countries. Because of this, more than three-quarter of the world has a shortcoming to afford a full-scale monitoring infrastructure for water quality control and will not be able to construct this infrastructure soon (Villar et al., 2012). On top of this limitation, results from such sediment measurements at large scale could not provide adequate information. It lacks to provide the information related to identifying the catchment part which is prone for more sedimenttransport and could not answer to the why questions which would be the very important information for prioritized mitigation plans. The high cost of facility and maintenance discourage the implementation of such monitoring networks to provide long-term, large scale, and uninterrupted observations, which are needed for energy and water resources development studies (Wren et al., 2000). Consequently, scientists in the area are still in searching economically feasible, accurate and spatiotemporally representative type of sediment modelling and monitoring techniques.

Followed the above problem and the effort, there is a shift toward applying remote sensing technology, hydrologic models and integration of the two. Remote sensing, mostly done by processing the interaction involved in between incident radiation and the targets of interest using imaging or non-imaging sensors, has become emerging technology for SSC monitoring and as complementary tools for hydrologic models. Recent advances in satellite technology, sensory, image acquisition and processing, and data accessibility have drawn much attention in using remote sensing approach in determining SSC, especially in highly turbid inland waters. As a result, many techniques including acoustic, pumping sampling, laser diffraction, nuclear, and methods based on focused beam reflectance, optical

backscattering, optical transmission, and spectral reflectance (Doxaran et al., 2002; Chen et al., 2004). Applying the hydrologic model is unthinkable with the absence of remote sensing technology. Many of the hydrologic models estimating sediment transportation and deposition rate (e.g. SWAT) use remote sensing technology as a tool to generate and map spatiotemporal input data.

Thus, direct and indirect application of remote sensing in monitoring and monitoring sediment transportation has multiple advantages over the conventional field-sampling technique. In-situ sampling followed by laboratory analysis is the most commonly used method for sediment monitoring in Rivers. This method involves site selection, water sampling, transportation of the samples, laboratory processing (drying and weighing), and post-analysis. It passes long chain, consumes more time, labour-intensive, and provides only point data at gauging stations. Since the construction of gauging stations and the maintaining of a conventional monitoring system is costly, it has been estimated that three quarters of the world cannot afford a full-scale monitoring infrastructure for sediment monitoring stations and will not be able to construct this infrastructure in the near future (GEMS, 2003; Villar et al., 2012).

2.*2.1.1 Direct application of remote sensing*

Remote sensing technology can provide synoptic, continuous and long-term observations to the variability of sediment concentration in different water bodies (oceans, seas, lakes and Rivers) directly. Various visible and near-infrared band combinations of remote sensing including in-situ spectral measurement using spectroradiometer, laboratory experimentation

and different satellite images had been tested and found effective in detecting SSC in coastal (Islam et al., 2003; Doxaran et al., 2003; Wang et al., 2010; Fang et al., 2010; Wang et al., 2012) and lake environments (Ritchie and Cooper 1991; Ma and Dai, 2005). The advances in satellite technology, sensory, image acquisition, processing, and data accessibility have drawn much attention in using remote sensing approach in determining SSC of highly turbid inland (lake and River) waters. The Islam et al. (2001), Chu et al. (2009), and Wang and Lu (2010) are some of the researchers tested the efficiency of remote sensing in the monitoring of SSCs in Rivers.

The principle working to apply remote sensing technology in monitoring SSC from inland water is just using the fact that suspended sediments increase the radiance emergent from surface waters in the visible and near-infrared region of the electromagnetic spectrum (Ritchie and Schiebe, 2000). According to the conservation of energy, the light that arrives at the surface of water called radiance is divided in to refracted (diffused attenuation), reflected and absorbed energy which depends on the optical property of the turbid surface water (Mobley, 1994). This fact is summarized as

$$\mathbf{R_r + A_r + T_r = 1} \quad \textbf{(Eq.1)}$$

Where Rr = reflectance or reflectivity, A_r= absorptance or absorptivity and T_r=transmittance or transmission of the object (water body in this case) with respect electromagnetic radiation (r) under consideration.

The wavelength ranges effective in determining sediment concentration and the relation between irradiances and SSC varies spatially. This variation can be attributed to the

variation of sediment composition (such as type and grain size distribution), waterbody characteristics (depth, vertical variation in sediment concentration, and bottom reflection), and view geometry. To some degree, the air-water interface and atmospheric conditions also add to the complexity (Gray et al., 2000). Moreover, various other parameters such as River geomorphology can influence the relation between SSCs and reflectance and hence algorithm developed for a given River may not be applicable to another River. There are multiple empirical (Doxaran et al., 2009; Min et al., 2012; Long and Pavelsky, 2013), semi-empirical (Shen et al., 2013), and theoretical (Wang et al., 2009) models which can be used for estimation of SSCs.

There are multiple empirical models developed at different River systems. Empirical models are normally generated based on the relation between the apparent optical properties (AOPs) and the level of SSC using statistical analysis on some measured data. The empirical models take the form of linear regression and nonlinear regression describing the relation between a single band of spectral reflectance or ratio of reflectance in merged bands and SSCs (Yuming and Min, 1992; Doxaran et al., 2002). The linear and nonlinear empirical relation existed between SSC and reflectance can be explained with the radiative transfer theory (RTT). Without considering any atmospheric effect, the reflectance at any wavelength can be expressed as a function of the optical properties of the co-existing concentrations of pure water and constituents in the water (Eq. 2).

$$\boldsymbol{R_\lambda = C\left((\beta_w + \beta_s \mathbf{SSC} + \beta_c)/(a_w + a_s SSC + \alpha_c)\right)} \qquad \textbf{(Eq.2)}$$

Where R represents the reflectance of the turbid water at specific wavelength (λ), α_w represents the absorption coefficient of the turbid water, α_s is the cross-section value of absorption coefficient of suspended sediments, a_c is the absorption coefficient of other co-existing constituents, β_w is the backscattering coefficient of water; β_s is the cross-section value of the backscattering coefficient of suspended sediments; SSC is the suspended sediment concentration

The optical property of pure water is dominated by absorbance and transferring optic properties while the backscattering is lower. Water absorbs most of the energy in the near-infrared and middle-infrared wavelengths whereas other surface materials have a higher reflectance in these wavelengths. But in more turbid water, the backscattering become higher compared to the absorbance and transferring optical properties of the water. Most researches investigating the relationship between reflectance and SSC in Rivers with lower sediment load indicated linear relation. This is reasonable that in such cases the absorption is dominated by water when a_w is far outweighing as SSC. Ritchie et al. (1976) found a linear correlation (R = 0.85) between integrated spectroradiometer reflectance (700−800 nm) and amounts of SSC in Mississippi reservoirs. Chen et al. (1991) found that the relation between SSC and reflectance was linear at wavelengths of 700 to 1050 nm. Novo et al. (1991) reported that, for Oxisol sediment types, the relation between total suspended solid concentration and reflectance was linear and constant from 450 to 900 nm. Islam et al. (2001) and Wang et al. (2010) researches in the Yangtze River found linear empirical model performed R^2 of 0.98 and 0.73, respectively. Research by Ma and Dai (2005) in Lake Tailu, China, also found a linear empirical model relating SSC and reflectance. But, in

water systems with extremely higher sediment concentration the relation between SSC and reflectance become non-linear. The reason is that the absorbance by the water is dominated by the absorbance from the sediment (a_s). Often a second-order polynomial (Lodhi et al., 1997), logarithmic (Chu et al., 2009; Wang et al., 2009; Wnag et al., 2010; Wang and Lu, 2010) and Exponential (Schiebe et al., 1992; Dekker et al., 2001) function model are the common nonlinear empirical relation found between the SSC and reflectance at different wavelength ranges.

As the above review can indicate the predicting capability of empirical models to their respective data and situation is found higher (R^2>= 0.5). But, none of them was consistent and universal. They were varied based on the River systems (sediment types and level of concentrations), sensor types and band combinations. This implied the applicability of remote sensing approach based on empirical relations can be quite limited and may result in significant errors if applied to other situations. Hence, though empirical models are simple and rapid in processing large data sets, they are only applicable to situations with similar characteristics like those used in the model development. These empirical models generally do not transfer well to places outside the area in which they were developed. Therefore, for any new applications, one still must develop his or her empirical models, and he or she should not expect the same good performance of certain empirical models to reappear.

Unlike the empirical models, semi-empirical modelling types can be used in estimating suspended sediment concentration of inland and coastal water systems. Semi-empirical models are developed based on radiation theory that integrates the inherent optical properties (IOPs) and the apparent optical properties (AOPs) (Loisel and Stramski, 2000).

The predictability of semi-empirical models depends on the estimation of IOPs for sediment substances. The IOPs are affected by types of sediment, depth of water and other factors that affect the relationship between SSC and remotely sensed optical properties (Curran and Novo, 1988). As the IOPs are constituent specific and are sensitive in the simulation of the radiative transfer equation (RTE), the performance of most semi-empirical methods depends on accurate determination of the radiative properties of sediment constituents.

$$\boldsymbol{R_\lambda = b_w + \sum_{j=1}^{n} b_j C_j} \qquad \textbf{(Eq.3)}$$

Where R_λ represent the reflectance of the turbid water, b_w refers to the backscattering coefficient of pure water, C_j refers to the concentration of the j^{th} constituent in the water solution.

Such approaches have been found more accurate than that of the empirical algorithms and these models are more applicable for different water types with the capability to take the effects of water depth, particle size, and water-air interface into account. There are many types of research successful in such an approach. Eleveld et al. (2008) in the southern North Sea (R^2 = 0.87) and Santini et al. (2010) fine-tuned a physical model for the highly turbid Venice lagoon waters are some of the researches applied a semi-empirical model for estimating sediment concentration in their respective study areas.

But the models are not without defects. Detail IOPs of constituents in the water should be presented and considered in the application of different sensor types. The quantity and

quality of the remote sensor are essential for the success of such SSC remote sensing methods. Though the number of sensors currently established to view biological and physical processes within the water bodies is many, most of them have short revisit times and coarse spatial resolution with high spectral resolution and sensitivity. The Landsat series (30m) and the Moderate Resolution Imaging Spectroradiometer (MODIS, >=250m) typically are too coarse to describe inland water constituents.

Therefore, there should be means that split the mixed representation of spectral signatures of components in a given pixel. Spectral unmixing (SU) is widely used for analysing mixed hyperspectral data of coarse spatial resolution of imageries. SU provides a comprehensive and quantitative mapping of the constituents in each pixel. More precisely, SU can identify the spectral signatures of these materials (usually called endmembers) and can estimate their relative contributions (or abundances) to the measured spectra using either a linear (Elmore et al., 2000; Small, 2003; De Asis and Omasa, 2007; Meusburger et al., 2010) or nonlinear unmixing model (Arai, 2008; Bioucas-Dias et al., 2012; Altmann et al., 2013). The unmixing model converts the image DN's to numerical fractions of a few endmembers (Adams & Gillespie, 2006). As a rule of thumb, linear un-mixing is associated with mixtures for which the pixel components appear in spatially segregated patterns. If, however, the components are in intimate association, light typically interacts with more than one component as it is multiplied scattered, and the mixing systematics are highly nonlinear (Keshava & Mustard, 2002). The underlying physical assumption of anlinear unmixing is that each incident photon interacts with a single-pixel component only. A mixed pixel signal (r) can as such be described as a linear combination of pure spectral

signatures of its constituent components (i.e., endmembers), weighted by their subpixel fractional cover (Adams et al., 1986).

Even though, the question whether linear or nonlinear processes dominate spectral signatures of mixed pixels is still an unresolved matter, due to the relative simplicity and straightforward interpretation of the analysis the linear spectral un-mixing analysis (LSUA) strategy is commonly applied (Adams et al., 1995; Dobigeon et al., 2014). The mathematical LSUA technique applied to split spectral signature into respective constituents is:

$$\boldsymbol{R_\lambda = \sum_{r=1}^{N} a_{r,p} m_r + n_p} \qquad \textbf{(Eq.4)}$$

Where, N is the number of endmembers present in the image, m_r is the spectral signatures of the r^{th} endmember, $\alpha_{r,p}$ is the abundance of the r^{th} material in the p^{th} pixel and n_p is an additive term associated with the measurement noise and the modelling error.

As the Eq. 4 indicated the LSUA seems possible to use for estimating SSCs from imageries and advantageous over the conventional empirical approaches of applying remote sensing technology. But this potential is not well studied and exploited globally. Since most Ethiopian Rivers have their distinctive characteristics making different one another and optical properties of constituents in River systems is not studied, attempting to develop a River basin-based algorithm for Ethiopian Rivers could have paramount importance.

2.2.1.2 Indirect application of remote sensing

Apart from the direct detection to the sediment concentrations in Rivers, remote sensing is also effective for monitoring and mapping the factors controlling sediment concentrations in Rivers. Role of the remote sensing in paramtrizing and supplementing different hydrologic models including sediment rating curves (eg. Haregeweyn et al., 2006; Tamene et al., 2006b; Haregeweyn et al., 2008; Moges et al., 2016), the WEPP (Zeleke, 2000; Maalim et al., 2013), the AGNPS (eg. Haregeweyn and Yohannes 2003; Mohammed et al., 2004), the SWAT (eg Setegn et al., 2010, 2008; Mohammad et al., 2015), and the ANN (eg. Masoumeh and Mehdi, 2012; Melesse et al., 2011) is very important.

Vegetation characteristic (species type, abundance, composition and development stage) resulted from the comprehensive long-term interaction of landform, hydrology, soil, climate and human activities are a sensitive indicator and controlling factor for sediment concentration in rivers. It plays an important role in reducing soil erosion and then sediment yield by reducing the force of falling raindrops, increasing infiltration of water in to the soil, reducing the power of surface runoff, binding the soil mechanically, and maintaining roughness of the soil surface and through improving the physical, chemical and biological properties of soils (Meusburger et al., 2010). Canopy cover, leaf area index, root structures and biomass are among the plant part which contribute to controlling soil erosion and the sediment yield. The effect of vegetation on sediment yield varies spatially because of species change and its growing stage. Moreover, it shows a long-term temporal dynamic as a result of land-use conversions or gradual depletion of resources or short-term dynamics caused by rainfall characteristics and by human activities (Vrieling, 2006).

The vegetation cover and management effect on soil erosion and then sediment yield known as C- factor has been therefore used as a decisive parameter in multiple erosion and sediment modelling software. In the soil loss models, Universal Soil Loss Equation (USLE, Wischmeier and Smith, 1978) and its subsequent, the Revised or Modified Universal Soil Loss Eq. (R/MUSLE, Williams, 1975), C- factor is an implicit parameter determining soil loss. The MUSLE is also found impeded in the hydrological model Soil and Water Assessment Tool (SWAT) used for simulating sediment yield. It is also used in simplified stream power equation of Bagnolds (1977) to route sediment transportation in reaches. Other than in the USLE and its successive, the C-factor has been also used in other erosion models such as in the Morgan and Finney method (Morgan et al., 1984), areal nonpoint source watershed environment response simulation (ANSWERS, Beasley et al., 1980), water erosion prediction project (WEPP; Zeleke, 2000) and agricultural non-point source (AGNPS, Haregeweyn and Yohannes, 2003; Mohammed et al., 2004). Thus, reliable spatiotemporal C-factor estimation is essential for accurate modelling of soil erosion and sediment yield estimation, which in turn, is needed for sound mitigation and adaptation planning.

2.2.2 Hydrologic modelling for sediment yield

Modelling the process of soil erosion and sediment transportation using hydrologic models can help our understanding to the issues related to the critical sources and factors controlling erosion and sediment transport. There are multiple potential hydrologic models which simulate the soil erosion/sedimentation processes in River basins. These models are primarly classified in to empirical, conceptual and physical-based. Sediment rating curves

(Haregeweyn et al., 2006; Tamene et al., 2006b; Haregeweyn et al., 2008), Hydrologic Engineering Centres River Analysis System, (HEC-RAS; HEC, 1995), Water Erosion Prediction Technology (WEPP, Nearing et al., 1989) tested by Maalim et al. (2013), Agricultural Non-Point Source Pollution (AGNPS; Young et al., 1989) tested by Haregeweyn and Yohannes (2003) and Mohammed et al. (2004), Soil and Water Assessment Tool (SWAT; Arnold et al., 1998) tested by Setegn et al. (2010, 2008), Mohammed et al. (2015), and the Artificial Neural Network (ANN; Masoumeh and Mehdi, 2012).

Soil and water assessment tool (SWAT) developed by Arnold et al., (1998) is one of the semi-distributed hydrologic models found effective in modelling sediment yield of different scales of River basins. It is the most popular model applied for understanding the hydrologic processes including sediment yield of small to large scale River basins. Since it is distributed and processes-based model, it has fewer uncertainties and provides relatively adequate information compared to that of lumped models. SWAT simulates the hydrology of the watershed in two phases. The land phase of the hydrologic cycle controls the amount of water, sediment, nutrient and pesticide loadings to the main channel in each sub-basin. The water or routing phase of the hydrologic cycle controls the movement of water, sediment, nutrients and pesticide loadings through the channel network of the watershed into the outlet. The model calculates the surface erosion within each Hydrologic Response Unit (HRU) with the Modified Universal Soil Loss Equation (MUSLE; Williams, 1975).

$$\mathbf{Sed = 11.8\times (Q_{surf} \times Q_{peak} \times A_{hru})^{0.56} \times K_{USLE} \times C_{USLE} \times P_{USLE} \times LS_{USLE} \times CFRG} \qquad \mathbf{(Eq.5)}$$

where Sed is the sediment yield (metric ton day^{-1}), Q_{surf} is the surface runoff volume (mm ha^{-1} day^{-1}), Q_{peak} is the peak runoff rate (m^3 s^{-1}), A_{hru} is the area of the HRU (ha), K_{USLE} is the USLE soil erodibility factor, C_{USLE} is the USLE cover and management factor, P_{USLE} is the USLE support practice factor, LS_{USLE} is the USLE topographic factor and CFRG is the coarse fragment factor.

The sediment routing model that simulates sediment transport in the channel network consists of two components operating simultaneously: deposition and degradation (Arnold *et al.,* 1995). The amount of deposition and degradation is based on the maximum concentration of sediment in the reach and the concentration of sediment in the reach at the beginning of the time step. The final amount of sediment in the reach is determined as

$$\mathbf{Sed_{ch} = Sed_{ch,i} - Sed_{dep} + Sed_{deg}} \qquad \textbf{(Eq.6)}$$

where Sed_{ch} is the amount of suspended sediment in the reach (metric ton day^{-1}), Sed_{chj} is the amount of suspended sediment in the reach at the beginning of the time period (metric ton day^{-1}), Sed_{dep} is the amount of sediment deposited in the reach segment (metric ton day^{-1}), and Sed_{deg} is the amount of sediment re-entrained in the reach segment (metric ton day^{-1}). The amount of sediment transported out of the reach is calculated as

$$\mathbf{Sed_{out} = Sed_{ch} \times V_{out}/V_{ch}} \qquad \textbf{(Eq.7)}$$

Where Sed_{out} is the amount of sediment transported out of the reach (metric t day−1), Sed_{ch} is the amount of suspended sediment in the reach (metric ton day^{-1}), V_{out} is the volume of

outflow during the time step (m^3 day^{-1}), and V_{ch} is the volume of water in the reach segment (m^3 day^{-1}).

The interest to use such hydrologic models for different purposes has been growing worldwide. It plays a great role in understanding the impact of land use alteration (Mango et al., 2011a; Mango et al.,2011b; Getachew & Melesse, 2012),climate change (Setegn et al., 2010; Dessu and Melesse, 2012, 2013; Assefa, et al., 2014) and evaluating the performance difference of management scenarios (Wang et al., 2008; Setegn et al., 2009, 2010; Grey et al., 2013; Yesuf et al., 2015) on reducing soil erosion and sediment yield of River basins. However, most of the hydrologic models including SWAT are initially developed after long time experiments in the US and Europe with a temperate to sub–humid climate and data rich areas. Lack of input data at the required temporal and spatial scales has been a typical limitation of the models. Consequently, sediment modeling in Ethiopia has generally not been very successful because of both limited sediment data for validation. At the same time the underlying hydrology of tropical sub humid areas is not understood very well. Runoff predictions in these models are based on the SCS curve number that is not suitable with the monsoon climate condition in the Ethiopian landscape (Liu et al., 2008, Bayabil et al., 2010, Tilahun et al., 2012). More recently, researchers (Easton et al., 2008, Steenhuis et al., 2009, Tilahun et al., 2012) have started to use a locally modified SWAT. An attempt to consider the topography of Ethiopia has made in this modification.

The fluvial processes and sediment load as well as the availability of sediment to be transported vary spatially and temporally as a response of inconsistent vegetation and other

parameters. The effect of vegetation on soil erosion and then sediment yield varies based on specie type, growing stages and their abundances (Zhou et al., 2006) which cause for different canopy covers, leaf area index, biomass, and root structure which intern have different hydrologic intervention. Consequently, vegetation contributes to the spatiotemporal variability of sediment yield and called C-factor. The C- factor value is place and time specific parameter which conceptually determined directly by the ratio of the long-term in-situ measurement of soil loss from vegetated land (Wischmeier and Smith, 1978).

The SWAT parameter setups specifically the vegetation cover management effects (C-factor) database included in SWAT consists of empirical values from long-term experiments in the United States, which may not be applicable to other countries. Therefore, the SWAT based studies in developing countries must have area and time specific database. But most studies have been considered it inadequately. It has been considered at land use unit type level or has been taken constant values from literature which results constant C- factor values for large area. This can't reflect the effect of spatial variation of vegetation on soil loss (Song et al., 2011). This implies the need for cost effective and spatially distributed estimating technique.

Space remote sensors especially the visible and near infrared (NIR) portion of spectrums and their combinations have been tested and found effective in detecting effect of vegetation on soil erosion and then sediment yield (Vrieling, 2006). The C- factor is place and a time-specific parameter which conceptually determined directly by the ratio of the long-term in-situ measurement of soil loss from vegetated land to that of corresponding

bare land measurements (Wischmeier and Smith, 1978). This approach is cost infeasible to apply to large River basins otherwise to plot - field scales (Panagos et al., 2015). Unlike this field measurement, the spatial and temporal variability of vegetation and the correlation with soil erosion and sedimentation (C-factor) can also be modelled using remote sensing. Different approaches of remote sensing have been employed for monitoring and mapping the condition of vegetation cover and its relationship with soil loss and sediment yield. Some of them are discussed in the following sections.

2.2.2.1 Classification approach for modelling C-factor

Previously, remote sensing has been used as an alternative approach to mapping land use classes and then a field measured C-factor values has been assigned to each land use classes. This land-use classification C-factor has often been used to map land-use types that differ in their effectiveness to protect the soil from transportation. To achieve this objective, direct linear regression has been performed between image band (MSS, TM, ETM+) ratios and C-values and then different inter/extrapolation mechanisms have been applied for spatial mapping (Gertner et al., 2002; Wang et al., 2003). Other researchers have also been used point data collected in the field by investing huge cost or done simply by assigning values from literature into a classified land cover map (eg. Betrie et al., 2011; Gizachew, 2015). This method, however, resulted in C-factor estimates that are constant for relatively large areas, and do not adequately reflect the spatial variation of vegetation and then its effect on soil loss that exists within land-use type and geographic areas (Griensven et al., 2012). It also introduces errors from classification (Wang et al., 2002). Such problems could be higher in River basins which lack the land-use plan and with changing climate

variables. To increase the spatial variability and decrease the influence of classification errors, direct linear regression between image bands or ratios and C-factor values determined in the field (Cihlar, 1987; Stephens and Cihlar, 1982) and a joint sequential co-simulation with Landsat TM images (Gertner et al., 2002; Wang et al., 2002, 2003) has been performed for mapping the C-factor. However, these methods are costly and obtaining the appropriate number of sampling points for interpolation is rather difficult.

Most SWAT based studies of sediment transportation and deposition in developing countries have been relied on the land use-based determination of C-factor. The spatial representation of C-factors in most SWAT studies in developing countries has been considered at a land-use level or has been taken constant values from literature which results in constant C-factor values for a large geographic area. This can't reflect the detail spatial variation of vegetation effect on soil loss (Song et al., 2011). Griensven et al., (2012) have critically reviewed to the researches in the Nile River basin which used SWAT for modelling hydrologic processes. The appropriateness of the models was evaluated based on three criteria including performance indicators (fit-to-observations, fit-to-reality and fit-to-purpose). Accordingly, it was found that the representation of the temporal dynamics of SWAT application is satisfactory. However, little confidence has been given to the potential of SWAT in representing to the spatial heterogeneity of the processes. According to this review, the very important gap of the researches was the lack of attention to the vegetation and crop processes. None of the papers reported any adaptation to the crop parameters or any crop-related output.

About 20 researches on sediment yield using SWAT for Ethiopian river basins published in international journals were reviewed (eg. Betrie et al., 2011; Steenhuis et al.,2009; Gebremichael et al., 2013; Hassen et al.,2015; Shimelis et al.,2010; Michael & Jain, 2013; Ayana et al.,2012; and …). The researches have used the R^2, NSE, PBIAS and RSR statistical tools to evaluate the performance of the model in estimating sediment yield in the respective study area (Table 2).

Table 2: Summary statistics of SWAT Peroformance in previous researches (R^2, NSE, RSR and PBIAS)

Constituents	**Statistics**	**Calibration**				**Validation**			
	Model Performance	R^2	NSE	PBIAS	RSR	R^2	NSE	PBIAS	RSR
	n	5	9	4	4	5	9	4	4
Sediment yield	Max.	0.86	0.88	28	0.67	0.84	0.83	30	0.69
	Min.	0.52	0.07	− 14.6	0.23	0.51	-1.7	-10.5	0.29
	Ave.	0.73	0.66	16	0.28	0.75	0.46	10.5	0.51

The above Table 2 shows summary statistics from the literature review of reported for Ethiopian watershed R2 (coefficient of determination), NSE (Nash-Sutcliffe efficiency), RSR (ratio of the root mean square error to the standard deviation of measured data) and PBIAS (percent of bias) values

According to Moriasi et al. (2007) model evaluation guideline for PBIAS, RSR and NSE, the performance of SWAT in predicting sediment yield relied on between satisfactory to good performances only. The hypothesis here is that the inappropriate parametrization of C-factor contributesto the less performance of the SWAT model in the studies.

2.2.2.2 Modelling C-factor using vegetation index based remote sensing

Vegetation indices are a specific class of spectral band ratios and which exploit the fact that green vegetation has a high reflectance in the NIR and low reflectance in the red part of the spectrum. The normalized difference vegetation index (NDVI, Tucker, 1979), which is defined as the NIR reflection minus red reflection divided by the sum of the two, has been used directly as an indication of the protective cover of vegetation (Thiam, 2003) or was related to vegetation cover with regression analysis (Symeonakis and Drake, 2004). NDVI has been explored for mapping the C- factor by relating it directly using regression analysis (de Assis & Omasa, 2007; Zhou et al., 2008; Durigon et al., 2014).

But, space remote sensing (satellite image) driven NDVIs were found to have less correlation with the C-factor due to the high sensitivity of the index to vitality (Jong, 1994 and Frederiksen, 1993) and poor sensitivity to the vegetation senescence. The vegetation vitality effects are during the early growth stage when non-vigorous vegetation covers are overestimated by NDVI due to the intense chlorophyll activity and during vegetation senescence when the NDVI usually decreases even when the covers remain the same. Moreover, the effect of soil reflectance has been considered inadequately in the NDVI analysis technique (Escadafal, 1994).

Even though researchers have developed different adjusting indices, for example, Bonn et al. (1997) have developed the soil adjusted crop residue index (SACRI) to improve the detection of dry vegetation, and Baret & Guyot. (1991) has also developed the transformed soil adjusted vegetation index (TSAVI) to consider the effect of soil reflection, none of

them was found complete. The efficiency of these indexes in estimating the C-factor varied regionally and even temporally. Due to the intervention of reflectance from soil types, estimating C-factors of semi-arid areas and on dry seasons using NDVI were found less efficient compared to the application on humid areas and wet seasons (Ustin et al., 1986; Tueller& Oleson, 1989). Arid and semi-arid areas consist of complex spectral properties due to different mosaics of vegetation, intensive land use pressures, sensitivity to climate fluctuations, dynamic soils' spectral property (colour change, mineralogy, textures, presence of sand and rocks), surface roughness and various other factors. These variabilities, as well as the spectral interaction between the sparsely distributed plant canopies, make vegetation cover using indexes in arid and semi-arid regions more complicated.

Despite the above limitations of the vegetation index methods, C-factor has been commonly estimated using classification and regression/correlations analysis with different indices. The normalized difference vegetation index (NDVI), soil adjusted crop residue index (SACRI, Bonn et al., 1997) and transformed soil adjusted vegetation index (TSAVI, Baret and Guyot. 1991) are commonly used to estimate spatial C-facto values. The use of C-factor in SWAT-MUSLE simulating sediment yield from such methods can therefore under or overestimation (Asis & Omasa, 2007; Durigon et al., 2014).

2.2.2.3 Spectral un-mixing analysis approach for modelling C-factor

The advantage of remote sensing is not limited to its quick and easy way for estimating land surface parameters in broad areas with limited investment cost and reasonable

accuracy, but also has dynamic potential to be applied to a different discipline. The LSUA approach has been commonly applied to different disciples due to its mathematical simplicity and sufficiency of accuracy (Bioucas-Dias et al., 2012; Shi & Wang, 2014). Recently, the linear spectral unmixing analysis (LSUA) has been found as a most accurate and quick way of estimating vegetation parameter of soil erosion and then sediment yield commonly abrivated as C-factor (Ma et al., 2003; Shi and Wang, 2014). LSUA uses the concept that the spectral signature of a given mixed pixel is the linear, proportion-weighted combination of the end-member including vegetation, rock, water and bare soil. Therefore, the C - factor is dependent on the linearly combined effect of these components. Using the vegetation, bare soil, water body and rocky land rations spectrum as an endmember, the C factor using the LSUA is mathematically computed as

$$\textbf{C-factor} = \frac{F_{bare}}{1+F_{veg}+F_{rock}+F_{water}} \quad \textbf{(Eq.8)}$$

Where, F_{bare}, F_{veg}, F_{rock} and F_{water} are the fractions of bare soil, vegetation, rock and water respectively. These fractions can be computed as

$$F_i = \sum_{j=1}^{n} \mathbf{A_j} * \mathbf{S_{eij}} + \mathbf{€_i} \textbf{ and } \sum_{j=1}^{n} \mathbf{A_j} = \mathbf{1}, \mathbf{0} \leq \mathbf{A_j} \leq \mathbf{1} \quad \textbf{(Eq.9)}$$

Where i is the number of spectral bands used, j=1, n (number of end-members), Ri is the spectral reflectance of the mixed pixel in band i, A_j is the fraction of the pixel area covered by the end-member j, F_{eij} denotes the reflectance of the end-member j in band i, and $€_i$ is the residual error in band i. The residual error ′€′refers to the difference between the measured and modeled reflectance values in each band and could be substituted by root

mean square error (RMSE), which is useful in assessing the validity of selected endmembers.

$$€ = [\frac{1}{i}\sum_{i=1}^{i}(\boldsymbol{F}_{\mathbf{measured}} - \boldsymbol{F}_{\mathbf{modeled}})^{1/2}] \qquad \textbf{(Eq.10)}$$

This approach has multiple opportunities over the conventional (classification and Indices) techniques of estimating vegetation distribution and then C-factor of large areas. Unlike the classification and indices technique, it considers both the photosynthetic and non-photosynthetic variables of C factor. Moreover, it has often been implemented to deal with the problem of mixed pixels unlike the classification system of estimating C-factor (Adams et al., 1986; Van der Meer, 1995). Omassa et al. (2007), de Assis and Omassa, (2007) has applied spectral unmixing analysis to map the spatial values of C-factor and then used to delineate the erosion risk areas. Accordingly, more than 0.90 correlation coefficients (r) between the results from the modelling and physical measurements were presented. Meusburger et al. (2010) has found best result from LSU determination of C-factor (R^2 = 0.85) compared from the NDVI (R^2 = 0. 64). Song et al. (2011) have also demonstrated C-factor from spectral unmixing to integrate into SWAT and then produces reasonable improvements in sediment yield prediction. The Nash–Sutcliffe efficiency coefficient (ENS) and R^2 for sediment yield were generally above 0·70 and 0·60, respectively. Moreover, spatially detail soil erosion risk map at the HRU level could be illustrated which is not common in the classification and index approaches. This technique is mainly used in semi\ arid environments, where it has the advantage that different soil characteristics within a scene can be accounted for.

But, the LSUA approach is not without delimitations. The assumptions including (1) the landscape is composed of a few fundamental endmembers, each of which is spectrally distinct from the others; (2) the endmember spectral signatures do not change within the area of interest; and (3) the composite remotely sensed signal for a mixed pixel is linearly related to the fractions of endmember presences, are misleading. These assumptions are simply oversimplification of the real world. There are significant endmember signature variations within a geographic area. For example, the vegetation endmember can be grass, coniferous, and broadleaf trees, each of which has a very different spectral signature from the others (Roberts et al., 1993; Song, 2005).

2.2.3 Endmember selection and variability control

2.2.3.1 Endmember selection

The critical step in LSUA is selecting the types, numbers and the corresponding spectral signatures of endmembers (Elmore et al., 2000; Theseira et al., 2003). The advantage of this step is helpful that is the spectral signatures are at the same relative measurement scale as the image to be analysed. The challenge is to identify the pure pixels that can be treated as endmembers (Song, 2005). The multiplicity and/or spectrally similarity of the endmembers together with the coarseness of the remote sensing data lead to endmember fraction images that are physically inaccurate as judged.

The techniques ranging from manually testing different sets of endmembers (e.g., Radeloff et al., 1999; Somers et al., 2010) to iteratively testing different endmember combinations (Garcia-Haro et al., 2005; Franke et al., 2009) have been proposed to identify the optimal

number and type of endmembers in scenes. The spectral signatures of the endmembers can be derived from spectral libraries built from field or laboratory measurements (e.g. Asner & Lobell, 2000) or directly from the image data themselves using radiative transfer models (Dennison et al., 2006; Eckmann et al., 2008). Different advanced analysis techniques including pixel purity index (PPI, Boardman et al., 1995), the virtual endmember concept (Tompkins et al., 1997), and N-FINDR (Winter, 1999) have been applied. The identification and estimation of endmembers abundance in a pixel using these methods have multiple sources of error caused by inaccurate atmospheric correction (Gong & Zhang, 1999), insufficient consideration Signal-to-Noise Ratio (Plaza et al., 2004) and model structure input noise (Borel & Gerstl, 1994). The major source of error, however, lies in the lack of the ability to account for sufficient temporal and spatial-spectral variability (Bateson et al., 2000).

Most commonly, the abundance of endmembers in pixels is computed based on the mean spectrum defined for each of the presented endmembers. The standard endmember spectra are subsequently assigned to each image pixel and subpixel cover fractions are calculated using the SUA (Adams et al., 1993). This approach is straightforward and considered very useful for fast photo interpretation and field investigations with high accuracy (Adams & Gillespie, 2006). Nevertheless, the use of fixed endmember spectra, as in SUA, implies that variation in endmember spectral signatures, caused by spatial and temporal variability in the condition of scene components and differential illumination conditions, is not accounted. This approach can work better in relatively homogeneous ecosystems, but because of the spectral complexity of many natural and semi-natural landscapes, the use of

fixed endmember spectra results in significant fraction estimate errors (Bateson et al., 2000).

2.2.3.2 Endmember variability

The variability within an endmember class (intra-class variability) and the similarity among endmember classes (inter-class variability) are the common endmember variabilities identified (Zhang et al., 2006). In some environments, similarity among reflectance spectra of the different endmembers of interest provides an additional difficulty to obtain accurate classification results. The similarity between endmembers results in a high correlation between the endmember spectra (R), which in turn leads to a drop-in estimation accuracy. To solve this problem, numerous solutions have been proposed and are still coming (Somers et al., 2010a, 2010b). Somers et al. (2011) hypothesized that all the available techniques are founded on five basic principles which should be integrated to allow a proper tackling of endmember variability in SUA. The iterative mixture analysis cycles, spectral feature selection, spectral weighting, spectral transformations and spectral modelling. A short review of these methods is given here.

1. **Iterative mixture analysis cycles**were introduced by Roberts et al. (1998). This technique permits multiple endmembers for each component and thereby refutes the fixed endmember restriction made in SUA. It is the most widely used technique and successfully tested in urban (e.g., Powell & Roberts, 2008; Franke et al., 2009) and extraterrestrial environments (e.g., Combe et al., 2008) using both multi- (and hyperspectral optical and thermal imageries.

2. **Spectral feature selection:** Asner and Lobell (2000) highlighted that a careful selection ofwavelengths, robust against spectral variability (i.e. minimizing intraandmaximizing inter-class variability), could significantly improvesubpixel quantification of fractional material cover, while the problemof computational complexity typical of iterative mixture cycles couldbe reduced. The approach wassuccessfully tested in (semi-)arid ecosystems (Asner & Heidebrecht,2002).
3. **Spectral weighting**: This is another alternative technique for reducing the effect of endmember variability in SUA. This can be done either by equally weighting assuming equally important effects or by giving higher weight to the spectral bands less sensitive to endmember variability (Chang & Ji, 2006; Somers et al., 2009d). Experimental results demonstrated that the latter generally performsbetter than the first (Chang & Ji, 2006).
4. **Spectral transformation**: Instead of original reflectance data, modified spectral information was used as input in the SUA.A tied spectrum concept (Asner and Lobell,2000), Normalized Spectral Mixture Analysis (NSMA; Wu, 2004), Derivative Spectral Unmixing (DSU; Zhang et al., 2006) are the common one. But these techniques have respective potential to introduce high frequency noise.
5. **Spectral modeling:** the alternative name given to this approach is the radiative transfer model. To reduce the spectral effects of soil moisture variations, a radiative transfermodel for moist soil background wasimplemented (Lobell & Asner, 2002; Somers et al., 2009b).

Even though the above techniques have their respective potential implemented to reduce endmember variability, none of them is complete in solving the endmember variability fully. Currently, researchers draw attention to the high complementarities between the different techniques and demonstrated an integrated approach (Asner and Lobell, 2000; Rivard et al., 2008). This approach promotes the integration of spatial, temporal and spectral information for reducing endmember variability.

2.2.4 Sensors and remote sensing instruments

The successful direct and indirect application of remote sensing to monitor and model sediment transportation and deposition depends on the sensors' resolution used and the management applied. Coarse (temporal, spatial, spectral and radiometric) resolutions of sensors, the intervention of atmospheric conditions, and absence of accurate geo-referencing of multi and hyperspectral images are some of the challenges. These challenges together with multiple factors affecting reflectance in flowing water kept remote sensing less exploited technology in sediment monitoring and modelling.

There are much ground-based, space and airborne sensors arranged for earth observation and to gather information on the physical and biological processes occurring within water bodies. Although ocean colour sensors such as the Coastal Zone Colour Scanner (CZCS), the Sea-viewing Wide Field-of-view Sensor (SeaWiFS) have short revisit times with high spectral resolution and sensitivity, the spatial resolution (>1km) is typically too coarse to describe inland water features adequately. Landsat series, Moderate Resolution Imaging Spectroradiometer (MODIS), Advanced Space-borne Thermal Emission and Reflection Radiometer (ASTER), Indian Remote Sensing (IRS), etc. all with different spectral,

radiometric and spatiotemporal resolutions are some of the imageries found potential in providing synoptic water quality data including suspended sediment concentration and modelling other environmental components(Chen et al., 2004).

The Landsat (TM, MSS and ETM) series having 30m spatial resolutions have been applied for different purposes. These types of imageries are relatively with good spatial resolution and have advantages for historic analysis. The advantages of Landsat sensors over other sensors are coverage of long-time series starting from the 1970s onward and its free accessibility. The spectral and radiometric resolutions of the Landsat series have also substantial importance in predicting suspended sediment transportation and sedimentation (Liu et al., 2003). As a result, many researchers have used it for monitoring sediment concentrations in different water systems (Doxaran et al., 2003: R^2 =0.88; Ma and Dai. 2005: R^2=0.91; Islam et al., 2003: R^2 = 0.83; Wang et al., 2009: R^2 = 0.88). Apart from this direct application, the Landsat series can be used to drive the C-factor using different techniques (Alejandro &Omasa, 2007; De Asis et al., 2008). If the range of suspended sediments is between 0 and 50 mg/l, reflectance from almost any wavelength will be significantly related to suspended sediment concentrations linearly (Ritchie and Cooper, 1988; Ritchie et al., 1990). As the range of suspended sediments increases to 200 mg/l or higher, curvilinear relations must be developed with reflectance in the longer wavelength (Ritchie and Schiebe 2000). But, the temporal resolution of these imageries is too coarse (15 days) to handle the fine temporal variability. The revisiting time of Landsat series is too long to see daily and hourly changes.

Moderate Resolution Imaging Spectroradiometer (MODIS) with 250 – 1000m spatial resolution are more commonly used in surface water quality studies and reservoir sedimentation assessment. MODIS is a key instrument viewing the entire earth's surface in each one to two days. It offers near-daily global coverage acquiring data in 36 spectral bands and 250m spatial resolution covering wavelength from 400 to 14400nm. MODIS has been applied to see the suspended sediment concentration of Rivers (Wang and Lu, 2010). Essayas et al., (2014) has also applied it and found effective in predicting the historic trend of suspended sediments in Lake Tana, Ethiopia. But, the retrieval of reflectance from the River surface using MODIS data is hampered by the low spatial resolution which may result in few pure (none mixed) water pixels depending on the River width and image acquisition geometry. Mixing of spectral from different objects (vegetation, water and land) in single pixel is a challenging issue in Rivers (Villar et al., 2012).

There are also grounds borne sensors of reflectance from objects. They are very important to develop a scientific understanding of signal-object and signal-sensor interactions. These studies, at a laboratory or field levels, help in the design and development of for the identification and characterization of the characteristic land surface features. One major ground-based remote sensing instrument is spectroradiometer. It has been applied in a quality monitoring (suspended sediment concentration, phytoplankton and total solid substrates) of coastal and inland water resources. The advantage of these ground based remote sensing instrument over the space and air based remote sensing is that the fineness of in its spatial resolution. Moreover, unless the cost challenging, one can increase the temporal resolution of the measurement by ground remote sensing instruments as he\she

likes to make it frequent. However, its application to the suspended sediment concentration monitoring still needs further detail analysis beyond the resolution of the instrument might has.

2.3 Remote sensing for extracting turbid River water from land

The application of remote sensing for River water studies depends on the difference of the optical remote sensing properties of pure water bodies and other impurities. Water absorbs most of the energy in the near-infrared and middle-infrared wavelengths, whereas other surface materials have a higher reflectance in these wavelengths. But due to the inpurities (E.g. SSCs) in the water and hetrogenities in most rivers are at finer scale than the resolution of most sensors, applying remote become complicated. To date, various water body extraction algorithms for optical imagery have been developed, and they can be categorized into five basic types: (1) hard classification (Hung and Wu, 2005; Tulbure and Broich, 2013); (2) single-band thresh holding (Jain et al., 2005; Xu., 2006); (3) spectral water indexes (Feyisa et al., 2014; Xie et al., 2014; Yang et al., 2015) ; (4) spectral unmixing (Ghrefat, and Goodell., 2011; Hommersom et al., 2011; Guo et al., 2015); and (5) automatic subpixel water mapping method (ASWM; Huan et al., 2019). The first three techniques have their own respective advantage to splicity and precision. However, these methods can only obtain water maps at the pixel level, which may not meet the precise requirements of the practical applications in small and narrow river systems. The spectral mixture analysis (SMA) and automatic subpixel water mapping method (ASWM) can be used for water mapping at sub-pixel resolution and for the post-sub-pixel mapping process (Wang et al., 2015).

The typical processes of SMA consist of two steps—endmember determination and abundance estimation (Shi and Wang, 2014) and for each step, prior knowledge or manual intervention is usually required (Li and Zhang, 2011; Somers et al., 2011; Zare et al., 2013). As all the land-cover types are usually involved in a SMA analysis, this is too complicated when the turbid water is the only land-cover type of concern. Several previous studies have simplified the SMA process for subpixel water mapping, e.g., Sun et al. (2011), and Ma et al. (2014) proposed subpixel water mapping methods based on MODIS 250m data using a linear mixture model, and Pardo-Pascualetal. Hung and Wu, (2005) used the single-band intensity gradient to determine the shoreline position at a subpixel precision. Sethre et al. (2005) applied the IMAGINE Subpixel Classifier to detect subpixel-scale ponds. Even though several sub pixel-level water body extraction methods have been proposed in the literature, none of them have considered extracting turbid water from land features. In the highly erosion risk river basins, an extremely turbid flash flood having confused optical properties distributed sparsely in a subpixel-scale size. In such pixels, both reflectance from macroscopically (E.g. land features and turbid water) and microscopicall (E.g. water, sediment, organic matter etc.) pure components are mixed. Consequently, the obvious water extraction remote sensing methods often fail to distinguish the narrow rivers with turbid water and estimate sediment concentration in the turbid water. The wider surface areas having low albedo surfaces and terain shadows, which are easily confused with the water bodies in a mountainous river basin (E.g. Tekeze basin), also bring a big challenge to apply it.

2.4 Mitigating excess sediment yield

There are different land management intervention approaches including the physical soil and water conservation, biological conservation and integration of the two. The effectiveness of these conservation measures is not equal everywhere. Their efficiency to mitigating sediment yield and the cost they required varies spatially (Amare et al., 2014). Accordingly, different models have been introduced to test their efficiency before they come into practice.

In Ethiopia, the efforts of soil and water conservations have hardly supported with proper planning and designing. There are some applications of models to simulate effects of soil and water conservation practices at a plot, field and basin-scale (Descheemaeker et al., 2006; Gebremichael et al., 2005; Chekol et al., 2007; Betrie et al., 2011). The researches by Kassawmar et al., (2018), Descheemaeker et al., (2006) and Gebremichael et al. (2005) showed that a considerable sediment reduction by reforestation and stone bunds at a field scale respectively. Chekol et al., (2007) found that simulation using parallel terraces with the reduction of slope length by 75% gave the highest reduction in sediment yield from upper Awash basin. Betrie et al., (2011) also showed that applying filter strips, stone bunds and reforestation scenarios can reduce sediment yields both at the sub basins and basin outlets of Blue Nile. These studies have indicated the effectiveness of sediment management types to minimize soil erosion and then sediment yield depends on the actual physical and socioeconomic conditions of the river basin. However, there are fewer literaturesstudying the effects of mitigation measures at a large scale.

2.5 Summary

Sediment transportation and deposition is the major River basin problem causing significant loss of land productivity, environment and remained the main challenge of surface water development throughout the globe. Due to the spatiotemporal variability of the driving factors (eg. climate and land-use dynamics) sediment transportation is a quite complex parameter of water resources developments. Literatures implied that the sediment transportation problem and its linkage with spatiotemporal variability of climate and land use are inadequately modelled. Even there is an argument that the acute problems of sediment transportation and deposition are related to lack of detail understanding on abundance, nature and its relationship with driving factors due to the absence of cost-effective and accurate sediment monitoring and modelling technology. Consequently, there is a need for further researches to advance the sediment monitoring and modelling techniques. This paper summarized the current development in using remote sensing monitoring and modelling techniques to quantify SSC, especially for Rivers.

Though it is at sporadic level, the conventional monitoring systems (in-situ sampling followed by laboratory analysis) have been widely applied. This monitoring system lacks spatial and temporal variability of sediment transportation and is a costly long process. Recently, instead of the conventionalin-situmonitoring system; the remote sensing technology, physically distributed models (eg. SWAT), and their integrations have been widely employed in mapping and monitoring sediments. The advances seen in satellite technology, sensory, image acquisition and processing, and data accessibility have drawn

much attention in using remote sensing approach for enhancing decision supporting system of sediment management.

The application of remote sensing in sediment concentration monitoring and modelling mainly lays either on direct estimation of the concentration and/or indirectly on modelling the driving parameters and then complementing other hydrologic models. The SSC of River systems, a critical parameter for water resources and energy development, has been monitored using the various visible and NIR bands of satellite imageries directly. Apart from the direct application of remote sensing for monitoring sediment concentration and other constituents in River systems, the technology can also be used in modelling the factors that can affect the rate and pattern of sediment transportation and deposition in the Rivers and reservoirs. Even though remote sensing technology is potential to provide insight into time long and wider spatial scale information, it is not without delimitations. The spatial, temporal and spectral resolutions of most sensors are too coarser to capture the variabilities in the hydrologic processes. The ground and space plated sensors provide mixed reflectance values at a specific area of place (pixel), time and spectral resolutions. The spatial pixel sizes of most remote sensors are often large enough that numerous disparate substances can contribute to the spectrum measured from a single pixel. Hence, the accuracy of remote sensing technology in modelling and monitoring the hydrologic processes and driving parameters is affected by the approaches of the analysis used. Conventionally, classification and regression/correlations analysis of the spectrum in a pixel and the targeted variable has been the common approach of using remote sensing technology for modelling and monitoring the hydrologic processes and driving factors. This

might present general knowledge about the targeted variable. But it may not yield any further insight into the other substances that might also reside within and around boundaries of the pixel.

Consequently, the desire to extract from a spectrum the constituent materials in the mixture, as well as the proportions in which they appear, is important to numerous tactical scenarios in which sub-pixel detail is valuable. Spectral Unmixing (SU), decomposing remote sensed electromagnetic spectra into a combination of spectrally pure (endmembers) signatures weighted, is becoming a promising technique developed by the efforts of earth and planetary scientists. SU can be used for analysing multi and hipper spectral data collected from space, air and ground plated sensors. It provides a comprehensive and quantitative mapping of the elementary materials that are present in the acquired data. More precisely, SU can identify the spectral signatures of these materials (usually called endmembers) and can estimate their relative contributions (or abundances) to the measured spectra. Both linear and nonlinear approach can be applied for unmixing the reflectance signature of surface objects. Unlike the nonlinear one, the linear approach is the quick and easy way of spectral unmixing technique. The spectral unmixing analysis, especially the linear which considers a given pixel/reflectance value as a linear combination of primary components (endmembers) is advantageous for maximizing the use of remote sensing for modelling and monitoring hydrologic variables.

The SWAT is the most popular semi-distributed hydrologic model for understanding spatiotemporal variability of sediment yield of large River basins. At the same time, it has also multiple potential problems. The SWAT parameter setups specifically the vegetation

parameter of soil erosion and sediment (C-factor) database included in SWAT consists of empirical values from long-term experiments in the United States, which may not be applicable to other countries due to differences in vegetation systems and management practices. The spatial representation of C-factors has been considered at land-use level, which results constant C-factor values within a large land-use area and lack ability to reflect the effect of spatial variation of vegetation on soil losses. Despite these problems of SWAT, none of the researches in Ethiopia was made internal calibration points or other spatially distributed data sources (e.g. remote sensing data). As to the researcher knowledge, none of the studies in Ethiopia has used locally adapted vegetation parameters nor did any of the studies to consider vegetation dynamics in Ethiopia. It is therefore recommended that to modify the C-factor of SWAT to make it fit-to-observations, fit-to-reality and fit-to-purposes.

CHAPTER THREE:

MATERIALS AND METHODS

This chapter systematically addresses the core components of the research methedology chapter that encompases: Study area description, Data type and source, Method of data acquisition, Model development, Data analysis and model performance evaluation, and General flow chart of the research methods.

3.1 Study area description

3.1.1 Tekeze River basin location

The Tekeze River one the major freshwater resources of Ethiopia is the main tributary of Atbara River, which is, in turn, one of the main tributaries of the Nile. Tekeze River Basin is situated in the north-western part of Ethiopia (Fig. 2) and forms the northernmost part of the Nile Basin within Ethiopia. It consists of three main Rivers Tekeze itself, Angereb and Goange. These River basins join in Sudan and form the Atbara River. The Tekeze headwaters rise at an altitude of 3,500 m.a.s.l from the Meket mountain range near Lalibela and flows north until it turns westward along the Ethio-Eritrean border covering a distance of 600 km until it crosses the Ethio-Sudan border near Humera at an altitude of 550 m.a.s.l. The Tekeze River Basin has an area of 82,350 km^2, covering parts of the Tigray, Afar and Amhara regional states in Ethiopia. It is the second largest tributary of the Nile from Ethiopia and covers about a quarter of the Nile drainage area. This basin stretched from 13^o 21'N, 38^o45' E on its northern part to 11^o34' N 38^o 58'6" E on its southwestern part.

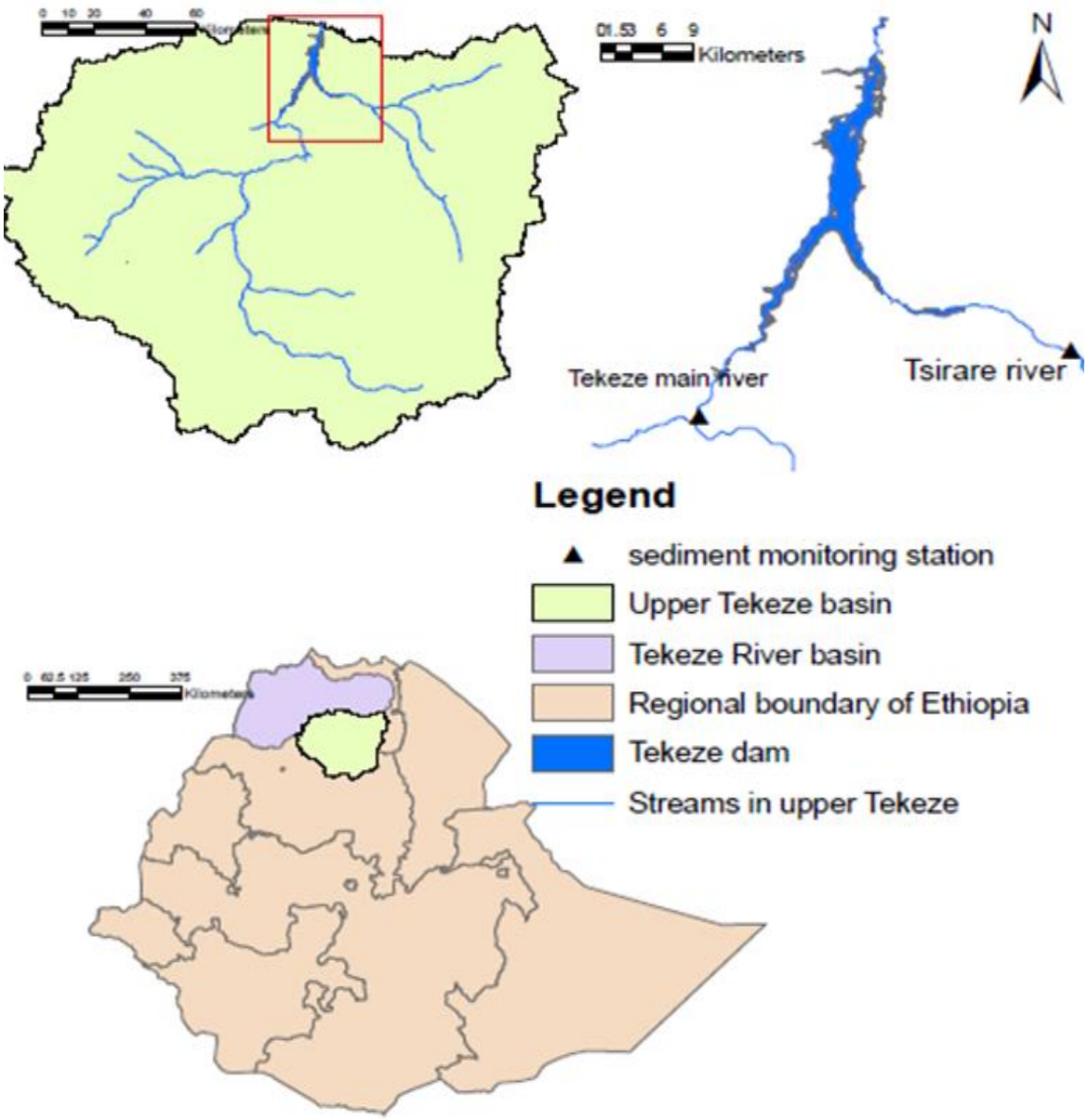

Fig.3: Location and map of upper Tekeze River basin

3.1.2 Topography of Tekeze basin

The basin has extremely variable topography (Appendix 6). The altitude ranges from 500 m in most of the western lowlands to over 4000 m on the Ras Dashen Mountains. Broadly, the basin can be divided into three physiographic regions: the highlands, intermountain valleys

and grabens and the western lowlands. A significant portion (70%) of the basin belongs to the highlands (over 1,500 m amsl) situated west of the Afar Rift. This region is characterised by flat-topped plateaus to undulating topography with intervening large volcanic mountains which form water divides and act as regional groundwater recharge zones. The highlands are deeply cut by major rivers and their tributaries which form deep canyons and gorges with steep and narrow river valleys. These areas have high surface runoff and are characterized by waterfalls and rapids. Along the course of these valleys, there are numerous springs that emanate along the contacts of the different rock units (mainly between the Mesozoic sedimentary rocks and the Trap series volcanics) and talus deposits and hence act as discharge areas. The western lowlands are found in a strip of about 150 km long and 30 to 100 km wide adjacent to the Sudanese border. Here, the elevation varies from 500 m to 1000 m with flat to slightly undulating topography

3.1.3 Climate of Tekeze basin

The Tekeze basin has highly variable rainfall concentrated in one or two rainy seasons separated by relatively long dry seasons. The mean annual rainfall in the Tekeze River basin ranges from 600 mm to over 1200 mm (Belete, 2007). Generally, the altitude-rainfall relation is highly influenced by topography and agroecology niches or micro-climate. The coefficient of variation in annual rainfall for the Tekeze ranges from 20% in the highlands to 40% in eastern lowland (Belete, 2007) which is higher compared to 8% for the whole of Ethiopia. The mean air temperatures in the basin vary from 10°C on the highlands to above 26°c on the lowlands (Belete, 2007). The climatic differences resulted in the classification

of the basin into four traditional agro-ecological zones namely Wurch (very high altitude), Dega (high altitude), Woina Dega (mid altitude) and Kolla (low altitude) (MoWR, 2008).

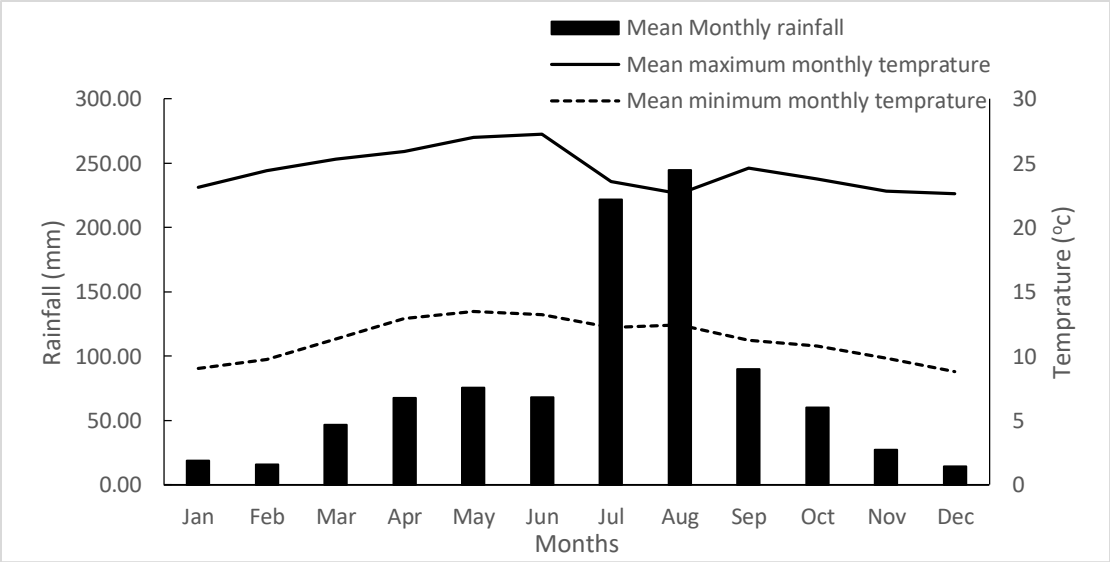

Fig.3*:* Mean monthly rainfall, maximum and minimum temperature records (1967-2016) of the upper Tekeze basin

3.1.4 Hydrology of Tekeze River

The Tekeze River basin together with Abay, Baro-Akobo, and Mereb are part of the Nile River system, flowing generally in the Western direction toward Sudan and terminating in the Mediterranean Sea. The total mean annual flow from the River basin is estimated to be 8.2 BMC. Its water covers 13%, 22% of the Main- Nile flow into Aswan High Dam Reservoir at dry and wet season respectively (Tafesse, 2002; Degefu, 2003; Belete 2007). From January to June, the Atbara Riverbed is almost dry, broken only by pools and ponds (Degefu, 2003). But in late summer, when torrential rains fall on the Ethiopian plateau, the Atbara provides about 20% of the Nile's flow (Zaghloulet al., 2007). The groundwater resource is not so promising except in a few areas.

3.1.5 Soil properties of Tekeze basin

The soils on the basin are EutricVertisols on the level lands; Eutric Leptosols, Eutric Vertisols, Eutric, and Calcic Cambisols and Haplic Luvisols on the sloping lands; EutricLeptosols on the steep lands; and Leptosols on composite landforms. EutricVertisols with soil depths of more than 50 cm are dominant on the level lands while Leptosols are the most common soils on the sloping lands. Moderately deep soils cover less than 5% of the area. Soil type map is presented in Appendix 6.

3.1.6 Land use and other socioeconomic activities in Tekeze basin

The major land use and land cover classes of the basin includes intensively cultivated land (7%), sparsely cultivated (58%), open woodland (12%), open grassland (5%), sparsely vegetated (0.2%), complex land (15%), and others (2.8%) (NEDECO, 1997; Belete, 2007). Most of the climax vegetation of the basin has disappeared and the Afro-alpine and sub-afro-alpine heath vegetation lay between 3700 and 3900 m.a.s.l around Simien Mountains.

3.2 Data type and sources

3.2.1 Input data used

The overall research work demanded the acquisition of reliable data which was crucial for the study. The following shows the major data types used.

1. Daily meteorological data including precipitation, temperature, humidity and solar radiation (observed and estimated)
2. Daily sediment and River discharge data (observed and estimated)
3. Topographic, soil, land use\land cover and other thematic data

4. Remote sensing data including higher temporal and spatial resolution satellite images (landsat7/8 images, and MODIS surface reflectance)
5. Primary data: reflectance, soil loss, suspended sediment load, grain size distribution and land use-land cover

3.2.2 Source of data

1. Due to the poor handling and non-systematic data management in Ethiopia, finding the original data from the data owners is usually difficult. In the case of missing data, other sources (eg. global data) and different data filling techniques (detail is discussed below), were employed. The major data sources of the identified data types are are discussed below.
2. The meteorological data were collected from the national meteorological agency of Ethiopia and to fill the missed data the global data metrology data sources, climate forecast system reanalysis (CFSR,https://globalweather.tamu.edu), were used. The soil property layer, sediment load, River discharge and other secondary data mentioned above were collected from the Ministry of Water Resources, Irrigation and Electricity (MoWIE) of Ethiopia.
3. The satellite images and digital elevation models (DEM) were collected from the United States Geological Survey (USGS, https://www.usgs.gov/earthexplorer).
4. Field survey and laboratory analysis were used to generate the primary data types

3.3 Method of data acquisition

Most of the secondary data were acquired free of charge from the institutions and links listed above and the primary data was from field survey and laboratory analysis. Attempts were done to access needed satellite images from free available web sites. Primary data were collected on the field and laboratory following scientific and standard measuring, sampling and monitoring procedures.

3.3.1 Reflectance of sediment types

The spectral profile variability of sediment solution was tested at laboratory, on-site and from landsat and Moderate-Resolution Imaging Spectroradiometer (MODIS) images. The laboratory and field detection of spectral profiles were carried using a high-resolution ground remote sensing instrument called FieldSpec ®HandHeld2TM Spectro-radiometer (ASD Inc. Boulder, Colorado, USA).The visible (VIS) which is photo-synthetically active radiations including the Blue (400 - 525nm, B_1), Green (526 - 605nm, B_2), Yellow (606 - 655nm, B_3), Red (656 – 750, B_4), as well as the Short Wave Near Infrared (SW-NIR, 750 - 1075nm) categorized in to 750-950nm (B_5) and 951 – 1075nm (B_6) ranges were applied to determine the spectral signature of sediment-laden water both at laboratory and field to each flood occurred during 2017 summer. Images of MODIS codded as MOD09A1 providing an estimate of a surface spectral reflectance at Band 1 through Band 4 corrected for atmospheric conditions were used.

3.3.1.1 Field experiment

The on-site reflectance measurement and sampling of sediment-laden water were done on a carefully selected section of the Rivers including the Tekeze River (12^{o} 48´ 12.99´´N, 38^{o} 36´ 20.14´´E) and Tirare River (13^{o}01´ 6.56´´N 38^{o}54´43.15´´E). To select these locations and sections the less sloppy with minimum turbulence effect, uniformity the flood water in areal distribution and safety to the researcher's life were considered. Moreover, these locations were around rocky and bare land cover types which are characterised with static spectral profile. Parallel to each of the field reflectance measurements, sediment-laden water from the upper 20 cm depth of the flash floods occurred during the 2017 summer (July 2, 2017 – September 3, 2017) in the rivers were sampled to laboratory.

3.3.1.2 Laboratory experiment

Laboratory experiments were carried to characterize the signals from different sediment types and levels of concentration. Processing and detecting spectral signatures were carried out in the soil laboratory at Mekelle University, Ethiopia. To investigate the effect of grain size, colour and level of sediment concentrations on the spectral properties of sediment-laden water, four types of grain size distribution (natural, clay, silt, and sand) and four colours of sediment including light grey (5YR7/1) collected from Tekeze main River, whitish (5YR8/1) collected from main tributary called 'Tsirare', and a reddish yellow (5YR7/5) and grey (5YR6/1) sediments collected from small tributaries were considered. The 5YR7/5 and 5YR7/1 are relatively the extreme red and black in the basin respectively. So, they are represented as red and black sediment types in this research. The levels of

sediment concentration considered in this study were the 2g, 5g, 10g, 15g, 20g, 25g, 30g, 40g, 50g and 60g each in 1liter of distilled water. The natural grain size distributions of the sediment types sampled to the laboratory were presented in table 3.

Table 3: Physical properties of the sampled sediment

Sediment type	Color	Grain size composition (%)		
		Clay (<0:002mm)	Silt (0:002 - 0:05mm)	Sand (>0:05mm)
Black sediment	5YR6/1	61.58	14.67	23.75
Red sediment	5YR7/5	56.89	19.01	24.1
Tsirare River sediment	5YR8/1	59.56	15.32	25.13
Main River's sediment	5YR7/1	58.55	18.03	23.42

Sediment-laden water from the upper 20 cm depth and spectral reflectance of the floods occurred during the 2017 summer (July 2, 2017 – September 3, 2017) in the main River and Tsirare River were continuously sampled and monitored simultaneously. The suspended sediment concentration in each of those flash floods was determined following the conventional approach. The sediments were pre-processed following four steps: (1) drying in air and pulverization; (2) filtration by passing through 2mm mesh sieves to remove gravels; (3) mixing with water to filter the tiny residues floating upon the surface of the water, and (4) drying in an oven at 105^{o}C for 12 hours.

3.3.1.3 Ground remote sensing instrument used and organization

The reflectance from the turbed water in laboratory and in the Rivers as well as the reflectance from different land cover types were detected using high-resolution spectro-

radiometer.The scientific name of the ground remote sensnsing instrument used is"*FieldSpec ®HandHeld2TM Spectro-radiometer" developed by* ASD Inc. Boulder, Colorado, USA. The instrument has awarded to the researchers after a strong competition at international level for the *Goetz instrument support program* prepared by the producing company each year.The information is available in the link https://www.malvernpanalytical.com/en/about-us/our-brands/asd-inc/student-support-programs/goetz-instrument-program. The instrument acquires remote sensing data at 1nm intervals, ranging from 325 to 1075nm with a resolution of 1nm and accuracy less than 3nm at 700nm were used. A 5"x 5" spectral reflectance panel which reflects all incoming energies was used as the calibration standard to know incoming energy from the solar system and the artificial source of light. The panel was checked for diffused reflectance nearly 100% of the incident light throughout the spectral range. The wavelength-specific reflectance $R_f(\lambda)$ was computed using the following formula (Eq.11)

$$R_f(\boldsymbol{\lambda}) = \frac{\mathbf{R_{rad}(\lambda)}}{\mathbf{R_p(\lambda)}} \mathbf{C_{al}(\lambda)} \mathbf{(Eq.11)}$$

Where $R_f(\lambda)$ is the wavelength specific reflectance, $R_{rad}(\lambda)$ is the wavelength-specific radiance from the sediment solution surface, for each sample, which is measured by the spectro-radiometer three times. $R_p(\lambda)$ is a white reference that is collected by putting the reference panel above the water surface. The white reference was updated before each measurement of the water sample. C_{al} (λ) is the calibration factor for the reflectance panel that comes with the product.

The measurements were repeated three times and the averages were used in the calculation. To have known amount and source of energy all laboratory measurements were carried at night.Two 500W halogen lamps organized at 45^{o} to the sample in the two directions, the spectro-radiometer was arranged at 90^{o} to the sample, 1 litter volume cylinder painted with black colour and laptop connected using a USB cable with the spectro-radiometer were organized.

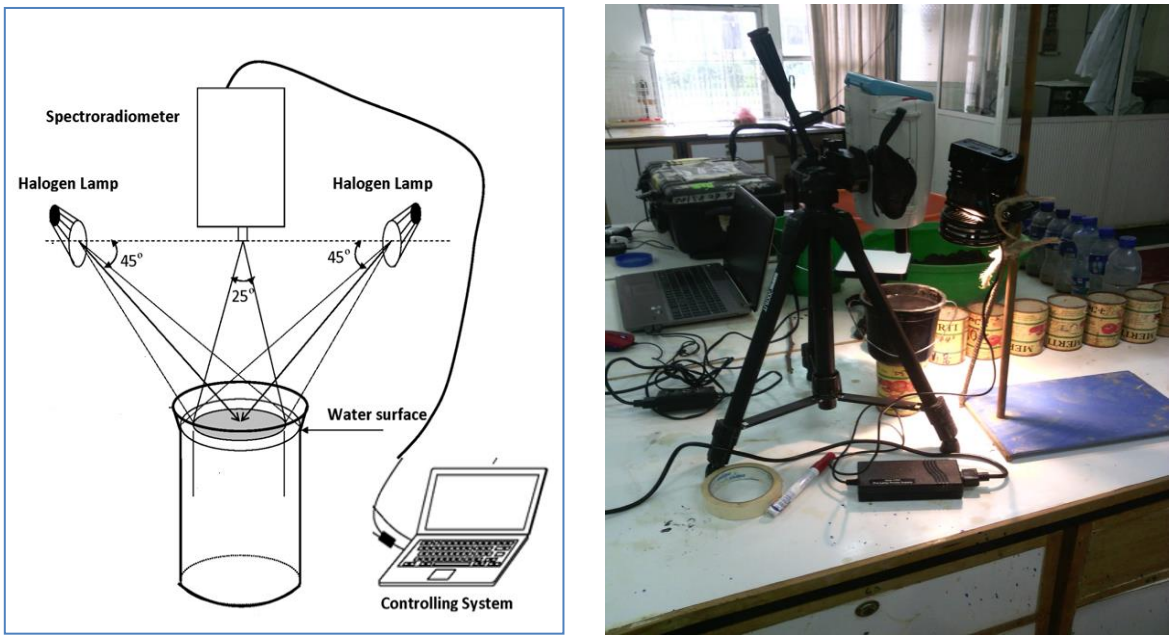

(a) (b)

Fig 4. The organization of spectroradiometer (a) and photo in the laboratory (b)

3.3.1.4 Processing imageries

Moderate-Resolution Imaging Spectroradiometer (MODIS) codded as MOD09A1 Version 6 product providing an estimate of the surface spectral reflectance corrected for atmospheric conditions were used. The surface reflectance images during 2017's summer

months including the June, July, August and September were considered. The images dated on these months which look free of cloud cover around the Tekeze dam were freely downloaded from https://earthexplorer.usgs.gov. In this research, the wavelength ranging 459-876nm which designated as Layer 1 (620 - 670), Layer 2 (841- 876), Layer 3 (459 - 479) and Layer 4 (545 - 565) were processed. For convenience and to fit the naming used in our field and laboratory experiments, we have replaced the above default name by Band 1 (459 - 479), Band 2 (545 - 565), Band 3 (620 - 670) and Band 5 (841 - 876). Geometric correction and geo-referencing of each image at the world geodetic system 84 (WGS 84) and Universal Transversal Mercator (UTM) was carried out using four (4) easily identified ground control points (i.e River intersections and Tekeze dam's concrete fill centre). Finally, pixels located at the main River of Tekeze (12^{o} 48´ 12.99´´N, 38^{o} 36´ 20.14´´E) and Tsirare tributary (13^{o} 01´ 6.56´´N 38^{o}54´43.15´´E) from each MODIS image were targeted in this study.

3.3.2 Assessing historic and current sediment loadof Tekeze River

To achieve the designed objectivesa historic and current time series sediment data was needed. Consequently, the historic sediment yield data has collected from the Ethiopian ministry of water, energy and irrigation (MoWEI). The daily River flow and sediment load for the wet seasons during 2004 – 2009 measured at *Embamadre* and dam site gauging stations were used for the model calibration and validation.

3.3.3 Soil map

The soil types of the study area were extracted from the SOIL-FAO database, Food and Agriculture Organization of the United Nations (FAO, 1995). The soil properties (e.g.

particle-size distribution, bulk density, organic carbon content, available water capacity, and saturated hydraulic conductivity) were generated using the Soil Land Inference Model (Zhu et al., 2001). The soil map from Ethiopian Ministry of Water Resource and Irrigation, from harmonized soil map for East Africa, ftp://ftp.soilgrids.org/data/AF/recent at 250m spatial resolution and soil map of FAO were used to prepare needed soil map for upper Tekeze basin.

3.3.4 Meteorological data

Daily precipitation, minimum and maximum daily temperature, solar radiation and wind speed for the study area were collected from the Ethiopian meteorological agency (EMA). This data was complemented and improved using the global climate data at https://globalweather.tamu.edu.Since the meteorological stations in the basin are not adequate and most of them were established recently, the data from EMA was with a lot of missed data and limited parameter. Hence, we have used weather data from global climate data sources. This data was first bias corrected withthe data spatially weighted meteorological observation at 13 stations (Fig.1) from the study and near the study area.

3.3.5 Land use /land cover and C- factor

The major sources of land use/land cover information are satellite images. Two Landsat images, freely available at https://earthexplorer.usgs.gov including enhanced thematic mapper plus (ETM+7) for 2006 & 2010 and the images from Landsat 8 for 2016 scenes covering the study area with paths/rows of 169/51, 169/52, 168/51, 168/52 and 170/51 under less than 10% cloud cover were selected for generating land use classes and estimating the spatial minimum C-factor. Before driving the intended land use/land cover

and C-factor information the Landsat images were passed all needed preprocessing. Atmospheric correction was done using the dark object subtraction algorism (DOS). The pre-processed layers (bands) were stacked, images mosaicking and then sub-setting images only for the study area were done using ENVI 5.1 software. Geometric correction and geo-referencing of each image at the world geodetic system 84 (WGS 84) and Universal Transversal Mercator (UTM) was carried out using four (4) easily identified ground control points (i.e road intersections, Tekeze dam's concrete fill centre and churches). Once all Landsat images get pre-processed, they were used for mapping land use/land cover and C-factor of the upper Tekeze basin which was basic requirements for SWAT set up.

To determine C-factor from the Landsat images, it requires conversion of the digital number (DN) recorded at the sensor to satellite radiance; conversion of satellite radiance to satellite reflectance at the sensor and finally the conversion to ground reflectance by removal of topographic and atmospheric effects. The DN of both Landsat recorded in 8 bits were converted to exo-atmospheric reflectance units as described in the users' handbooks for Landsat 8 (http://www.gsfc.nasa). This involved a conversion from DN to radiance, which took advantage of the LMIN and LMAX (spectral radiances for each band at digital numbers 0 or 1 and 255) values provided in the image metafile and then converting the radiance values to reflectance using the respective formula in the respective users' handbooks.

3.4 Model development

3.4.1 LSUA model from laboratory experiment

To minimize complexity, linear spectral unmixing algorism was selected in this study. In this approach, the mixed reflectance of sediment-laden water at a specific wavelength is the sum of linearly combined reflectance from each primary component. The spectral reflectance of a volume of turbid water can be conceptualized into a composite signal by using the weighted sum of the primary constituents of the water such as clean water, non-phytoplankton suspended sediments, and phytoplankton. Distilled water and dry sediment were the only components of the water sample in this experiment as it was a simulation of flood water. Based on this, the water reflectance at each SSC level was translated to the spectral mixing coefficient of primary water constituents. Accordingly

$$\mathbf{R(\lambda) = SMC_wR_w(\lambda)+ SMCsRs(\lambda)} \qquad \mathbf{(Eq.12)}$$

Where SMC_w and SMCs are Spectral Mixing Coefficients of water and sediment respectively. Rw (λ) and Ps (λ) represented the spectral patterns of clean water and dry sediment. The spectral mixing coefficient for sediment (SMCs) and water (SMCw) in each band and each concentration (SSCs from 2 - 60g/l) were estimated by solving the following equations.

$$R(B_1) = SMCwRw(b1) + SMCsRs(b1) \quad (Eq.13)$$

$$R(B_2) = SMCwRw(b2) + SMCsRs(b2) \quad (Eq.14)$$

$$R(B_3) = SMCwRw(b3) + SMCsRs(b3) \quad (Eq.15)$$

$$R(B_4) = SMCwRw(b4) + SMCsRs(b4) \quad (Eq.16)$$

$$R(B_5) = SMCwRw(b5) + SMCsRs(b5) \quad (Eq.17)$$

$$R(B_6) = SMCwRw(b6) + SMCsRs(b6) \quad (Eq.18)$$

where $R(B_i)$, $Rw(B_i)$, $Rs(B_i)$ (i = 1; 2; 3; 4;5;6) were stood for the reflectance sediment laden water, standard reflectance for clean water, and standard reflectance of dry sediment at the i^{th} band, respectively. The standard clean water and dry sediment reflectance (Fig. 5) in this study were considered the spectro-radiometer based measurement in laboratory for the distilled water and pre-processed soil samples for each soil colours.

3.4.2 Application of LSUA to MODIS terra images

Pixels located at the main River of Tekeze (12^o 48´ 12.99´´N, 38^o 36´ 20.14´´E) and Tsirare tributary (13^o 01´ 6.56´´N 38^o54´43.15´´E) from each MODIS image were targeted in this study. To select these pixels non-changing land cover types (eg. rock, bare soil) around the boundary of the Rivers and to minimize turbulence effects gentle slope of the Rivers were used as criteria. Moreover, these sites were assumed as representative of the higher concentration and variable sediment types in the Tekeze River.

The spatial resolution of the MODIS surface reflectance images was coarse (500m) compared to the width of the Rivers targeted (averagely 60m). The resolution of the image is too coarser to have a pure pixel mad-up of the river section with water flow unless we considered the stagnant water around the dam. Instead, the pixels were made-up of at leastfrom two of the ground cover components (eg. water body, bare soil, rock and vegetated land) existed in the basin. Accordingly, the reflectance of the pixels is supposed

to be a weighted sum of the reflectance from the respective components. Even though the components in pixels can be combined in a nonlinear way based on the physical arrangement of the components on the field (Arai, 2008; Bioucas-Dias et al., 2012; Altmann et al., 2013), for simplicity linear combination of the reflectance has been applied commonly. In such combinations, it was supposed that the reflectance of the mixed pixels at a specific wavelength is the sum of linearly combined reflectance from each primary component.

The reflectance profile of most ground cover components is highly dynamic due the variability of weather and human intervention. Unless these variabilities are carefully managed and addressed, the accuracy of the remote sensing for modelling and monitoring the sediment concentration in Reivers can be hampered. In this study, we have used two pixels carefully selected one from the main River and the second from tributary Tsirare River. The rocky and bare-land ground cover components were mixed with turbid water cover components in the selected pixels of the main and tributary Rivers in the upper Tekeze River, respectively. Moreover, the reflectance from the turbid water component is a result of reflectance interaction from constituents existed in the flowing water. The same as to the assumptions used in the laboratory and field experiment in most research, we have assumed the reflectance from each constituent to be combined linearly constrained to some errors.

Therefore, a new subpixel analysis approach called Double Stage Spectral Unmixing Analysis (DLSUA) was proposed to drive the SSCs from such coarse resolution imageries. In this case, 1st the pixels' reflectance was unmixed into rock/bare-land cover component

and to turbid water reflectance and 2nd the reflectance of the turbid water from step one was further unmixed into the constituents' reflectance. Each of these steps is described mathematically here below.

$$\mathbf{R}_{p} = \mathbf{A}_{\mathbf{rock/bare}}\mathbf{R}_{\mathbf{rock/bare}} + \mathbf{A}_{\mathbf{tw}}\mathbf{R}_{\mathbf{tw}} \pm \mathbf{€i} \;\&\; \mathbf{A}_{\mathbf{rock/bare}} + \mathbf{A}_{\mathbf{tw}} = \mathbf{1} \qquad \textbf{(Eq.19)}$$

Where R_p is the spectral reflectance of the mixed pixel in band i, $A_{rock/bare}$ is the fraction of the pixel area covered by the rock or bare soil, $R_{rock/bare}$ denotes the reflectance of the rock or bare soil in band i, A_{tw} and R_{tw} refers to the area of the pixel covered by the turbid water and reflectance of the pixel contributed by the turbid water respectively, and $€_i$ is the residual error in band i. The residual error '€'refers to the difference between the measured and modelled reflectance values in each band and could be substituted by root mean square error (RMSE), which is useful in assessing the validity of selected cover components.

$$\mathbf{R}_{tw} = \mathbf{SMC}_{\mathbf{w}}\mathbf{R}_{\mathbf{w}} + \mathbf{SMC}_{\mathbf{s}}\,\mathbf{R}_{\mathbf{s}} \qquad \textbf{(Eq.20)}$$

Where R_{tw} is part of the reflectance in the pixel contributed by the turbid water, SMC_w and SMC_s are Spectral Mixing Coefficients of water and sediment respectively. R_w and R_s represented the distinctive spectra of clean water and dry sediment respectively.

Eq.19 was used to unmixed the pixel level reflectance value intocomponent-based reflectance of the selected pixels. And Eq.20 was used to unmixed reflectance of the turbid water into respective constituents' reflectance existed in the water. By substituting Eq. 20 to the reflectance from the turbid water (R_{tw}) in Eq.19 and through rearranging, it can provide the following equation (Eq. 21).

$$SMCs = \frac{R_p - (A_{rock/bare} R_{rock/bare} + A_{tw}\,(SMC_w R_w))}{A_{tw}\ R_s} \pm €i \quad \textbf{(Eq.21)}$$

The relation between the SSCs and their respective Spectral Mixing Coefficient (SMC) values from different sediment types were determined in laboratory experiment and verified in field. The exponential regression equation was found to be the best fit to the relation between SSCs and respective SMCs (Eq.22).

$$\mathbf{SSC = \alpha e^{(\beta(SMCs))}} \quad \textbf{(Eq.22)}$$

Where SSC and SMCs refer to the Suspended Sediment Concentration (g/l) and the Spectral Mixing Coefficients values respectively, 'α' and 'β' are coefficients.

To compute the SSCs from the MODIS surface reflectance for the targeted pixels Eq.21 was substituted to the SMCs in Eq.22. Finally, these computed SSCs values were compared to the observed SSCs at respective dates.

The above DLSUA model was compared with the SSCs estimation performance of the empirical regression model developed in laboratory experiment. A natural logarithmic transformation was used to rearrange into SSC values (Eq. 23).

$$\mathbf{SSC = (\ln (R_p/a))*b} \quad \textbf{(Eq.23)}$$

Where SSC and R_p refers to the suspended sediment concentration (g/l) and the reflectance respectively, 'a' and 'b' were coefficients.

3.4.3 Application of LSUA for estimating C- factor and integration into SWAT

3.4.3.1 LSUA and endmembers selection

Most pixels (smallest land unit sensed) of remotely sensed imageries are composed of mixed spectral information. Landsat 8 is among the images which hold multiple endmembers having different spectral signature mixed in each pixel. This is due to the limitations of the coarse spatial resolution of the satellite instruments and the heterogeneity of features on the ground. Because of this reason, driving information (eg. spatiotemporal vegetation) from such coarse resolution images were less accurate. Such problems are very common especially in arid and semi-arid areas like the Tekeze basin where the vegetation is scarce, and the land is shared among the smallholders cultivating in different systems. Therefore, a subpixel analysis technique called spectral unmixing analysis was proposed to minimize such inaccuracies. Even though the components in pixels can also be combined in nonlinear way based on the physical arrangement on the field (Roberts et al., 1993; Myneni et al., 1995), Linear Spectral Unmixing analysis (LSUA) was chosen in this study due to simplicity. It was applied to estimate components' (endmembers) proportion in the study area. The identification of endmembers, the most important step in the performance of LSUA, was done with the help of frequent field visit and google earth. The spectral value of each endmember for each of the six bands (2-7) of Landsat 8 acquired at the wet season of 2016 was processed using ENVI 5.1. Mathematically it can be represented by

$$F_i = \sum_{j=1}^{n} A_j * S_{eij} + €_i \text{ And } \sum_{j=1}^{n} A_j = 1, 0 \leq A_j \leq 1 \quad \text{(Eq.24)}$$

Where i is the number of spectral bands used, j=1, n (number of end-members), Ri is the spectral reflectance of the mixed pixel in band i, A_j is the fraction of the pixel area covered by the end-member j, F_{eij} denotes the reflectance of the end-member j in band i, and €$_i$ is the residual error in band i. The residual error ′€′refers to the difference between the measured and modeled reflectance values in each band and could be substituted by root mean square error (RMSE), which is useful in assessing the validity of selected endmembers.

$$€ = [\frac{1}{i}\sum_{i=1}^{i}(\mathbf{S_{measured} - S_{modeled}})^{1/2}] \qquad \textbf{(Eq.24)}$$

3.4.3.2 Estimation of the C-factor using LSUA

The C-factor was estimated following the concept that dense vegetation prevents soil particles from displacement by the two water-related factors (raindrop and runoff). Apart from the vegetative cover, ground covers such as surface rocks and water can protect soil from the erosive forces of raindrop and run-off impacts. Therefore, the higher covers from the above factors were considered with low C-factor values. But a soil which is free of any cover was considered with high C-factor values. To estimate the C-factor, the shadow fraction was first removed and the fractions (vegetation, bare soil, water and rock) were rescaled by a normalization factor with the sum of the vegetation (F_{veg}), bare soil (F_{bare}) and rock and/or urban ($F_{rock/urban}$) fractions equal to 1. Finally, the C- factor was computed using

$$\textbf{C-factor} = \frac{F_{bare}}{1+F_{veg}+F_{rock}+F_{water}} \qquad \textbf{(Eq.25)}$$

where, F_{bare}, F_{veg}, F_{rock} and F_{water} are the fractions of bare soil, vegetation, rock and water, respectively.

3.4.3.3 Accuracy assessment using field measurement

The C- factor could be determined directly by the ratio of in-situ measurement of soil loss from vegetated land to that of corresponding bare land soil loss measurements. Accordingly, 40 experimental plots each 2m*2m bounded using flexible corrugated iron were designed on randomly selected four classes of vegetation including cropped, forests, grass and shrub-bush land uses. A plastic container was placed in each plot in a way that the eroded soil from the bounded area can be collected to the containers. Each of those plots was repeated on nearby bare soils having the same driving factors except the vegetation. The measurement of displaced soil had been collected in each weekend and this was continued for the whole wet season in 2016 (June, July, August, and half of September). Finally, C- Factor for each experimental plot was computed using the formula.

$$\textbf{C – Factor} = \frac{E_{veg}}{E_{bare}} \qquad \textbf{(Eq.26)}$$

where, E_{bare} and E_{veg} stands for erosion on bare soil and lands covered by the vegetation. The C-factor values for the locations of the experimental plot from the C factor map generated using the LSUA were considered and compared with the C-factors from the experimental measurement.

3.4.3.4 Integrating spectral unmixinganalysis model into SWAT

SWAT is a time-continuous, semi-distributed, process-based River basin or watershed scale hydrologic model developed to predict the impact of land management practices on water, sediment and chemical yields with varying soils, land use, and management conditions over a long period (Arnold et al., 1998). It simulates hydrology and sediment at the hydrologic responsive units (HRU) by summarizing into sub-basin and then routing through the stream network to the basin outlet (Neitsch et al., 2011).

SWAT divides a basin into sub-basins. Each sub-basin is connected through a stream channel and further each sub-basin is divided into HRU. It is described as a unique combination of soil, land use and slope type in a sub-basin (Arnold et al., 2011). Water and sediment from each HRU are summarized in each sub-basin and then routed through the stream network to the watershed outlet (Neitsch et al., 2005, 2011). SWAT used soil, land use, climate and digital elevation model as input data to predict the sediment load and other processes of River basins over long period of time. The digital elevation model (DEM, 30m), land use map prepared from Landsat images in 2006, soil maps prepared by integrating the soil data from FAO and EMoWIE, and weather data collected from Ethiopian meteorological agency (EMA). The land use type parameters including (leaf area index, maximum stomatal conductance, and maximum root depth, optimal and minimum temperature for plant growth) were based on the default values available in SWAT. The parameterizations of soil types (e.g. particle-size distribution, bulk density, organic carbon content, available water capacity, and saturated hydraulic conductivity) were extracted from the SOIL-FAO database (FAO, 1995). The slopes of the basin were classified into five

classes 0-10, 10-15, 15-30, and 30- 45 and greater than 45% from the digital elevation model of 30m resolution. Finally, the land use, soil type, slope class maps were overlaid to drive the HRUs.

Apart from the above inputs, C-factor is a required parameter of SWAT for modelling sediment yield. Hence, according to the conventional approach, the mean C-factor values have been considered at land use type units and the assignment of a C-factor to an HRU in SWAT was originally determined by assigning the corresponding USLE-C value in 'crop.dat' according to the land use/land cover to which each HRU belongs. This produces a homogenous C factor map, with no/little spatial variation within and among land use type units. In the new approach, the pixel-based values of C- factor was integrated following three steps. 1. In this step, we have identified the spatial location of HRUs using ID code. 2. We have computed the average C-factor for each HRUs from the pixel base values of the C-factor. The C-factor values for each HRU were determined by dividing the sum of the C-factor values for all pixels in an HRU by the number of pixels in the HRU. This process was conducted using the zonal mean function in ArcGIS 10.1 with the remotely sensed C factor map as a value grid input and spatial location map of HRUs as a zonal grid input. 3. Finally, we have modified the source code of sediment routing for each HRUs and assigned the new C-factor values. The improved source codes were compiled with other original source codes and a new executable file SWAT2012.exe was generated for further sediment simulation.

3.4.3.5 Sensitivity analysis, Calibration and validation of SWAT

SWAT has many parameters that make calibration difficult. Hence, the first step in the calibration and validation process in SWAT is the determination of the most sensitive parameters for a given watershed or sub-watershed. The term sensitivity analysis refers to the identification of the most important influencing parameter in the model. Sensitivity analysis is important from two points of view: First, parameters represent processes, and sensitivity analysis provides information on the most important processes in the study region. Second, sensitivity analysis helps to decrease the number of parameters in the calibration procedure by eliminating the parameters identified as not sensitive. One-at-a-time (OAT) or local sensitivity analysis, and all-at-a-time (AAT) or global sensitivity analysis algorithms can be used. In OAT, all parameters are held constant while changing one to identify its effect on some model output or objective function. In this case, only a few model runs are usually enough. In the AAT, however, all parameters are changing; hence, a larger number of runs are needed in order to see the impact of each parameter on the objective function. In the current study, the OAT algorithm was selected for minimizing complexity. OAT uses directly compare the impact of three to five parameter values on the output signal, whereas AAT uses a multiple regression approach to quantify sensitivity of each parameter. The sensitive parameters of sediment transport in the upper Tekeze basin are tabulated in Appendix 7.

Model calibration is an effort to better parameterize a model to a given set of local conditions, thereby reducing the prediction uncertainty. Model calibration is performed by carefully selecting values for model input parameters (within their respective uncertainty

ranges) by comparing model predictions (output) for a given set of assumed conditions with observed data for the same conditions (Arnold et al., 2012). Model validation is the process of demonstrating that a given site-specific model can make sufficiently accurate predictions. This implies the application of the calibrated model without changing the parameter values that were set during the calibration, when simulating the response for a period other than the calibration period. The model calibration and validation process were conducted by using the SUFI2 (Sequential Uncertainty Fitting Version 2 programme) in SWAT- CUP. The SWAT-CUP is a computer programme for automatic calibration of SWAT models. The programme links SUFI2 procedures to SWAT.

3.4.4 Evaluating trend of climate change and sediment yield

Identifying the trends and linkages between basic climatic variables (precipitation and temperature) and sediment yield is fundamental to understand the influence of climate change on soil erosion and sediment transportation of a basin. The daily precipitation, maximum and minimum temperatures were considered in this study. These data were provided by the Ethiopian National Meteorological Service Agency. Visual inspection, linear and multiple regression analyses between neighbouring stations and other global datasets (eg. CFSR) were applied for data analyses and validation, detecting outliers, filling missing values and checking reliability for all gauging stations. The homogeneity and trend of sediment concentrations in the upper Tekeze basin in the year 2004 through 2017 simulated using the modified SWAT at the annual and seasonal time scale were evaluated using Petit and MK tests, respectively.

3.4.5 Testing different sediment yield mitigating scenarios for upper Tekeze basin

Sustainable basin's sediment management intervention involves introducing Best Soil and Water Management Practices (BSMPs). There are multiple BSMPs that have different potential of soil erosion and sediment transport reducing capability. The list of scenarios described in table 5 was used in this study.

Table 4: Describing the scenarios and LSUA-SWAT's parameters used

Scenarios	**Description**	**SWAT parameter used**		
		Parameter	Calibration value	Modified value
Scenario-0	Existing condition as obvious	USLE_C	HRU based	HRUs based
Scenario-1	Filter striping cultivation	FILTERW(.hr	0	1
Scenario-2	Integrating filter strip cultivation on agricultural land and stone bund/ terracing on non-agricultural land	SLSUBBSN (.hru)	It was varied through 9.1, 24 and 61m as slope varies to 0-10, 10-20 and >20%	10m for all slope class was used
		CN2(.mgt)		
		USLE_P(.mgt)	81	59
			1	1
Scenario -3	Parallel Terraces/stone bunds: Assume the slope length is reduced by 50%.			
Scenario-4	Integrating Parallel Terraces/stone bunds and Reforestation: The stone bund/terracing was for the land units below 30% slope			
Scenario-5	Reforestation:	-	-	-

The scenarios simulated and representations of the soil and water management in the LSUA-SWAT are depicted in table 3. In Scenario 0, the basin's existing conditions were considered. In scenario 1, it was assumed as filter strips were placed on all agricultural HRUs that are the combination of croplands, all soil types and in all slope classes. The effects of the filter strip were to filter the runoff and trap the sediment in a given plot

(Bracmort et al., 2006). The appropriate model parameter for the representation of the effect of filter strips was the width of the filter strip (FILTERW). FILTERW value of 1m was assigned to simulate the impact of filter strips on sediment trapping. This value was modified by editing the HRU (.hru) input table. The filter width value was assigned based on local research experience in the Ethiopian highlands (Hurni, 1985; Betrie et al., 2011).

In scenario 2, integrating filter strip cultivation on agricultural land and stone bund/ terracing on nonagricultural land was considered. In this scenario, the land mass of the upper Tekeze basin was classified into two classes based on slope. The first one was all HRUs having a slope of less than 30% and the second one was all HRUs having 30% and/or more slope class. Accordingly, we have introduced a strip cropping system to the first class and stone bund/parallel terracing into the later one.

In scenario 3, placing stone bund/parallel terracing in all HRUs was assumed. Placing stone bund/parallel terracing has a function to reduce overland flow, sheet erosion and reduce slope length (Bracmort et al., 2006; Betrie et al., 2011). Appropriate parameters for representing the effect of stone bunds were the Curve Number (CN2), average slope length (SLSUBBSN) and the USLE support practice factor (USLE_P). We modified slope length (SLSSUBSN) value by editing the HRU (.hru) input table, whereas USLE_P and CN2 values were modified by editing the Management (.mgt) input table. The SWAT model assigns the SLSUBBSN parameter values based on the slope classes. In this application, the SWAT assigned values were 61m, 24m and 9.1m for slope classes 0–10%, 10–30%, and over 30% respectively. But it was modified to 10m for below 30% slope classes and 9m for above 30 %. The USLE_P and CN2 were modified to 0.32 and 59 respectively.

In scenario 4, we simulated the impact of integrated sediment management (stone bund and reforestation). That is HRUs having below 30% to be with stone bunds and HRUs sloped 30% and above to have reforestation practices.

In scenario 5, we simulated the impact of reforestation by introducing it into non-agricultural HRUs. The reforestation has a function to reduce overland flow and rainfall erosivity and these effects were simulated by introducing land use change, not by parameters changes. It seems impractical to change agricultural land into the forest completely. Thus, we use the nonagricultural HRUs only. The parameters (e.g., plant, hydrological and erosion) related to the dry land forestation were modified from the database.

3.5 Data analysis and model performance evaluation

3.5.1 LSUA and empirical models for estimating SSC

The Pearson correlation coefficient (R_s) in R software was used to determine the statistical dependence between the two variables (between SSC and reflectance in our case). The correlation was tested between the reflectance of soil colours (black, red and intermediates) in 10 SSC levels (2-60g/l) and the six simulated bands including band one (B_1, 400 - 525 nm), band two (B_2, 526 - 605 nm), band three (B_3, 606 - 655 nm), band four (B_4, 656 – 750), as well as the Short Wave Near Infrared (SW-NIR, 750 - 1075 nm) categorized in to band five (B_5, 750-950nm) and band six (B_6, 951 – 1075nm). The performance of the generated models in simulating the SSCs in the upper Tekeze River reaches was evaluated

using the coefficient of determination (R) and root mean square error (RMSE) that is a model with higher R but lower RMSE were considered as well performing model.

3.5.2 Evaluating performance of LSUA integrated SWAT

Performance of conventional and modified SWAT model was evaluated using the Nash-Sutcliffe coefficient (NSE, Nash and Sutcliff, 1970), Coefficient of determination (R^2), root mean square of error- observations standard deviation ratio (RSR) and percent bias (PBIAS). The equations for each performance indicators are given from equation 28-32.

$$\boldsymbol{R} = \frac{\sum_{i=1}^{n}(X_i - X)(Y_i - Y)}{\sqrt{\sum_{i=1}^{n}(X_i - X)^2}\sqrt{\sum_{i}^{n}(Y_i - Y)^2}} \quad \text{(Eq.27)}$$

$$\boldsymbol{RSR} = \frac{\sqrt{\frac{\sum_{i=1}^{n}(X_i - Y_i)^2}{n}}}{\sqrt{\frac{\sum_{i=1}^{n}(Y_i - Y)^2}{n}}} \quad \text{(Eq.28)}$$

$$\boldsymbol{NSE} = \mathbf{1} - \frac{\sum_{i=1}^{n}(X_i - Y_i)^2}{\sum_{i=1}^{n}(X_i - X)^2} \quad \text{(Eq.29)}$$

$$\boldsymbol{PBIAS} = \frac{\sum_{i=1}^{n}(X_i - Y_i) * \mathbf{100}^*}{\sum_{i=1}^{n}(X_i{}^1)} \quad \text{(Eq.30)}$$

$$\boldsymbol{RMSE} = \sqrt{\frac{\sum_{i=1}^{n}(X_i - Y_i)^2}{n}} \quad \text{(Eq.31)}$$

Where R, RSR, PBIAS and NSE is coefficient of determination, Nash-Sutcliffe coefficient and root mean square error- observations standard deviation ratio respectively, X_i is observed value and Y_i is simulated values and X and Y are the means for the observed and simulated value respectively.

The Nash–Sutcliffe efficiency coefficient (NSE) ranges between −∞ and 1. It indicates a perfect match between observed and predicted values when NSE = 1). Values between 0.0 and 1.0 are generally viewed as acceptable levels of performance, whereas values less than 0.0 indicate that the mean observed value is better than the simulated value, which indicates unacceptable performance. Percent bias (PBIAS) measures the average tendency of the simulated data to be larger or smaller than their observed counterparts. Low magnitudes of PBIAS indicate accurate model simulation. Positive values indicate model underestimation bias, and negative values indicate model overestimation bias.

3.5.3 Trend of climate and sediment yield change

The long-term trends of the climate variables (precipitation and temperature) and the simulated sediment fluxes and their relation were analysed using the Mann–Kendall (MK) and correlation analysis techniques. The research generated a historic reanalysis of major climate variables and its effects on sediment flux.

Mann-Kendall test is used for the detection of a statistically significant trend in variables like rainfall and temperature. The Mann-Kendall (MK) trend test was used because it is simple, robust, can cope with missing values, and the data need not conform to any distribution (MK; Mann, 1945; Kendal, 1975). This method is very essential as it has no assumption made in the data to be tested. The Mann–Kendall test, is a rank based method that has been widely used to detect the trend of hydro-climatic time series data in different parts of the world (e.g. Abdul Aziz & Burn, 2006; Jones et al., 2015; Wang et al., 2015; Gebremicael et al., 2017). The procedure of MK testing starts by calculating the MK statistic (Yue et al., 2002).

Using the XLSTAT 2013 plug-in of Microsoft Excel, the monthly percentage contributions of rainfall over the years were subjected to the MK trend test shown in Eq. (33)

$$S = \sum_{k=1}^{n=1} \sum_{J=k+1} Sign\ (X_j - X_k) \text{Where}$$

$$\text{Sign } (\theta) = \begin{bmatrix} +\mathbf{1} \\ \mathbf{0} \\ -\mathbf{1} \end{bmatrix} \boldsymbol{if} \begin{bmatrix} \theta > \mathbf{0} \\ \theta = \mathbf{0} \\ \theta < \mathbf{0} \end{bmatrix} \text{(Eq. 32)}$$

Where S is the Mann-Kendall statistic. X_j and X_k are the data values in time j and k, respectively, j > k, and n is the length of dataset. The normalized test statistics Z of the MK test and the variance V(S) were calculated as shown in Eqs. (34) and (35).

$$Z = \begin{cases} \frac{\mathbf{S-1}}{\sqrt{\mathbf{V(S)}}} \\ \mathbf{0} \\ \frac{\boldsymbol{S+1}}{\sqrt{\boldsymbol{V(S)}}} \end{cases} \quad \boldsymbol{if} \quad \begin{vmatrix} \boldsymbol{S > 0} \\ \boldsymbol{S = 0} \\ \boldsymbol{S < 0} \end{vmatrix} \text{(Eq.33)}$$

$$V(S) = \frac{\mathbf{1}}{\mathbf{18}} \left[\boldsymbol{n}(\boldsymbol{n}-\mathbf{1})(\mathbf{2}\boldsymbol{n}+\mathbf{5})\right] \text{ (Eq. 34)}$$

where S and V (S) are the Kendall's statistics and variance, respectively. The MK test calculates Kendall's statistics S, which is the sum of the difference between data points and a measure of associations between two samples (Kendall's τ) given by Eq. 36

$$\tau = \frac{2S}{n(n-1)} \text{ (Eq. 35)}$$

Positive and negative values of those parameters (z and s) indicate an "upward trend" and "downward trend", respectively. In order to evaluate the trend results, the Z value combined with the computed two-tailed probability (P) were compared with the user-

defined confidence level (5 %) of the standard normal distribution curve.Pettitt test (Pettit, 1979) is an approximation for a sequence of random variables of the non-parametric method, has been used in this study and helps to indicate where possible change points are. The Pettitt test only detects the time of a change point, but a t-test was always applied to check the significance of the trend. A significance level of 5% has been applied in this study. The approximate significance probability (P) for a change point is defined by Eq. (6):

$$P= \mathbf{1- \rho} \quad \text{(Eq. 36)}$$

Where P is the probability of detecting the point of change and ρ is the existence of significant change point. The ρ -value (two-tailed) has been computed in this study using XLSTAT software with 10,000 Monte Carlo simulations at 99% confidence interval for checking the data homogeneity.

The homogeneity and trend of sediment concentrations in the upper Tekeze basin in the year 2004 through 2017 simulated using the modified SWAT at the annual and seasonal time scale were evaluated using Petit and MK tests, respectively.

3.5.4 Evaluating sediment management scenarios efficiency

The performance of the LSUA-SWAT model was evaluated using Nash-Sutcliffe Efficiency (NSE), Coefficient of determination (R^2), Root Mean Square of Error-Observations Standard Deviation Ratio (RSR) and Percent Bias (PBIAS). The mathematical operations for each statistical tool are presented in section 3.5.2. The scenarios were evaluated based on their capacity to minimize daily sediment yield at the

outlet of the upper Tekeze basin. The scenario which gives minimum sediment yield at the out of upper Tekeze basin was considered as best sediment management scenario in the study area.

3.6 General flow chart of the research methods

This study was focused on the potential of remote sensing in monitoring suspended sediment concentration of Rivers and in determining the vegetation dynamics effect on sediment yield (C factor). The linear spectral unmixing approach of remote sensing was applied in this study. The study used reliability checked and organized data from sediment laboratory (sediment concentration, sediment yield, sediment texture and spectral reflectance of sediment-water), Pre-processed remote sensing data (Landsat 7&8, MODIS, DEM), and historic real hydrological and meteorological data (Streamflow, sediment yield, precipitation and temperature). The steps of the approaches used in this study are depicted in the flow chart (Figure 4). The result and discussion part focused on (1) the identification of effective spectral bands and affecting factors, comparing empirical and LSUA models in simulating SSCs using on-field reflectance and MODIS surface reflectance data. (2) Evaluating the temporal and spatial variability of C factors using a remote sensing approach. (3) Integrating the spatial C-factor into SWAT and testing its efficiency in simulating sediment yield in the study area. (4) Analysing the trend of climate change (precipitation and temperature) in upper Tekeze basin and its relationship with sediment yield and (5) testing the sensitivity of upper Tekeze basin sediment yield to different sediment transporting mitigating scenarios.

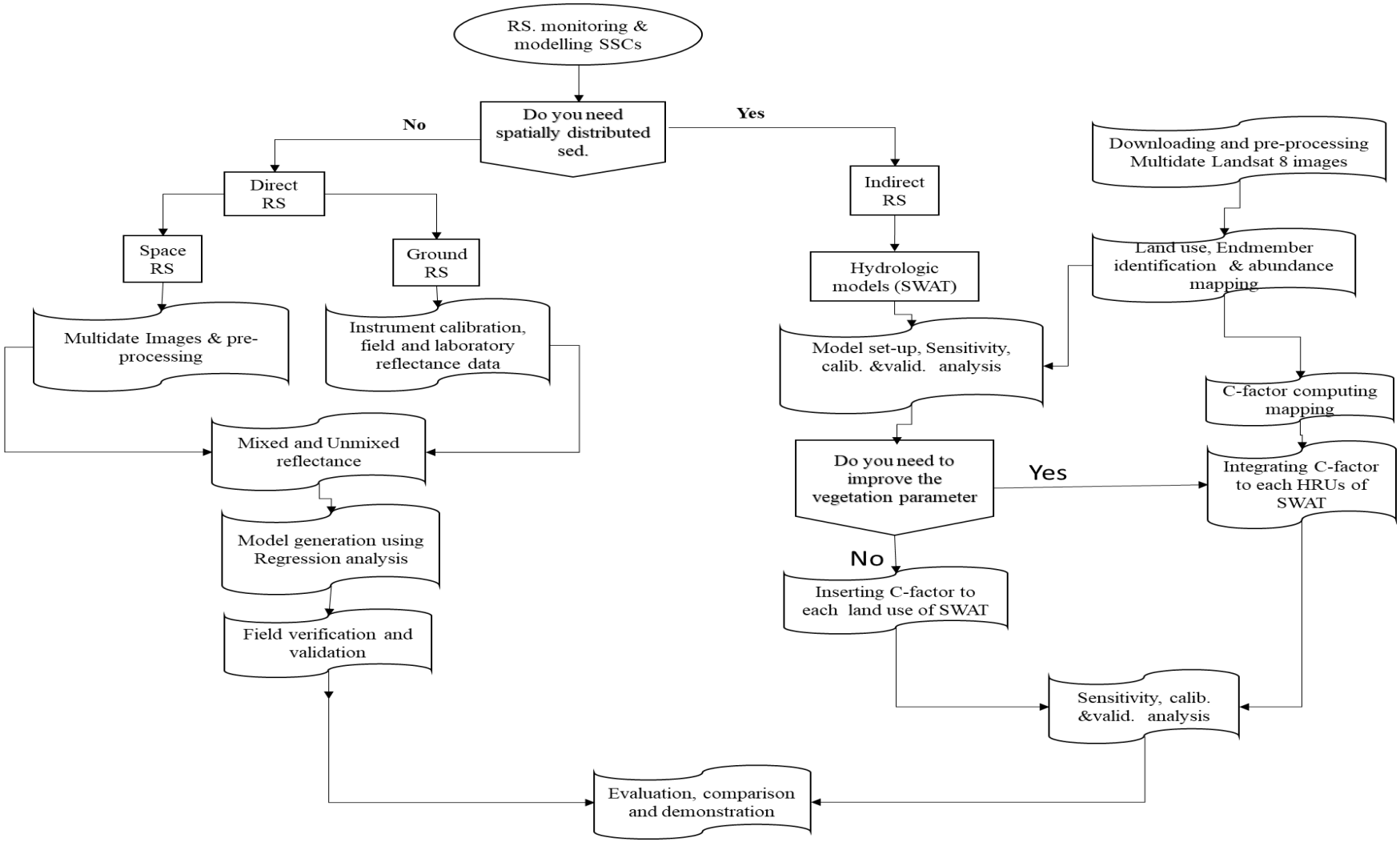

Fig. 5: Flow chart of the research methods

CHAPTER FOUR:
RESULTS

This section holds the results related to the direct and indirect application of linear spectral unmixing remote sensing technology for estimating sediment load in the Tekeze River system. Results related to the application of LSUA for direct estimation of suspended sediment concentration and comparative analysis with empirical remote sensing, integration of LSUA model with SWAT for mapping sediment yield and application of LSUA integrated SWAT for evaluating effect of climate change on sediment yield and comparative analysis on the best sediment management scenarios are presented in this section.

4.1. Spectral properties and modelling SSCs using remote sensing in laboratory

4.1.1 Spectralsignatures of SSCs

The spectral reflectance value curves along with the entire measured bandwidth (325 nm - 1075 nm) of the dry sedimentfor different sediment types sampled from the upper Tekeze River system as well as for the pure water are presented (Fig.6).

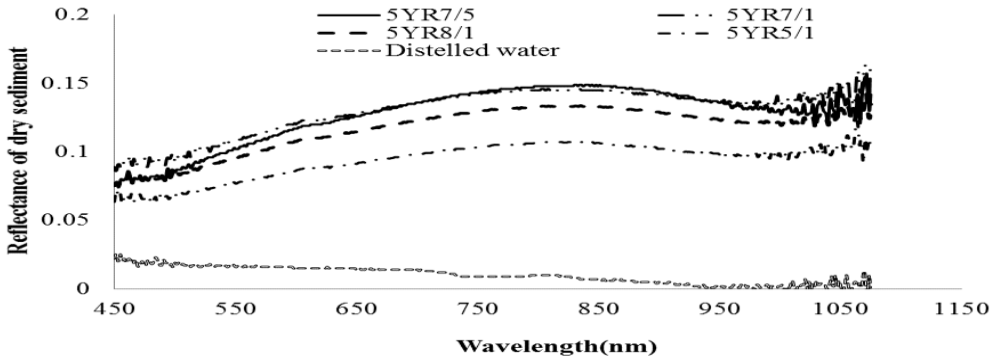

Fig. 6: Average reflectance of dry sediments 5YR7/5 (Red sediment), 5YR7/1 Tekeze River bed sediment), 5YR8/1 (Tsirare River bed soil) and 5YR6/1(black sediment)) and distilled water

The distilled water was with decreasing trend of reflectance values at the wavelength range used (450 – 850 nm). Unlike the spectral properties of the pure water, the reflectance values of the dry sediments from the Tekeze Rivers were continuously increasing trend.

To evaluate the effect of grain size distribution and level of concentration on reflectance values, a 2, 5, 10, 15, 20, 25, 30, 40, 50 and 60 g/l sediment solution for the clay, silt, sandy and natural grain size distribution were prepared. The spectral reflectance curves along with the entire measured bandwidth (325 nm - 1075 nm) showing the spectral characteristics for each level of concentration using the spectroradiomer were compiled (Fig.7 and Fig. 8).

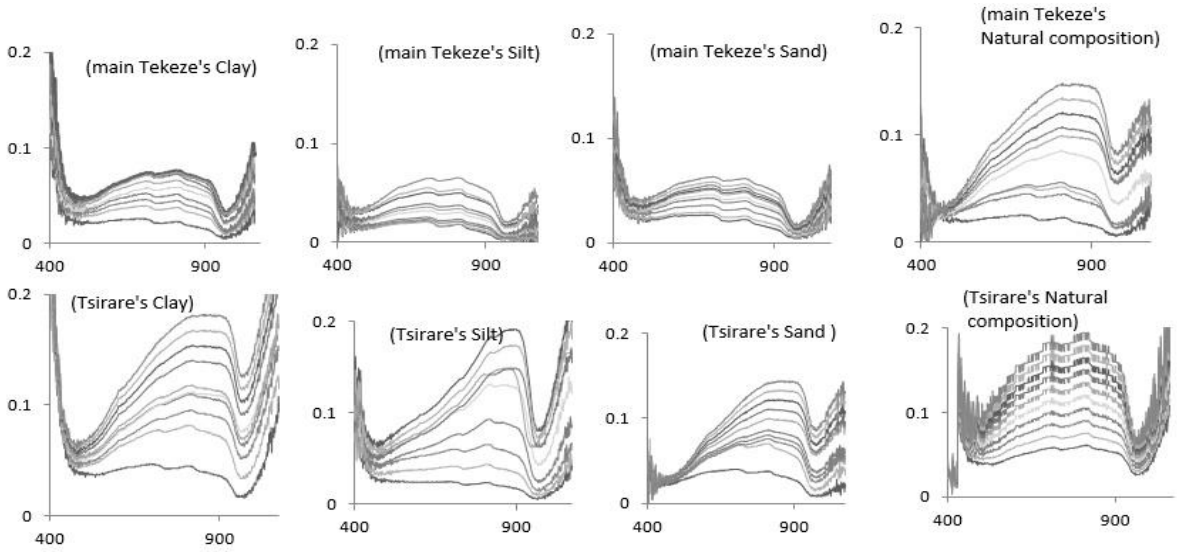

Fig. 7: Reflectance profiles of different sediment solutions collected from the Tekze River and Tsirare Rivers in the upper Tekeze basin.

The reflectance curves (Fig.7) are distributed progressively representing from the lower to higher water solutions of 2, 5, 10, 15, 20, 25, 30, 40, 50 and 60 g/l of the sediment types, respectively. The y and x axis represent the reflectance and wavelength range (nm) respectively. The curves represent the variability of reflectance of sediment solutions under the wavelength ranges 400-1075 nm.

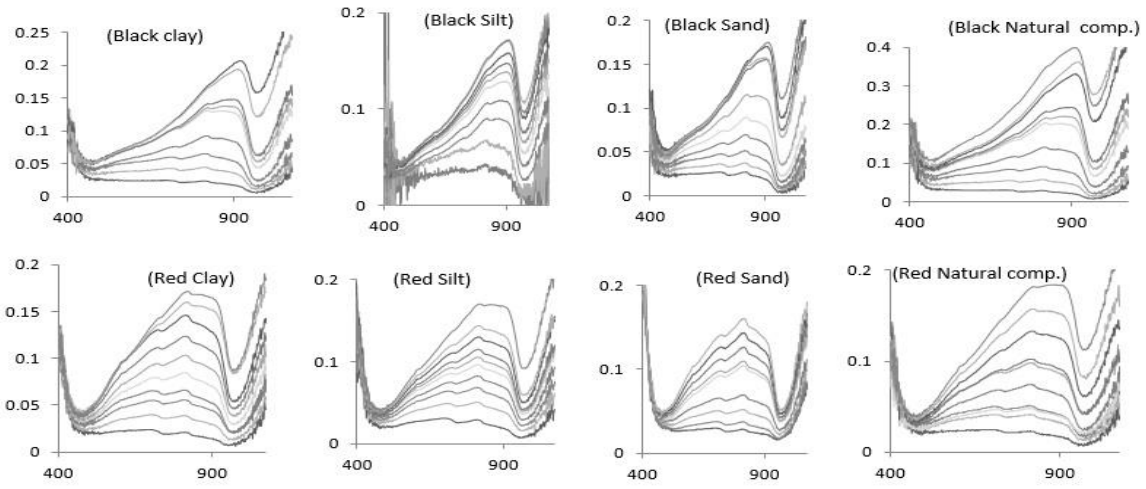

Fig.8: Reflectance profiles of black and red sediment solutions collected from reaches in the upper Tekeze River basin.

The reflectance curves are distributed progressively representing from the lower to higher water solutions of 2, 5, 10, 15, 20, 25, 30, 40, 50 and 60 g/l of the sediment types, respectively. The y and x axis represent the reflectance and wavelength range (nm) respectively. The curves represent the variability of reflectance of sediment solutions under the wavelength ranges 400-1075 nm.

As can be seen from Fig. 7 and 8, the spectral signatures of the sediment types were varied based on colour (5YR7/5, 5YR6/1, 5YR7/1 and 5YR8/1), grain size (natural, clay, silt and sand), level of concentrations (2, 5, 10, 15, 20, 25, 30, 40, 50 and 60 g/l), and wavelength ranges. The reflectance showed an increasing trend from coarser to finer grain sizes across the wavelength range (325-1075 nm) and relatively highest reflectance magnitude was found in the natural composition of grain size (Fig. 7& 8). Moreover, the reflectance was increasing as the levels of SSCs get increased. In the considered sediment types, overlapping reflectance values were observed in the wavelength ranging 325-450 nm and 950-1075 nm. But acute differences in reflectance values were observed in the wavelength ranging from 450-950 nm. The peak reflectance and more clear variability due to sediment type were observed at SW-NIR wavelength ranging from 750 to 950nm in all levels of SSCs (Fig. 7 & 8).

4.1.2 Correlation between reflectance and SSC in simulated bands

The Pearson correlation coefficient (Rs) was used to test the association between reflectance and level of SSCs for all sediment types over the bandwidth (450 - 1075 nm).

The Rs value was more than 0.55 in the wavelength used. Relatively higher correlations (Rs>0.7) were found in the wavelengths ranging 750-950 nm. The strength of the correlation between sediment concentrations and reflectance was also varied as the grain size gets varied. Stronger correlations (average Rs = 0.82) were found between reflectance and level of SSCs in fine grain size (clay) than the coarser (sand) sediment types (average Rs = 0.75) and the intermediate (silt) grain size (average Rs = 0.78). The reflectance from the natural grain sizes was loosely associated with its level of concentration (average Rs= 0.68). Comparatively, a higher correlation between SSCs and reflectance was found in the sediment type sampled from Tsirare coloured as 5YR8/1 (average Rs = 0.75) than the sediment type from the main River (5YR7/1), the black (5YR6/1) and the red (5YR7/5) sediment samples.

4.1.3 Empirical and LSU remote sensing models

4.1.3.1 Empirical remote sensing modelling

To use remote sensing for estimating sediment concentration we have to know first the relation between sediment concertation and reflectance. Having that relation, we can use the reflectance for estimating the sediment concentration transporting in Rivers. To do this we have used the wavelength ranging 750–950nm (B_5) in the current study. As explained in the previous section higher correlation between sediment concentrations and reflectance was found at B_5. The spectral profiles in Fig. 9 is developed from the relation between the SSCs (2, 5, 10, 15, 20, 25, 30, 40, 50, 60 g/l) with clay, silt, sand and natural grain sizes and their respective reflectance measured using a high-resolution spectro-radiometer in the wavelength 750-950 nm (B_5).

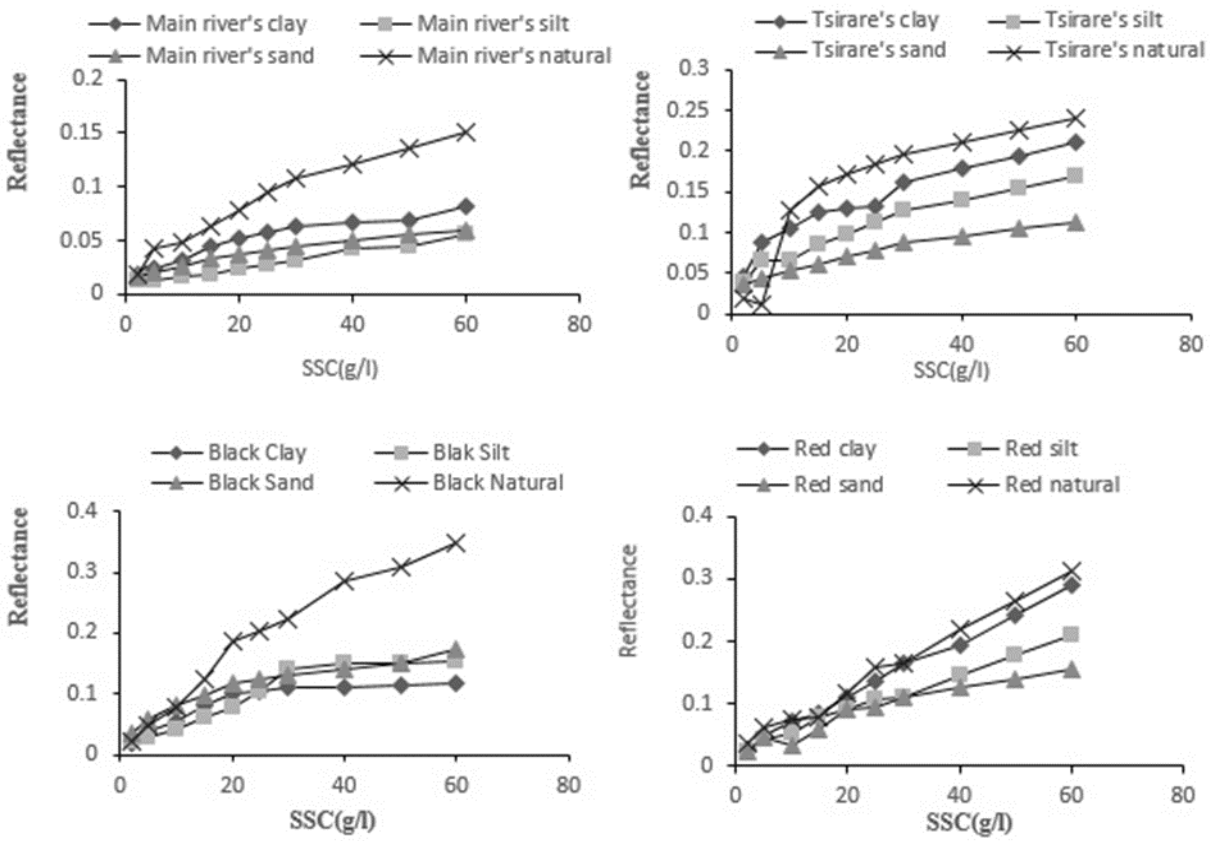

Fig.9: Reflectance profiles of SSCs under different grain size distribution and coulors in the wavelength range of band 5 (B_5, 750-950nm).

The scatter plots in Fig.9 were from reflectance measured using spectro-radiometer and SSCs under different sediment colours (5YR7/, 5YR8/1, 5YR6/1 and 5YR7/5) and grain sizes (clay, silt, sand, and natural). The scattering was not uniform among the sediment colours and grain sizes. Vast scattering was found in the sediment type from the main River than the sediments from the Tsirare River. Higher reflectance values were also presented from the natural grain size compared to the reflectance from other grain sizes in all sediment types.

The linear regression (the easy for operation) and other nonlinear regression model fitting curves were tested to fit the variability regressions between SSC levels and respective reflectance values. But, none of them was well fitted like the exponential equation (R^2>0.8). An exponential equation is given below (Eq. 38) was found well fitted to the relation between SSCs and reflectance.

$$\mathbf{R_f = ae^{(SSC/b)}} \qquad \mathbf{(Eq.37)}$$

Where SSC and R_f refers to the suspended sediment concentration (g/l) and the reflectance at 750-950nm (B_5) respectively, 'a' and 'b' were coefficients.

Table5: The coefficients regressed from the empirical model ($R_f = ae^{(SSC/b)}$) of the known SSCs (g/l) and the reflectance at Band 5 (750-950nm)

Grain size	Estimate	Sediment color			
		Main River (5YR7/1)	Tsirare River (5YR8/1)	Red sediment (5YR7/5)	Black sediment (5YR6/1)
Clay	a	0.03	0.06	0.04	0.04
	b	42.92	49.51	41.49	27.25
	R^2	0.80	0.89	0.89	0.86
Silt	a	0.01	0.06	0.03	0.04
	b	37.59	45.87	29.85	30.30
	R^2	0.88	0.85	0.89	0.87
Sand	a	0.02	0.07	0.06	0.03
	b	48.54	54.05	45.05	33.22
	R^2	0.86	0.86	0.83	0.88
Natural	a	0.02	1.62	0.05	0.05
	b	34.01	0.76	24.69	28.90
	R^2	0.85	0.89	0.88	0.85

According to the regression analysis between level of SSCs and respective mixed reflectance values (Table 5), the coefficient of determinations ($R^{2)}$ were found in the range of 0.8 - 0.89. Non-random estimates (a and b) were resulted from nonlinear regression analysis under a significance level of 99%.

4.1.3.2 Linear spectral unmixing analysis for modelling SSC

The linear spectral unmixing algorithm was introduced to maximize the accuracy of simulating SSC using remote sensing. The reflectance variability in 750-950nm (B_5) from the considered levels of SSCs was translated to the spectral mixing coefficients (SMCs) variability using Eq. 3. The graph describing the relation between the SSCs and their

respective SMC values of the sediment types sampled from the two Rivers were presented in Fig. 10.

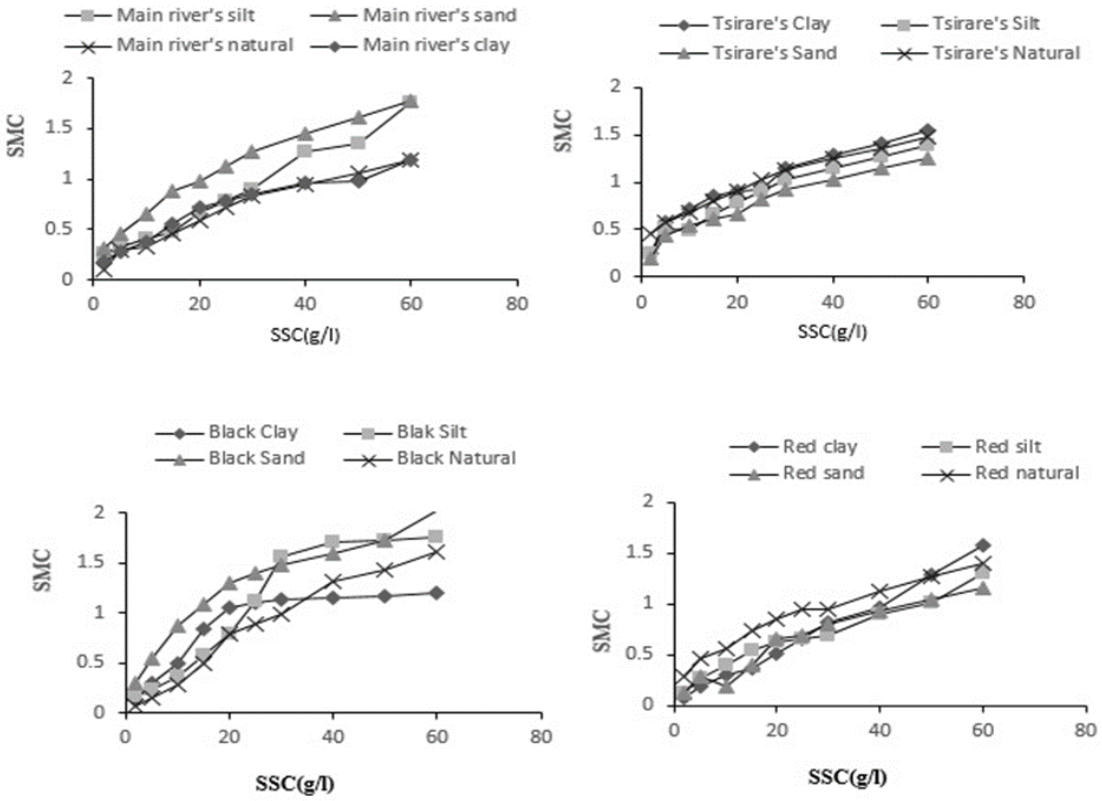

Fig.10: SMCs profiles of sediment laden water in the wave length range of 750-950nm (B_5) from the main River bed (5YR7/1, a), Tsirare River bed (5YR8/1, b) and other black (5YR6/1, c) and red (5YR7/5, d) sediments in basin

The exponential regression Eq.39 was found to be the best fit to the relation between SSCs and respective SMCs. The relation between SSCs and SMCs was determined to be as in Eq. 39.

$$SSC = \alpha e^{(\beta(SMCs))} \qquad \textbf{(Eq.38)}$$

Where SSC and SMCs refer to the suspended sediment concentration (g/l) and the spectral mixing coefficients values respectively, 'α' and 'β' are coefficients. The coefficients of determination (R^2) were above 0.89 in all sediment types (Table 7).

Table6: The coefficients regressed from the LSU model ($SSC = \alpha e^{(\beta(SMC))}$) from the known SSCs (g/l) and the SMCs at band 5 (750-950nm)

Grain size	Estimate	Sediment colour			
		Main River (5YR7/1)	Tsirare River (5YR8/1)	Red sediment (5YR7/5)	Black sediment (5YR6/1)
Clay	α	0.33	0.72	1.54	0.65
	β	2.64	3.12	1.96	2.58
	R^2	0.95	0.93	0.89	0.93
Silt	α	0.53	1.34	0.99	1.35
	β	2.77	1.87	2.85	1.51
	R^2	0.91	0.90	0.91	0.94
Sand	α	3.09	4.31	14.33	2.63
	β	0.32	0.47	0.35	0.51
	R^2	0.93	0.93	0.96	0.97
Natural	α	3.17	1.16	0.34	1.01
	β	0.73	58.05	2.934	2.85
	R^2	0.92	0.91	0.94	0.91

According to the regression analysis between the level of SSCs and respective SMC values computed by transformed reflectance values (Table 7), the coefficients of determinations (R^2) were found in the range of 0.89 - 0.95. Non-random estimates (α and β) were resulted from nonlinear regression analysis under a significance level of 99%.

4.2 Testing and validating the empirical and LSUA of SSCs models using in-situ data

The empirical (Eq. 37) and LSUA (Eq. 38) remote sensing models fitted to the natural grain size distribution sampled from the Tekeze main River and Tsirare Riverbeds deposition were further tested using insitu reflectance and compared against the SSCs of the flash

floods in Tekeze and Tsirare River occurred during the 2017's summer. The exponential equations constructed using the empirical remote sensing (Eq.37) and from the LSUs (Eq. 38) were first transformed to logarithm for convenience of linear regression analysis and used to simulate the SSCs transporting with the flash floods in the Tekeze Main River and the tributary Tsirare River using the estimates for the respective natural grain size of sediment developed from the laboratory analysis (Fig. 11). The daily SSCs at Tekeze River and Tsirare during the summer of 2017 were simulated using the empirical and LSU models and then compared with the SSCs measured using the conventional sediment sampling technique. The reflectance values (R_f) in Eq.37 were substituted by the reflectance values of the turbid water on field measured using the Spectroradiometer. The daily SSCs during the summer were measured using the traditional sampling technique.

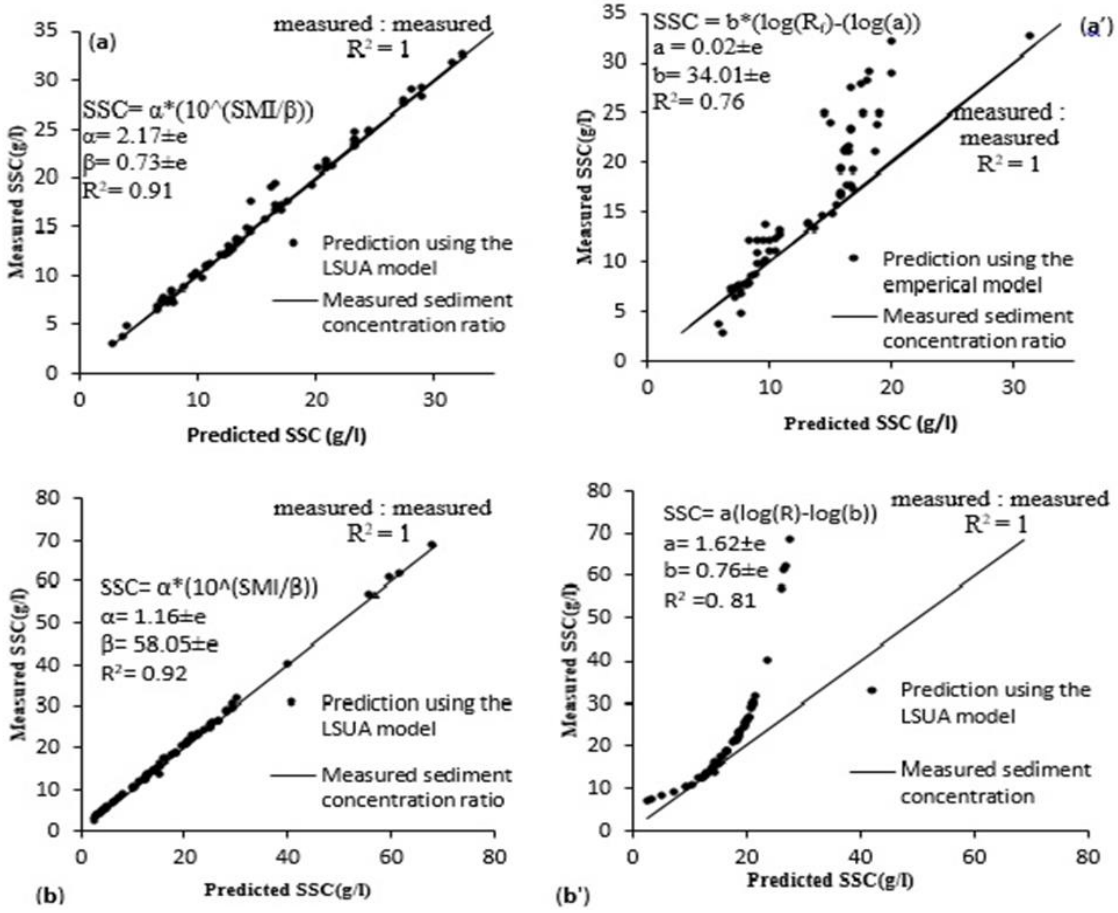

Fig.11: Comparing simulating potential of LSU analysis and empirical models for SSC at the Tekeze main River (a, a') and Tsirare River (b, b')

The SSCs predicted using the empirical remote sensing models for both Rivers were deviated from the measured SSCs (Fig. 10). Initially the performance of the empirical model in the laboratory was computed to be R^2=0.76, RMSE = ±10.87g/l in the main River and R^2 = 0.81, RMSE =±2.65g/l in Tsirare. But, performance of the same model to estimate the daily SSCs in the rivers using insitu reflectance values were lower than the above values. Especially, when the level of SSCs increased, the deviations from the measured SSCs were also increased (Fig.11). Unlike the empirical model, the LSU model (Eq.38)

performances were consistent in the laboratory and in the field to capture the variability of sediment concentration in both Rivers. The fit between the observed and the simulations using the LSU and empirical models to the SSC of flash flood events at the Tekeze main River and Tsirare tributary River occurred during the wet season of 2017 is presented below (Fig. 12 & 13).

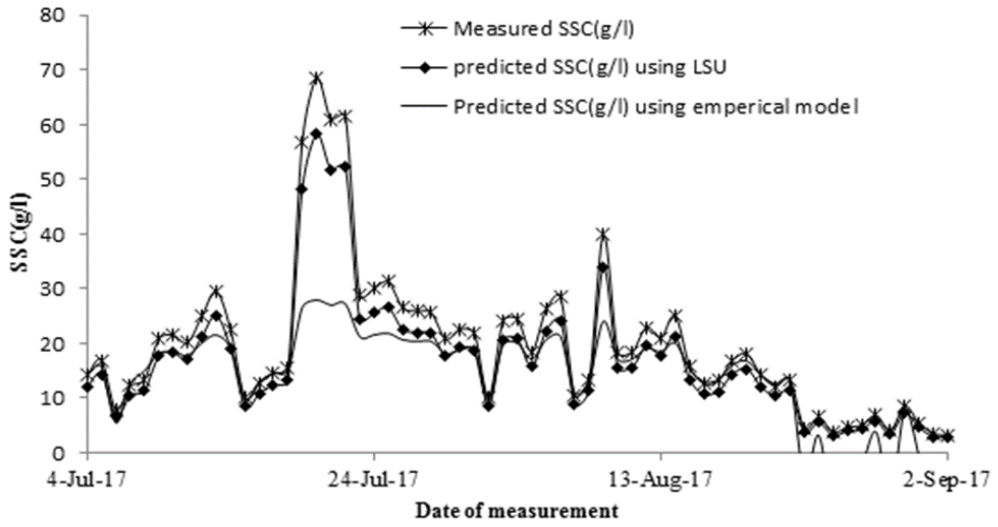

Fig.12: The fit b/n the measured and simulation using the LSU and empirical models to the SSC of flash floods events at the Tekeze main River starting from on 2July 2017 to 3 September 2017

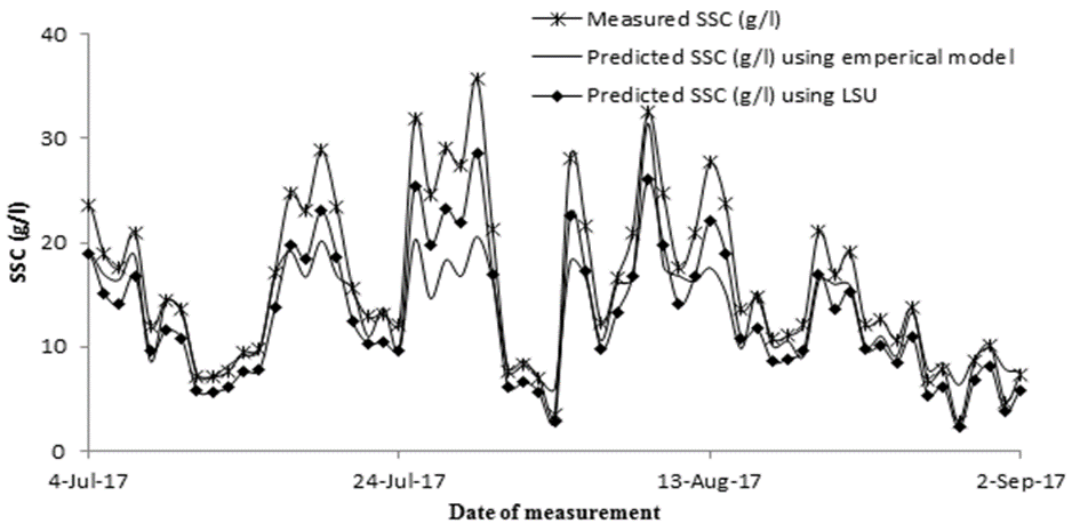

Fig.13: The fit b/n the measured and simulation using the LSU and empirical models to the SSC of flash floods events at the Tsirare River (b) starting from on 2July 2017 to 3 September 2017

As can be seen from Fig. 12 and 13 the empirical models were poorly performed in capturing the variability of SSCs compared to the LSU model. Especially, the peak sediment concentrations in both Rivers could not be captured using the empirical model. Unlike the empirical model, the LSU algorithms were well performed in capturing the variability of sediment concentration in both Rivers.

4.3 Estimating SSC from MODIS terra images

4.3.1 Spectral profile of selected pixels and nearby cover types

The spatial resolution of MODIS data is coarser (250-1000m) compared to the heterogeneity and geographic dimension of most River systems. Consequently, the pixels around Rivers are a mixture of two or more than two ground cover components. The reflectance values of pixels are therefore a combined effect of the cover components around

the geographic location of the respective pixels. Hence, characterizing the spectral reflectance profile of the primary components existed in the pixels of interest has paramount importance for spectral unmixing analysis approach.

Hence, two pixels one from the main River Tekeze and the second from the tributary Tsirare were selected. About 43% and 68% area of the selected pixel at the main River of Tekeze and Tsirare Tributary River mostly had rock and bare soil land cover types, respectively. The remaining part of both pixels was laid on turbid water cover type. Therefore, the mixed reflectance at the main River was from a linearly combined reflectance from the respective components in each targeted pixel. Accordingly, the reflectance values for of the selected mixed pixels were assessed as in Fig. 14.

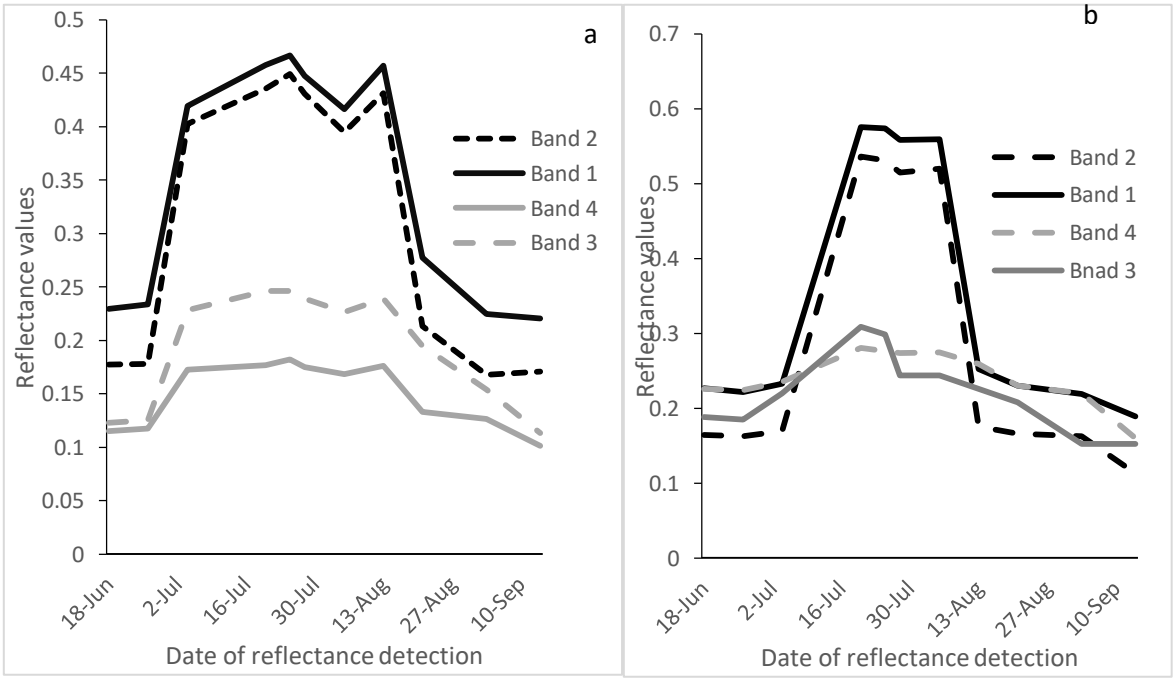

Fig.14: The daily variability of surface reflectance observed at the selected station of the Tekeze MainRiver and Tsirare TributaryRiver at band 1, 2, 3 and 4 of MODIS surface reflectance images

As can be seen from Fig. 14, even though the absolute values of reflectance at the pixel vary from band to band, the trend of reflectance variability through the whole bandwidth were consistent during the summer. That is higher reflectance values were derived from the targeted pixels of the images dated in July and August months of 2017. While lower reflectance values were derived from the same pixels at the images dated on June and September 2017. The variability of the absolute reflectance values at pixel level was varied from band to band and from River to River. Relatively, higher reflectance values were derived from Band 1 (620 – 670nm) and Band 2 (841-876nm) than from Band 3 (459-479nm) and Band 4 (545-565nm) for both Rivers.

The average reflectance values for the land cover components supposed to be mixed in the targeted pixels were assessed as in Fig. 15.

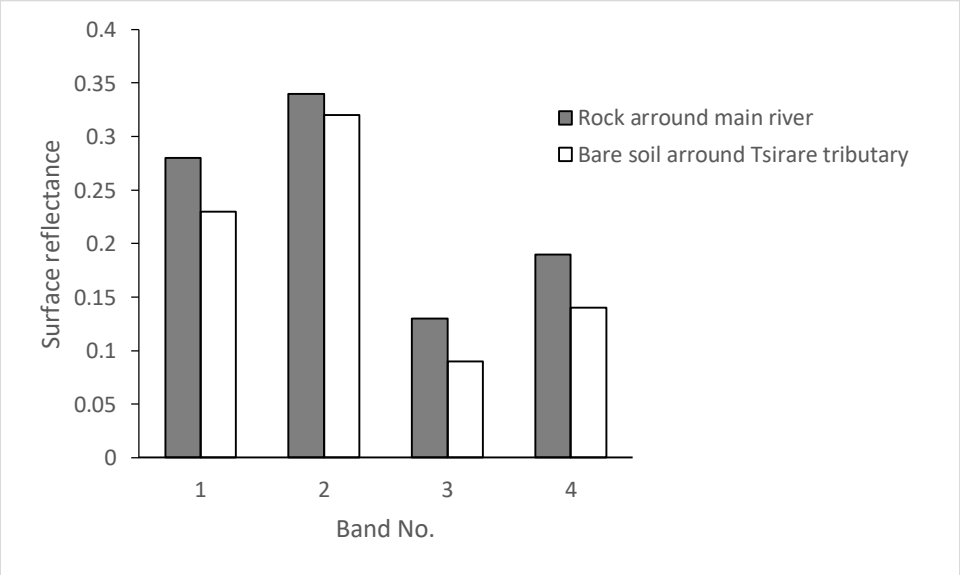

Fig.15: Average surface reflectance of non-changing land cover types of Tekeze Main River (rock) and Tsirare Tributary River (bare soil) at band 1, 2, 3 and 4 of MODIS surface reflectance images

Higher reflectance values of rocky and bare land ground cover components were found at the first two band width (Band 1&2) compared to the reflectance values of the cover components at Band 3&4. Slightly higher reflectance values were computed rocky land cover types than from the bare land.

4.3.2 Applying empirical regression model on MODIS

The daily SSCs of the two Rivers at the simulated station were predicted using the empirical model developed in the laboratory (Eq.37). The reflectance values were used from respective MODIS surface reflectance. The simulated daily SSCs were compared with the respective SSCs measured using the conventional sediment monitoring method (Fig. 16).

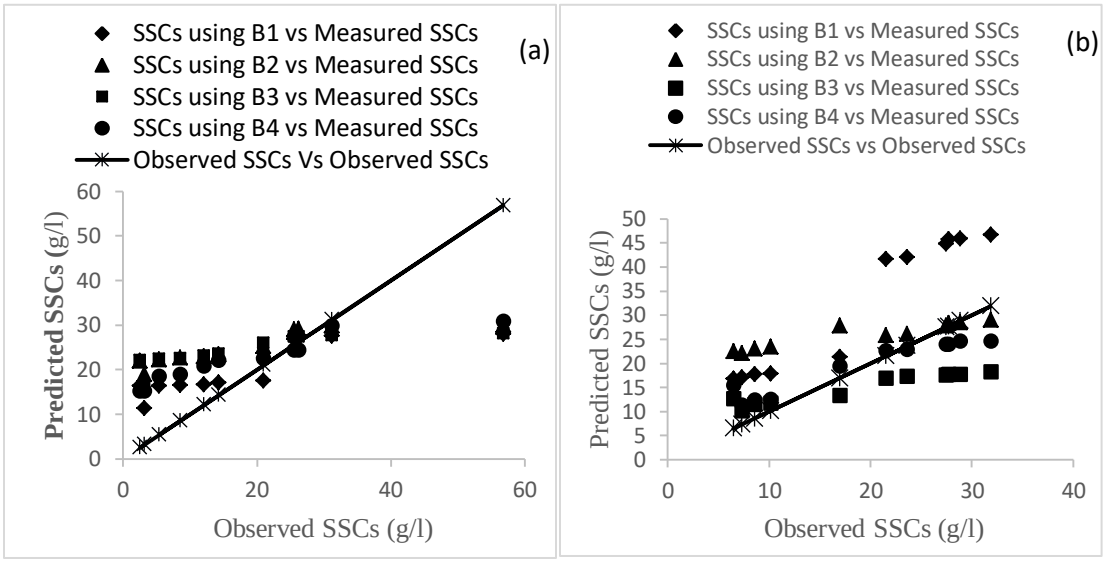

Fig.16: Scatter plot between predicted SSCs (y axis) and observed SSCs (x axis) of the Tekeze main River (a) and tributary Tsirare River(b)

Fig.16 is constructed based on the prediction made using the empirical regression model (SSC= (ln (Rp/a))*b). There was no consistent correlation between SSCs and the reflectance of the mixed pixels in Band 1- Band 4 in the selected pixels of both Rivers. In both Band 1 to Band 4 there was no consistent trend of reflectance as the SSCs get increased. In some of them there was reduction of reflectance with increasing of SSC and in some others, there was different level of change in reflectance for constant change of SSCs. The empirical regression model was performed with average coefficient of determination and RMSE of 0.78 and ± 14.17 in the main River as well as 0.69 and ± 18.22 in the tributary Tsirare River respectively.

4.3.3 Double stage Linear Spectral Unmixing Algorithm

To minimize the errors in estimating SSCs from direct use of MODIS imageries we have developed a new subpixel analysis approach called Double Stage Linear Spectral Unmixing Analysis (DLSUA). In this case, 1st the pixels' reflectance was unmixed into rock/bare cover components and to turbid water reflectance and 2nd the reflectance of the turbid water from step one was further unmixed into the respective constituents' reflectance. Once the daily reflectance values of the turbid water at the simulated station computed from the mixed pixels of MODIS, the respective Spectral Mixing Coefficients of sediments (SMCs) were calculated using Eq. 20. Then the SSCs for respective Rivers during for each date of the images used were computed using the nonlinear relations between the SSCs and SMCs developed from the laboratory experiment (Eq. 37). To evaluate the performance of the model the observed and predicted SSCs are plotted below (Fig. 17).

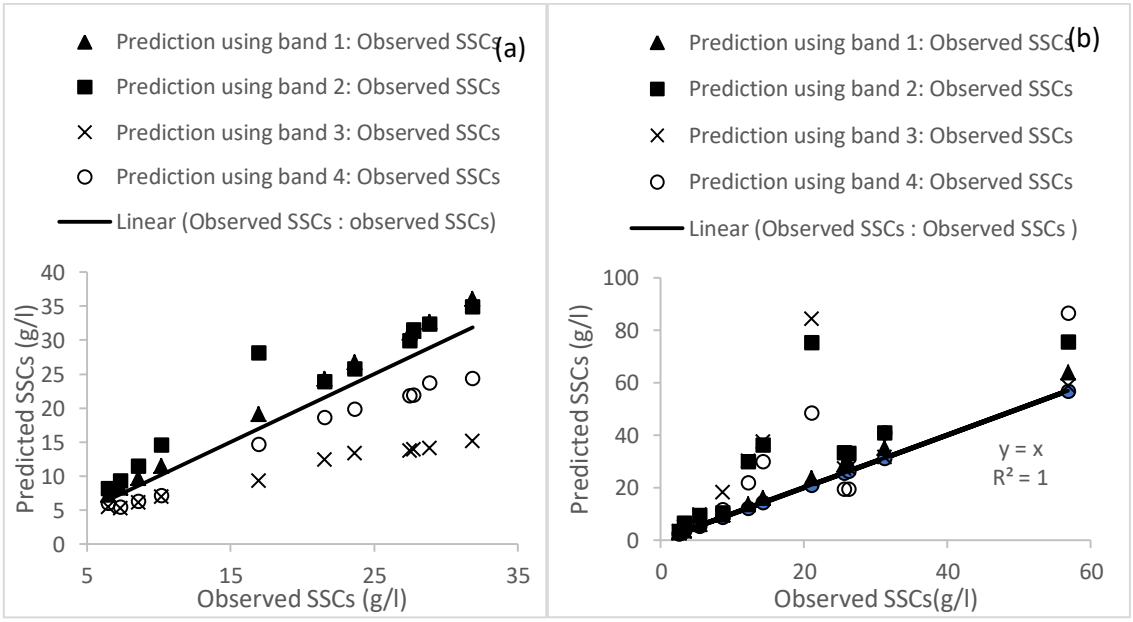

Fig.17: Scatter plot between predicted SSCs (y axis) and observed SSCs (x axis) of the Tekeze main River (a) and tributary Tsirare River (b). The predictions were made based on DLSUA model.

Though the predicted SSCs were not the same with the measured SSCs during each date, the deviations were in the accepted ranges. In the main River, the model was performed at an average Relative Mean Square Error (RMSEs) of 2.79, 4.42, 10.17 and 4.15 at Band 1 to Band 4 respectively. In the Tsirare Tributary River, the RMSEs were computed to be 2.97, 19.81, 21.31 and 14.05 at Band 1 to Band 4, respectively. The DLSUA approach estimated SSCs at the Tekeze main Riverwith average (R^2 = 0.90 and RMSE± 5.38) and in the tributary Tsirare River (R^2 = 0.76 and RMSE ± 14.54).The research indicated that the models developed from the Band 1 were performed well than from in the remaining Bands.

4.4 Integrating LSUA into hydrologic model

4.4.1 Identification and Characterizing spectral signature of ground cover

As in most rural areas, four principal ground cover components (endmeber) were identified in upper Tekeze basin. The vegetation, bare soil, rock and water bodies were the identified principal ground cover components (endmembers) in the upper Tekeze basin. The spectral value of each endmembers under the six bands (2-7) of Landsat 8 acquired at the wet season of 2016 were presented (Fig.18). As can be seen in Fig.18, the spectral signature of each endmeber were scattered in the wavelength ranges in between band 4 and band 6.

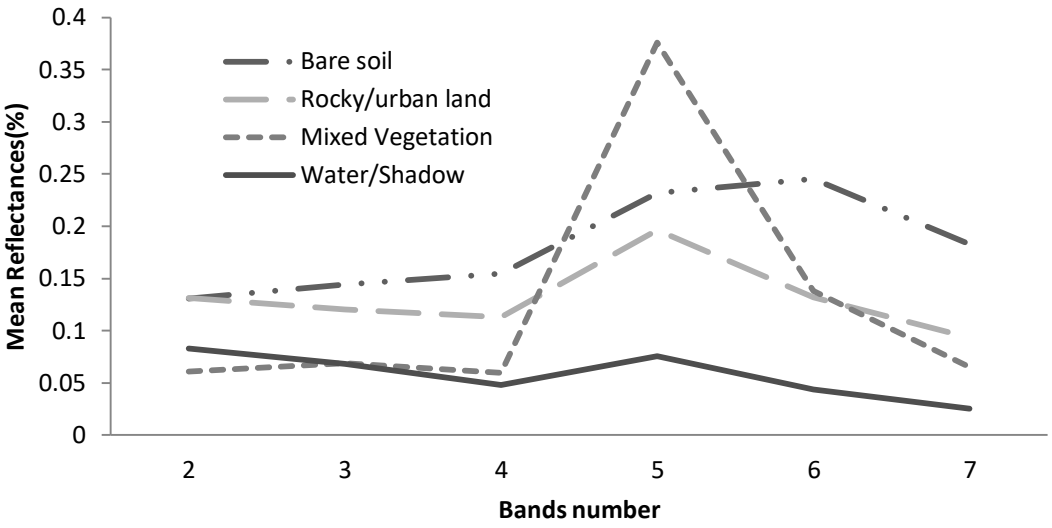

Fig.18: Spectral curves of identified endmembers in upper Tekeze basin computed from Landsat 8 dated on summer 2016 using ENVI 5.1

4.4.2 Mapping spatial abundance of ground covers in upper Tekeze basin

Based on the spectral signature profile (Fig. 18), the spatial abundance of the principal ground cover components was computed and mapped using ENVI 5.1. The spatial

abundance of each endmembers (vegetation, bare soil, water bodies and rocky lands) derived from the satellite image using the LSUA are shown in Fig.19. The overall average relative mean square error (RMSE) made during the LSUA from Landsat 8 was about 0.12.

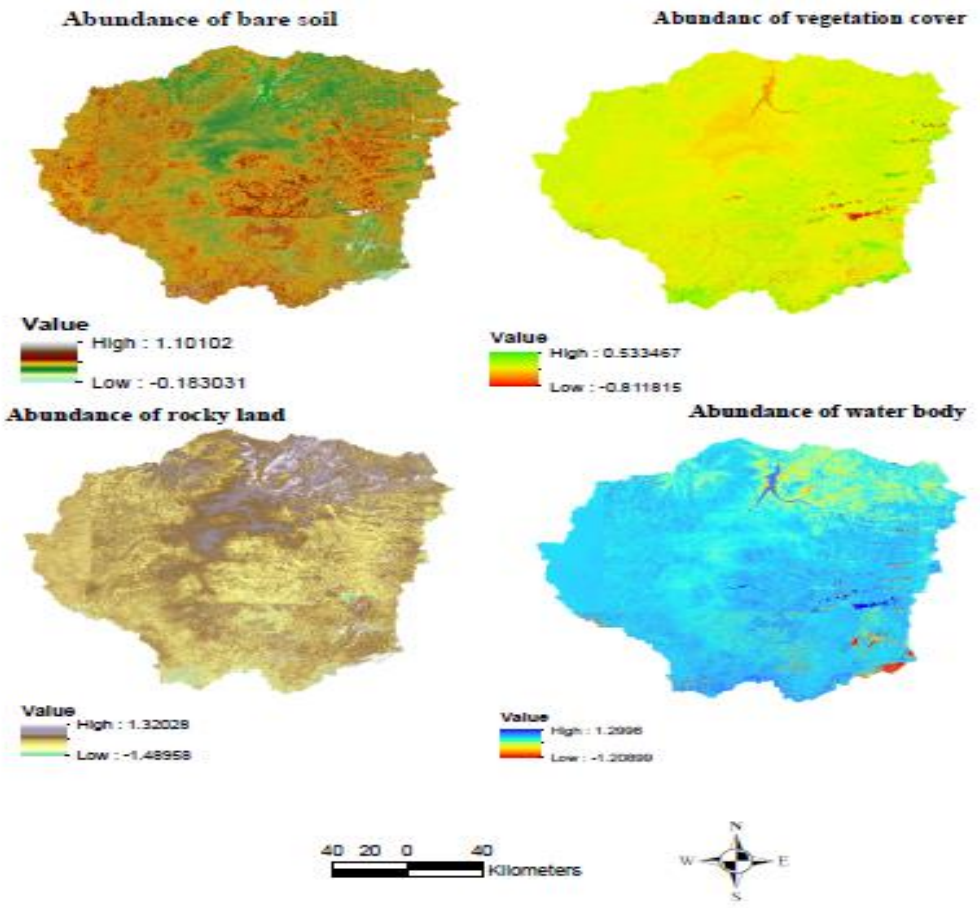

Fig.19: Spatial abundance of bare rock (A), water body (B), bare soil (C) and vegetated lands (D) in upper Tekeze basin derived from the landsat 8 dated on 11, Sep 2016

The maps show high spatial variability of the endmembers that represents the different cover conditions in the study area. Higher vegetation cover was found on the steeply lands and on the flat cultivable lands (Fig. 19). But, the central part of the basin where most

valleys found was found to be with less vegetation cover. Like the vegetation cover, the bare soil in the upper Tekeze river basin was higher in majority part of the basin except around the valleys. The water covers in the basin are the artificial lake of the Tekeze dam and the Hashenge natural lakes. But, unexpectedly the map for water cover (Fig. 19) seems there was water throughout the basin. This may be due to the excess moisture in the basinduring the study period.

After identifying the endmembers in the basin and mapped the spatial distribution of each of them, we have computed the spatial C-factor values in the basin following Eq. 3 and presented as in Fig. 19 below.

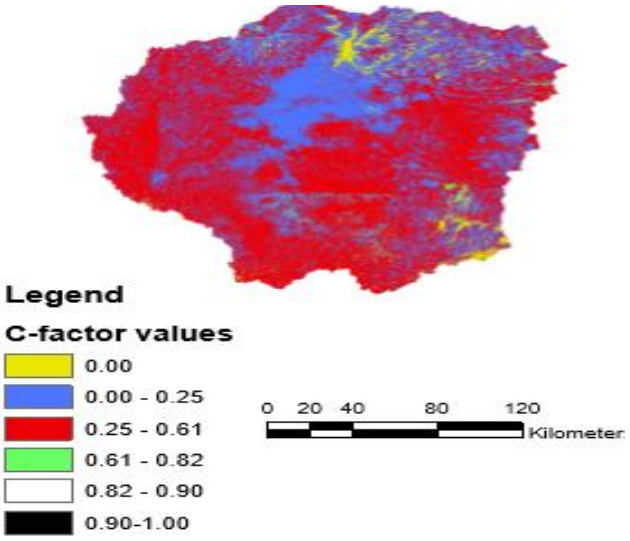

Fig.20: Minimum C- factor map produced from Landsat 8 of 2016 using LSUA (A) for the upper Tekeze basin

The C-factor values for the upper Tekeze basin was mapped (Fig.20) and compared with the respective C-factor values from field measurement (see appendix).Accordingly, the C-factor values mapped (Fig.20) illustrated that the C-factor values estimated using LSUA

was relatively consistent and not significantly deviated from the mean values of the field measurements suggesting that the range was reasonable. The C-factor in the basin was found in the range of 0-1 as obvious. Parallel to this, land use/land cover map for the upper Tekeze basin for the year 2005 were developed from Landsat 7. Accordingly, six land-use types including forested, shrub, grassed, intensively and moderately cultivated land and water bodies were identified and mapped (see appendix). The C-factor for each land-use type were derived from the C-factor map in Fig.20. Accordingly, the C-factor values for the water bodies, rocky land and forested land were in the range of 0 - 0.25. The C-factor values for shrub land, grass land and cultivated land were found to be in the range of 0.25 – 0.9.

4.4.3 Integration of LSUA into SWAT and evaluating its performance

The spatial C-factor estimated using LSUA from Landsat images of the study area was integrated into SWAT supposing that this can improve the sediment yield predictions. The modification of C-factors was made to an HRU in SWAT which was conventionally assigned to the corresponding 'crop.dat' according to the land use/land cover types. The conventional determination and assigning of C-factor creates a homogenous C-factor map, without any spatial variation within a specific land use area. To make use of LSUA remote sensing C-factor map, the source code in the subroutine for dealing with the C-factor was modified to assign the corresponding C-factor in the 'hru.txt' file for each HRU according to their HRU ID. Improved source codes were compiled with other original source codes and a new executable file SWAT2012.exe was generated for further sediment simulation. The time-series plot of measured and the prediction of daily sediment yields using the

conventional and modified SWAT at Tekeze hydroelectric dam station during 2004-2009 presented as in Fig.21.

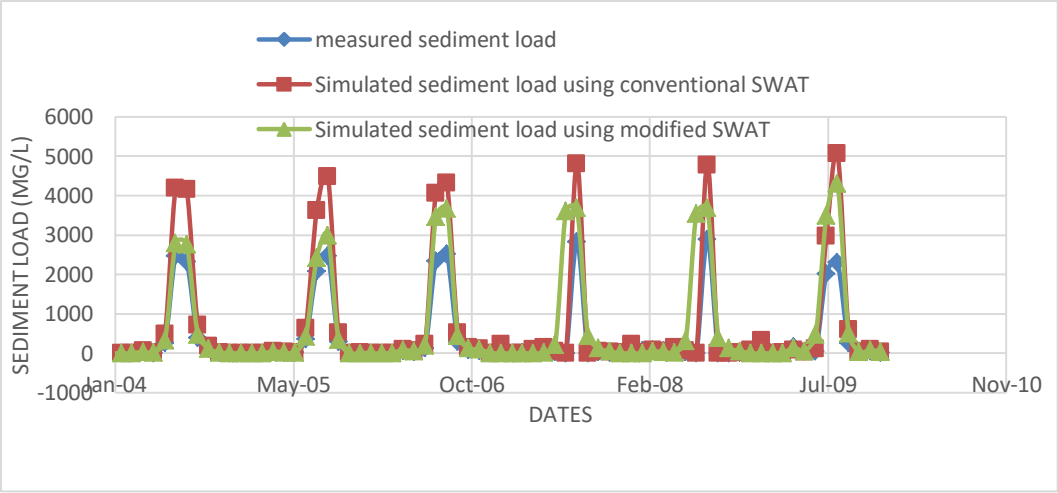

Fig.21:Time-series plot of measured and predicted monthly sediment yields at Tekeze hydroelectric dam station during 2004-2009 using the conventional SWAT and modified SWAT

Table 7: Summary statistics of calibration and uncertainty analysis of sediment yield prediction using the conventional and modified SWAT

SWAT used	Objective function values			
	NSE	RSR	PBIAS	R^2
Conventional SWAT	0.72	0.39	34.2	0.68
Modified SWAT	0.84	0.23	10	0.79

The NSE, RSR, PBIAS, and R^2 between the measured and the simulated sediment using the conventional SWAT were computed to be 0.72, 0.39, 34.2 and 0.68, respectively. While in between the measured and the simulated sediment using the modified SWAT were 0.84, 0.23, 10% and 0.79, respectively. The fit between the model sediment predictions using the modified SWAT and the observed concentrations were improved compared to the predictions by the conventional SWAT (Fig. 21). The LSUA integrated SWAT computed

sediment yields for each sub basin and saved its results in the files of 'output.sub', respectively. By dividing these values for the area of a computation unit and its related soil delivery ratio, it was possible to obtain the soil erosion intensity of the sub-basins in the upper Tekeze (Fig. 22).

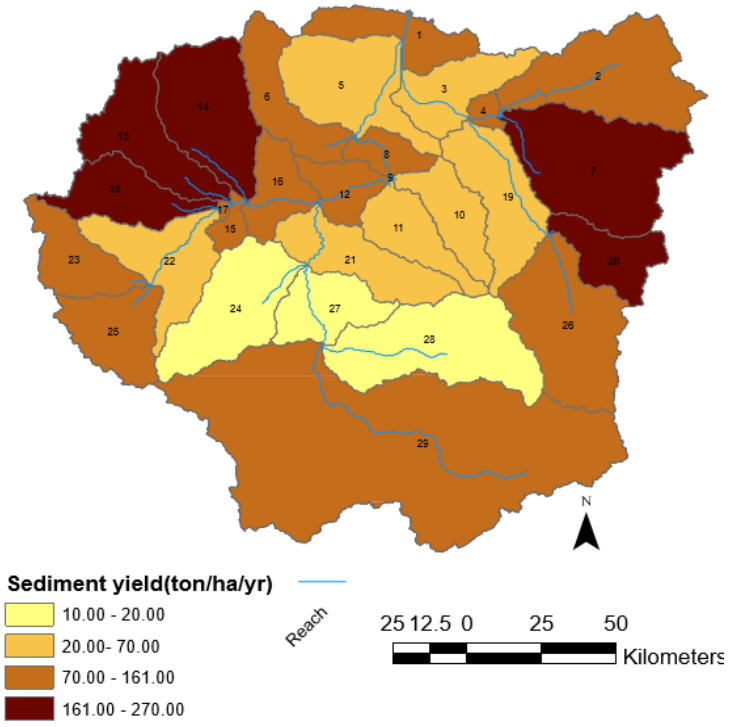

Fig.22: Sediment yield map developed from predicted sediment yield at each HRU using the modified SWAT model for the existing conditions in the Upper Tekeze basin

Sediment yield extent varies from 15 to over 267tha^{-1}yr^{-1}. The sediment yield level in the basin classified into lower (10–20 t ha^{-1}yr^{-1}), moderate (20–70 t ha^{-1}yr^{-1}), higher (70–136 t ha^{-1}yr^{-1}) and extremely higher (above 136 t ha^{-1}yr^{-1}) categories. This classification was made according Hurni (1983 and 1985). Hence, lower sediment yield was computed only from three sub basins including 24, 27 and 28 while the remaining sub basins were

computed to have moderate and above moderate status of sediment yield. This indicated that major part of the basin is under intensive soil erosion status. However, emphasis should be given to relative sediment yield level than the absolute values because the model was not calibrated and validated at the sub basin outlets due to lack of data.

The variability of monthly sediment yield at the Tekeze dam was also evaluated (Fig.22). The peak of sediment yield confined with the peak of rainfall in the basin. But it occurred early before the peak of water yield to the basin. This shows that sediment yield is well determined by the abundance of rainfall instead of by the water yield.

4.5 Climate and sediment yield variability

4.5.1 Point of changes and trends of rainfall

The variability of climate in the major seasons in the study area including the summer or wet season (June–August), winter or called dry season (December– February), the autumn mostly called harvesting season (September – November), and the spring called short rainy season (March–May) were considered in this study. Before detecting trends and correlations in between precipitation and sediment yield, the serial correlations existence in all datasets was tested at seasonal and annual time scales. Results of the trend analyses (Pettit &MK tests) were used to identify if the time series of annual and seasonal rainfall had a statistically significant breaking point and trend in the last 30 - 50 years, respectively.

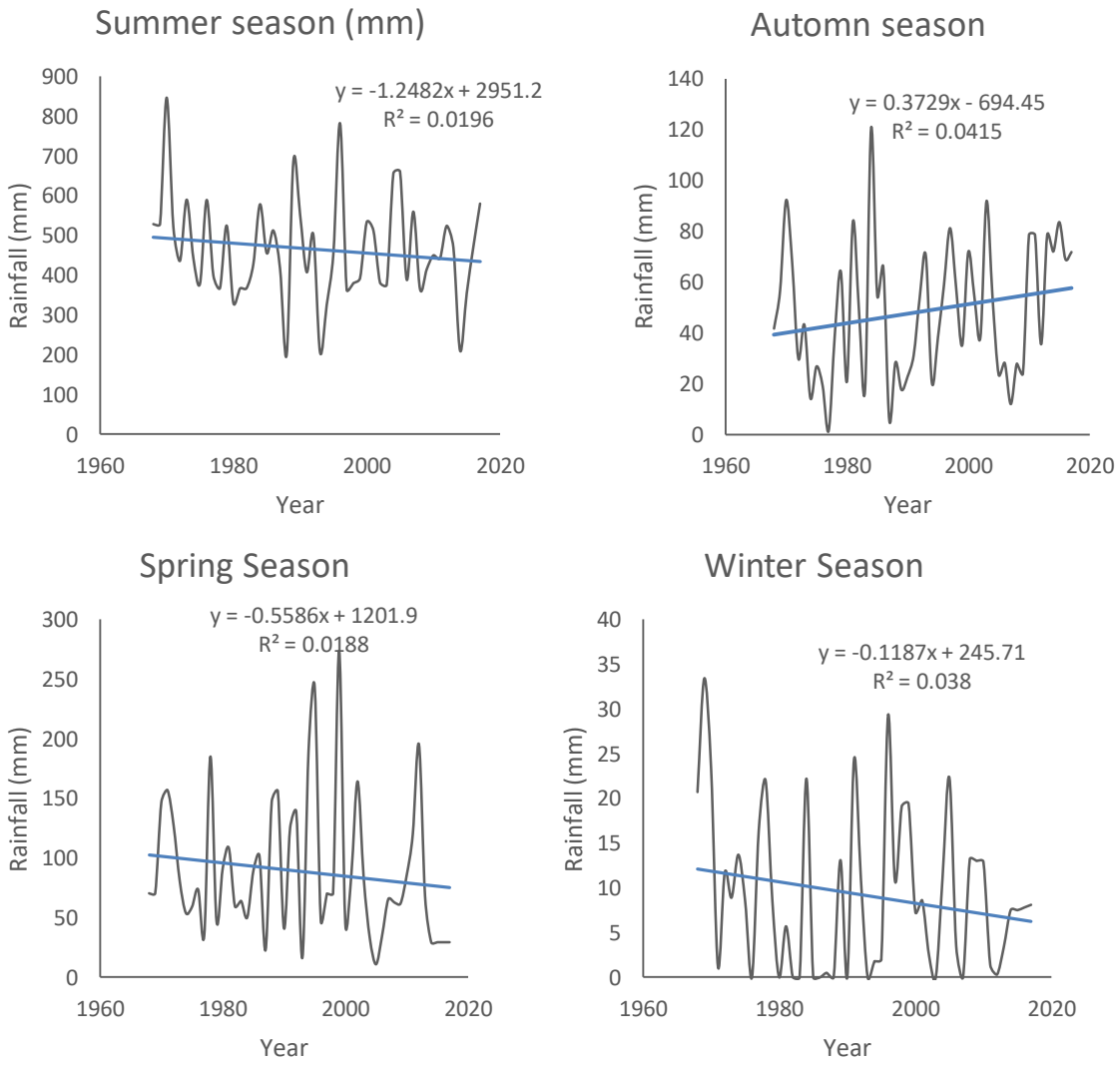

Fig.23: Variability of seasonal rainfall in the upper Tekeze basin

Accordingly, the results from the analysis have depicted that there are no significant trends in the rainfall of the basin both at annual and seasonal scales. The statistical indices of the test revealed a tendency of decreasing annual rainfall pattern. At the same time a decreasing of rainfall was observed in the summer, spring and winter seasons while an increasing of seasonal rainfall pattern at the autumn was observed in the study area (Fig. 23). However,

these trends were found to be nonsignificant. The Pettit test was used to identify if there is a breakpoint in the data series. Similar to the MK test, the statistical analysis of the annual and seasonal rainfall did not show statistically significant heterogeneity at 5 % significance level.

4.5.2 Point of change and trend of temperature

The trend of Tmax and Tmin of the years between 1968 - 2017in the upper Tekeze basin at the annual and seasonal time scale was evaluated using MK test. The graph showing the trends for seasonal Tmax and Tmin is presented here below (Fig. 24).

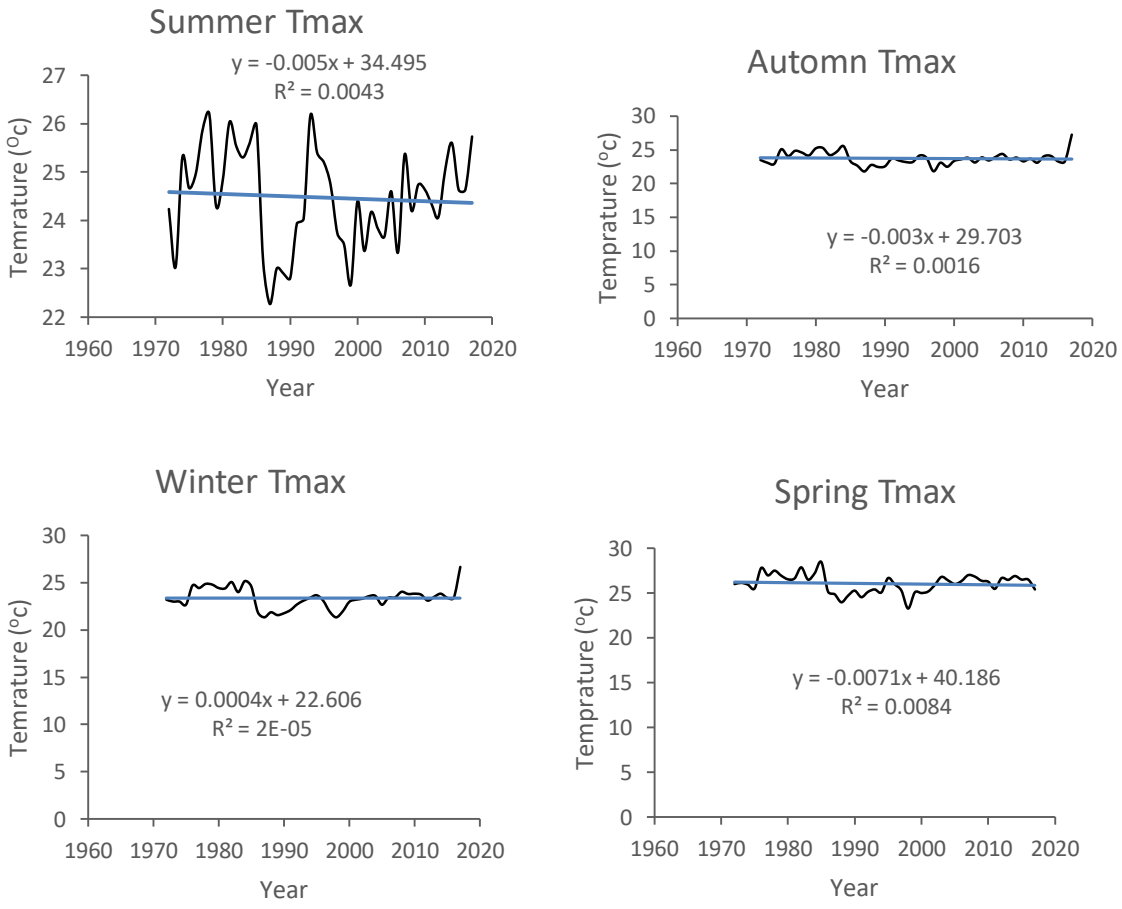

Fig.24: Variability of seasonal average maximum temperature in the upper Tekeze basin

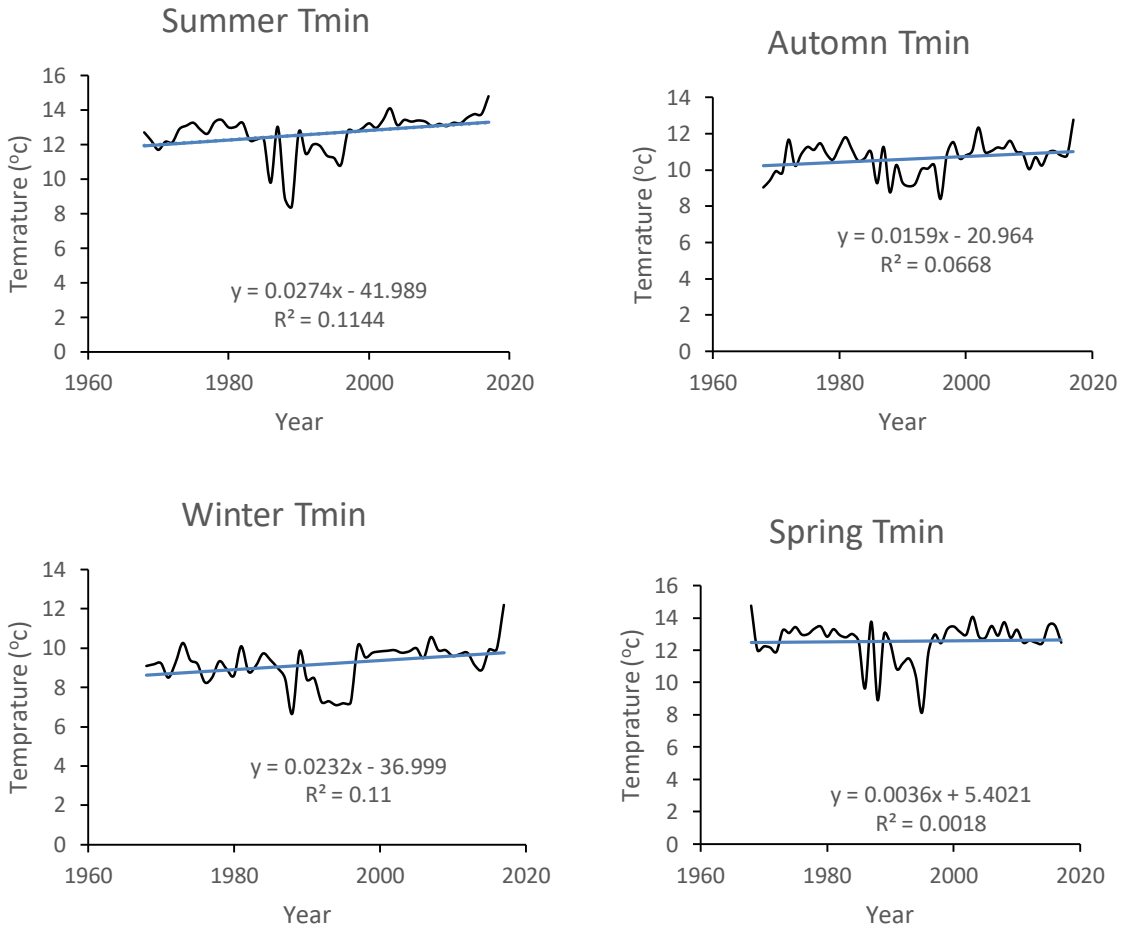

Fig.25: Variability of seasonal average minimum temperature in the upper Tekeze basin

The results from the analyses of trend on Tmax and Tmin at annual and seasonal time scale have depicted that there are no significant trends in the temperatureof the basin both at annual and seasonal scales (Fig. 24 & 25). The statistical indices of the test revealed a tendency of increasing and decreasing pattern of temperatureduring the considered years (Fig. 24 & 25). Generally, decreasing in Tmax and an increasing inTmin indicators were observed in this study. The Pettit test was also used to identify if there is a changing point in the data series. Accordingly, changing point was not found consistently in both the Tmax and Tmin of the Tekeze basin.

4.5.2 Trend of sediment concentration

The homogeneity and trend of sediment concentrations in the upper Tekeze basinin the year 2004 through 2017 simulated using the modified SWAT at the annual and seasonal time scale were evaluated using Petit and MK tests, respectively. The graphs showing the homogeneity and trends to each of the seasonal sediment concentration are given below (Fig. 26).

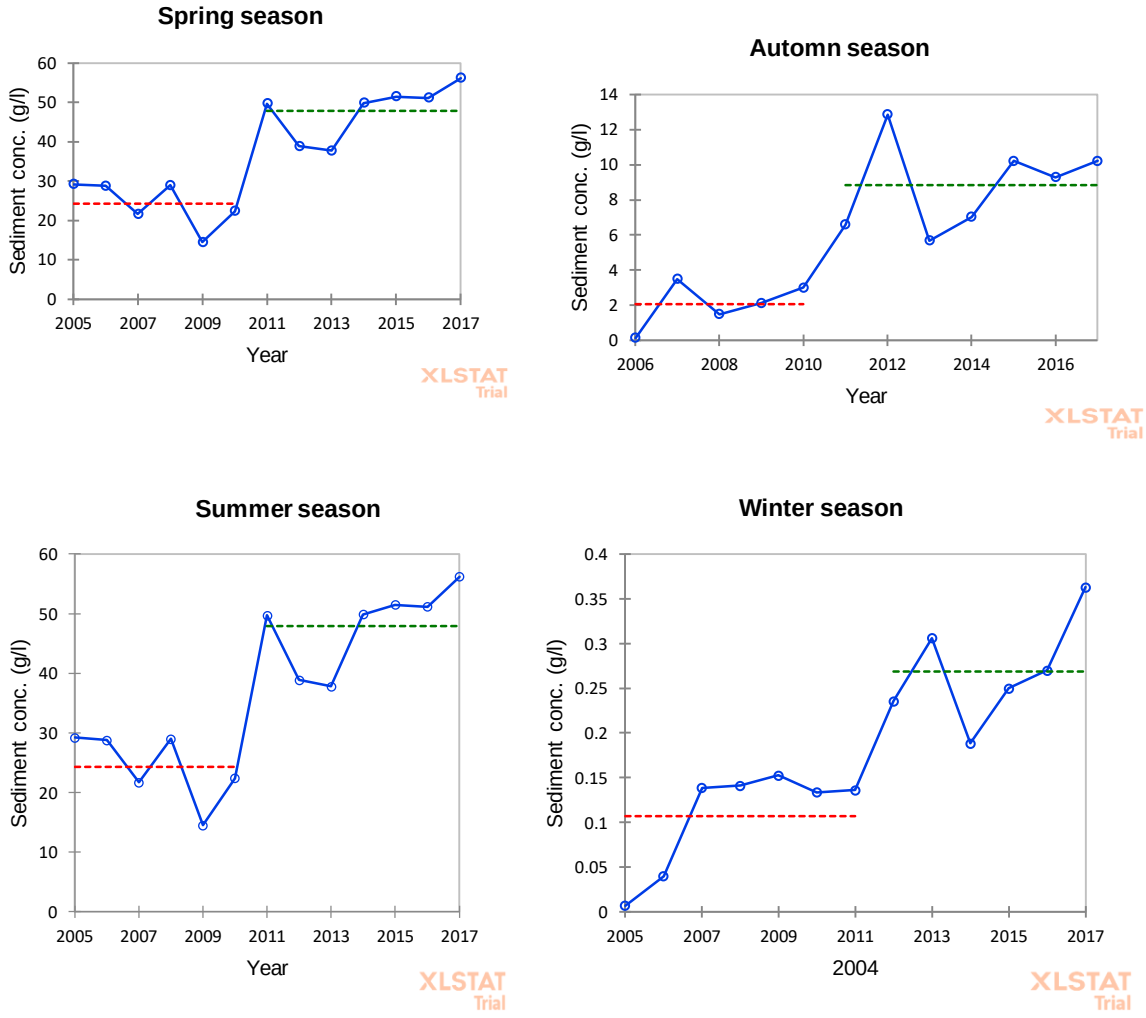

Fig.26: The homogeneity and trend of the seasonal sediment concentration in the upper Tekeze basin under the existing weather condition

The statistical analysis of both the homogeneity using the Petit test and the trend using the MK- test were statistically significant at 95 % interval of confidence. As the graphs show the year at which significant and abrupt change of sediment concentration seen in the basin is after 2011. The seasonal trend of sediment yield for the time series on 2004 – 2017 for the upper Tekeze basin is presented in Fig.27.

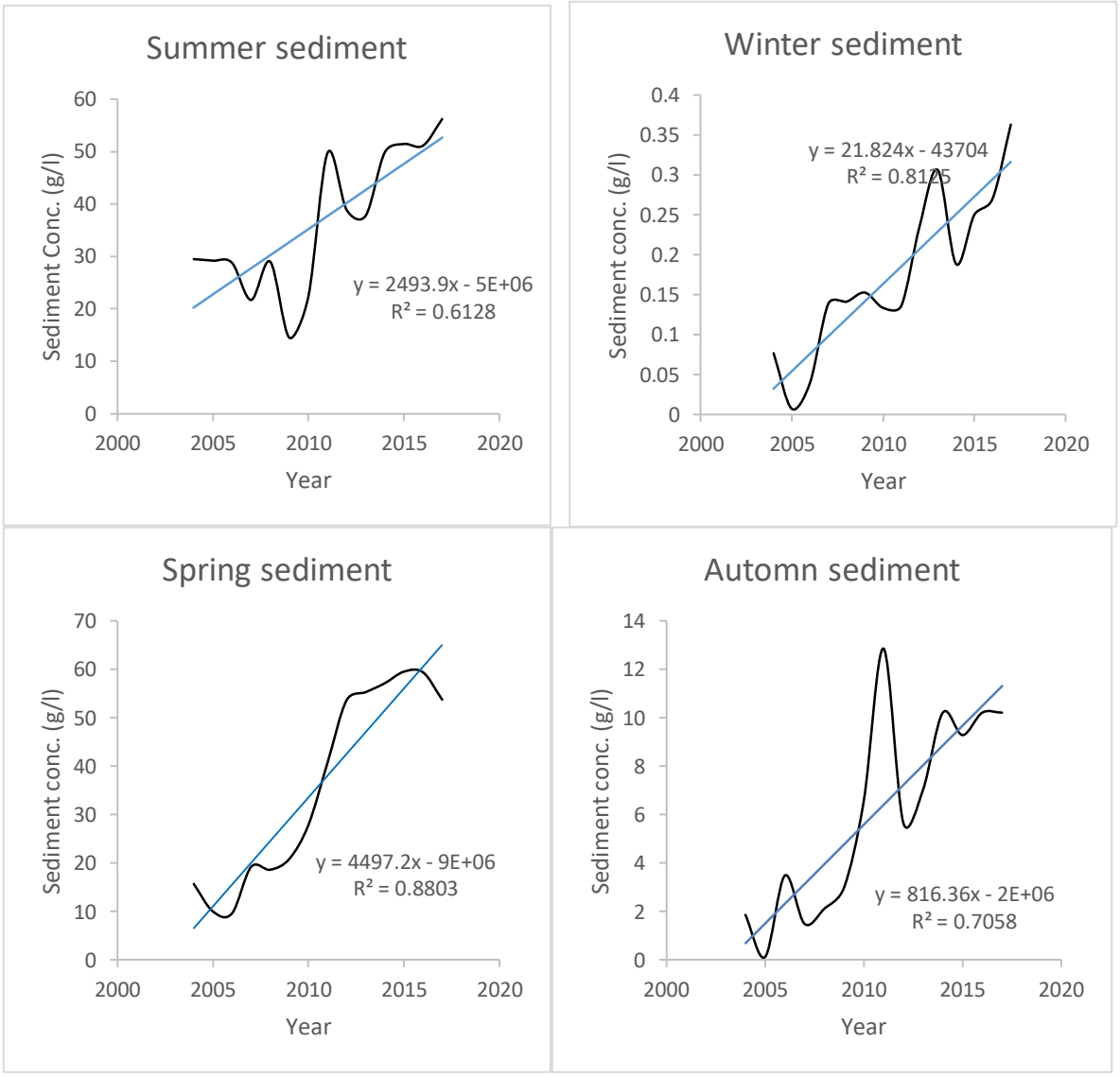

Fig. 27:Trend of seasonal sediment yield for the time series on 2004 – 2017 for the upper Tekeze basin

4.5.3 Correlation between climate and sediment yield

The variability of the monthly, annual and seasonal average sediment concentration at the Tekeze hydroelectric dam together with the rainfall and temperature in the basin were evaluated. Correlation and regression analysis between these sediments and climate variables were also evaluated. Accordingly, the Pearson correlation between the average rainfall and sediment concentration values for the spring, summer, autumn and winter seasons were computed to be 0.39, 0.21, 0.09 and 0.19, respectively. Higher and lower correlations were found during the spring and winter seasons, respectively. The values for coefficient of determination (R^2) of the linear regression analysis assuming the sediment concentration as dependent and rainfall as independent variable were 0.02 and 0.03 for spring and summer, respectively.

4.6 Selecting best sediment management scenarios in upper Tekeze basin

4.6.1 Sediment yield under different management intervention

Based on the inputs, the upper Tekeze basin was delineated in to 29 sub basins and 108 HRUs. The LSUA-SWAT model performed well in simulating the sediment yield at Tekeze hydroelectric dam. The observed average sediment yield at the outlet of the upper Tekeze basin (Tekeze hydroelectric dam) was 3.87×10^5 tyr^{-1}. The LSUA-SWAT model predicted 4.25×10^5ton yr^{-1} for the existing conditions. The NSE, RSR, PBIAS, and R^2 values during the calibration were 0.84, 0.23, 10% and 0.79, respectively. The model was performed poor in capturing the peak sediment hydrograph (Fig. 20).

4.6.2 Comparing efficiency of sediment management scenarios

Upper Tekeze basin was found with extreme soil erosion and sediment transportation. The sediment yield at the upper Tekeze basin was simulated using LSUA-SWAT model under different sediment management scenarios. The simulation results indicated various sediment yields for various sediment management scenarios. This variability was seen at the basin level.

Table 8: The possible percentage (%) of annual sediment yield reductions as the sediment management types from the Upper Tekeze basin at the outlet of the Tekeze hydroelectric dam

Scenario used	Mean reduction (%)	Standard deviation reduction (%)	Coefficient variation (%)	Minimum reduction (%)	Maximum reduction (%)
Scenario 1	27.20	8.21	30.20	11.26	41.50
Scenario 2	28.02	8.12	28.98	12.27	42.16
Scenario 3	38.24	7.90	20.67	18.25	50.70
Scenario 4	29.44	6.12	31.57	21.86	46.24
Scenario 5	9.48	6.89	72.72	0.97	28.36

The simulation of LSUA-SWAT model with different sediment management scenarios provided different results. The simulation to the introduction of filter strip scenario in to the upper Tekeze basin reduced the current annual total sediment yield ($4.25*10^5$ton ha^{-1}) by 27.20% on average. The simulation of sediment yield with assumption of strip cropping agricultural systems and stone bund/parallel terracing on non-agricultural land reduced the annual sediment yield by about 28%. The simulation of sediment yield by introducing stone bund/parallel terrace in the whole basin was reduced the annual sediment yield by 38.24%. The stone bund/parallel terracing integrated with reforestation scenario that is constructing stone bund/parallel terraces on the land below 30% slope and the reforestation on the land

above 30% slope was capable reducing the current annual sediment yield by 29.44% on average. Apart from these physical/integration with biological soil and water management practices, the biological soil and water management (reforestation on none crop land) was simulated and consequently 9.48% reduction from the current annual sediment yield was computed.

CHAPTER FIVE:
DISCUSSIONS

This section holds basically the discussion related to direct and indirect application of linear spectral unmixing remote sensing technology for estimating sediment in Tekeze River system. Application of LSUA for direct estimation of suspended sediment concentration (SSCs) and comparative analysis with empirical remote sensing, integration of LSUA model with SWAT for mapping sediment yield and application of LSUA integrated SWAT for evaluating effect of climate on sediment yield and selecting best sediment management option among scenarios are presented in this section.

5.1 LSUA for modelling suspended sediment concentration

5.1.1 Spectral profiles of water, sediment concentration and correlation

The distilled water was relatively with higher reflectance at the starting of the wavelength range used (375 – 1075 nm) with continuous decreasing trend. This finding was not different from previous studies (eg. Zhang et al., 2009; Röttgers et al, 2010; Ma et al.,2019;) saying pure water has higher reflectance at the blue portion of the visible part of the spectrum and virtually no reflectance in near infrared wavelengths range and beyond. Unlike to the spectral properties of the pure water, the reflectance values of the dry sediments from the Tekeze Rivers were continuously in increasing trend in all sediment types along the whole wavelength used (325-1075nm). Relatively, higher reflectance values were found to the sediments from the Tekeze main River than the Tsrare River in the upper tekeze River basin.

The spectral signatures of the sediment types were varied based on the colour, grain size distribution, level of concentrations and wavelength ranges. The reflectance showed an increasing trend from coarser to finer grain sizes across the wavelength range (325-1075nm) and relatively highest reflectance magnitude was found from the natural grain size distribution (Fig. 7 & 8). Moreover, the reflectance was consistently increased as the level of SSCs increased. In the considered sediment types, overlapping reflectance values were observed in the wavelength ranging 325 - 450 nm and 950 - 1075 nm. But, an acute and distinct difference in reflectance values were observed in the wavelength ranging from 450 to 950 nm. This indicate that the possible wavelength range for studing the level of SSC in upper Tekeze basin is 450-950 nm. But, the peak and clear variability of reflectance due to sediment types were observed at SW-NIR wavelength ranging from 750 to 950 nm in all levels of SSCs. This finding is consistent with many studies done in different areas (Novo et al., 1989; Bharrgava and Mariam, 1992; Doxaran et al., 2003).

The corelation between the SSC variables and reflectance in the Tekeze River was based on the variabilities of the level of concentration, grain size, and colour types as well as due to the wavelength variations. In general, reflectance increased as the grain size of the suspended sediment dropped from sand to clay sediment type and comparatively higher reflectance was presented in the natural grain size sediment concentrations. This shows that the mixing of different grain sizes in water can increase the absolute values of reflectance from the sediment solutions. The same result has been reported by other researchers (e.g. Doxaran et al., 2003; Chu et al., 2009). This can imply that mixing different sediment grain

size in water can increase the surface area of the solid sediments in water which has lower transmission and absorption but higher reflecting optical properties.

The spectral reflectance for all sediment types gradually increased with the wavelength in the 450 nm to 650-700 nm wavelength range, but progressively decreased with increasing wavelengths in the 700 to 950 nm wavelength region. Here, the rate of change in reflectance was not consistent in all sediment types and the whole wavelength. These make applying reflectance directly for estimating the SSCs difficult. Moreover, despite the higher reflectance values from the natural grain size distribution, the Pearson correlation between their level of concentrations and the reflectance were found comparatively very small. This evidenced that higher reflectance values may not mean a higher concentration of sediment. Moreover, the strength of correlation between the reflectance and SSCs were also varied based on the wavelength range used. Relatively higher correlations (Rs>0.7) were found between reflectance and the SSCs in the wavelength ranging 750-950 nm (B_5) than in the remaining wavelength ranges. This result was consistent with the studies in Yangtze River in which near-infrared (NIR) was found to be the best indicator of water turbidity (Wang et al., 2009b; Wang and Lu. 2010).

Nonlinear regression was found the best fit for the relationship between the reflectance and sediment concentrations from the upper Tekeze River. This finding was in line with Ritchie et al. (2003), and Pavelsky and Smith, (2009) that they found a nonlinear relation when the sediment concentration increased. The daily SSCs occurred in the upper part of the Tekeze River specifically at the immediate inlets to Tekeze hydroelectric dam were varied from the lower concentration 2 g/l to higher concentration 68 g/l. Therefore, the correlation between

SSC and reflectance must be validated before building a reliable model for the remote sensing of SSCs.

5.1.2 Comparing empirical and LSUA remote sensing models

Relatively more scattered curves were found between the SSCs and respective mixed reflectance values (Fig. 9) than the curves between SSCs and respective SMCs (Fig. 10). The more scattered curves from SSCs and respective mixed reflectance values showed that absence of distinct mixed reflectance values for different sediment concentration. This means that possibilities of getting different mixed reflectance values for the same level of SSCs and the viceversa in the River systems are higher. This was attributed to the variability of the inherent optical properties of the sediment tyepes in the River systems. This can be potential source of errors in sediment studies if we apply the empirical remote sensing which does not consider effects from the IOPs. Unlike the direct use of the mixed reflectance in the empirical remote sensing approach, applying the SMCs drived from based on the inherent optical property of each sediment types has minimized the scattering of the curves due to changes in sediment type. The curves from between the SSCs and respective SMCs were overlapped one over the other (Fig.10). This implied that the sensitivity of SMC values to the changes of sediment type in Rivers was found less compared to the mixed reflectance values. Hence, the accuracy of sediment concentration studies using remote sensing can be enhanced if the SMCs values are used instead of the mixed reflectance values.

The exponential equations fitted to the relation between SSCs and reflectance (Eq. 38) and SSCs and SMCs (Eq. 39) to the sediment types deposited in the Tekeze and Tsirare Rivers

were validated using insitu measurements of reflectance and SSCs of turbid flash floods in the Rivers. During the laboratory experiment, performance indicators of the generated empirical (R^2=0.76, RMSE=±10.87g/l in the main Tekeze River and R^2=0.81, RMSE=±2.65g/l in Tsirare tributary River) and LSUA remote sensing models (R^2 = 0.92, RMSE = ±0.76 g/l in Tsirare River and R^2 = 0.91, RMSE = ±0.73 in the main Tekeze River) were not equal. The LSU model (Eq. 39) has fitted better than the empirical model (Eq.38). Moreover, during the validation of the models using the insitu reflectance of the turbid flash floods in the Rivers, the model performance indicators of the empirical remote sensing models previously seen in the laboratory were not achieved. The remote sensing models have even performed below the accepted ranges. Especially, when the level of SSCs increased, the estimation using the empirical model was also more deviated from the observed SSCs of the Rivers. This can evidence to that empirical remote sensing models developed from the regression analysis between the known SSCs and reflectance is less accurate and non-universal in simulating SSCs. Such models only work to the site and time specific predictions of SSCs with reasonable accuracy. But it is limited in its universal application and may not extend to the full range of conditions present in the River systems. This indicates that the relation between SSCs and reflectance are sensitive to grain size, geological colours variabilities of sediment and level of sediment concentration. This finding is consistent with different investigation in other River systems (E.g. Islam et al., 2001; Ma and Dai, 2005; Chu et al., 2009; Wang et al., 2009; Wang et al., 2010; Wang and Lu, 2010).

Unlike the empirical model, the LSUA model was consitently performed in capturing the variability of sediment concentration in both Rivers. Hence, the LSU remote sensing-based simulations of SSCs were well fitted to the measured SSCs than the estimation by the empirical model. This showed that the LSU method is relatively accurate and less sensitive to the variability of grain size, colours and level of sediment concentrations. The researches by Oyama et al. (2007, 2009) on the remote sensing of non-phytoplankton suspended sediments demonstrated that the spectral mixing modelling approach (R^2 = 0.96) estimated non-phytoplankton suspended sediments (1mg/l to 100 mg/l) more accurately than the traditional empirical model for the same sediment concentrations.

5.1.3 Comparing the empirical and DLSUA models

Unlike the ground remote sensing in the above, the space based remote sensing (using the sensors in satellite) is the most crucial and cost-effective application of remote sensing technology. Coarse (temporal, spatial, spectral and radiometric) resolutions of sensors, intervention of atmospheric conditions, absence of accurate geo-referencing of multi and hyper spectral images are some of the challenges. These challenges together with multiple factors affecting reflectance in flowing water kept satellite based remote sensing less effective technology in sediment monitoring and management practices.

The endmembers (turbid water, rocky and bare lands) in the targeted pixels were characterised to have different reflectance values and unequal reflectance weight contribution to the recorded reflectance values (Fig. 18). Many researchers (eg. Liu et al., 2003; Zhang et al., 2006) have reported the variability within an endmember class (intra-class variability) and the similarity among endmember classes (inter-class variability) are

the common endmember variabilities identified. It is because of this, the critical step in LSUA is selecting the types, numbers and the corresponding spectral signatures of endmembers (Elmore et al., 2000; Theseira et al., 2003). This difference together with coarseness of the remote sensing data leads to endmember fraction images that are physically inaccurate.

To minimize the errors in estimating SSCs using the space based remote sensing (eg. MODIS imageries), we have developed a new subpixel analysis approach called *Double Stage Linear Spectral UnmixingAnalysis* (DLSUA) and its performance were evaluated and compared with the commonly applied empirical remote sensing approach. The DLSUA approach was successfully improved the estimation of SSCs at the Tekeze main River (R^2 = 0.90 and RMSE = ±5.38) and its tributary the Tsirare River (R^2 = 0.76 and RMSE =±14.54) from that of empirical regression remote sensing model performed at (R^2 =0.78 and RMSE =±14.17) and (R^2 = 0.69 and RMSE= ±18.22) for the Rivers, respectively. Hence, this study indicated accurate SSCs quantification by means of space remote sensing depends on detail analysis of the optical properties of the constituents existed in the mixed pixels.

The DLSUA were successful in managing such variabilities. Near to real SSCs in Tekeze River were estimated from MODIS surface reflectance using the DLSUA modelling approach. Compared to the in-situ SSC measurements and direct regression (empirical model) methods, the DLSUA remote sensing approach was found advantageous. (1) DLSUA was fewer sites and time-specific, because the independent variable used in the spectral unmixing model almost significantly varies with SSC concentrations and is less affected by the other constituents. Therefore, a model can be constructed in advance using a

controlled experiment in the laboratory or a simulation can be achieved in advance by using a radiative transfer model of natural waters. (2) It is convenient to combine the bands information and to control the effect of confounding factors. (3) It was convenient to use imageries with coarse resolution in small Rivers.

In general, this research presented a methodology to estimate SSCs in Flash floods from MODIS data. The key to successfully apply the Double Stage Linear Spectral Unmixing based estimation of SSCs from satellite data is to identify the component/end-member and optical properties of each component and determining the mixing coefficient of each component is important. But the following points must be furtherly investigated. (1) For nonlinear combination of components/end- members in a spectral mixture modelling approach for a water body. (2) This study ignored factors such as shape, organic substances and chlorophyll that can affect the optical characteristics of turbid waters.

5.2 Integrating LSUA and hydrologic models

Apart from the direct application of remote sensising as in the above section (5.1) the LSUA remote sensing approach can be used indirectly for complementing the sediment yieldmodellingusing the hydrologic models. Remote sensing is potential in monitoring and preparing input data for hydrologic models. Even we have ground to say no one can think about applying conceptual or physically distributed hydrologic models without the remote sensing and GIS technology. The C-factor is one of the required inputs in hydrologic models for predicting sediment yield. This parameter has been determined commonly using the field measurement, and remote sensing (eg. land use classification, NDVI and its

derivatives). But these approaches have multiple drawbacks. Hence, in this research we have discussed another approach called LSUA and its capability to capture the C–factor variability in place and time. An effort was also made to change the assignment of C–factor in to HRUs instead of to land use type units in SWAT.

5.2.1 Characterizing spectral signature and abundance of ground covers components

As in many studies (eg. Tompkins et al., 1997; Elmore et al., 2000) stated, themost difficult and may be the key step to successful LSUA is appropriate endmember selection. Selecting endmembersinvolves identifying both the number and type of endmembers andtheir corresponding spectral signatures. Too manyendmembers or endmembers that are spectrally similar lead toendmember fraction images that are physically inaccurate as judged.

Hence, after continuous field assessment using a portable reflectance measuring tool the vegetation, bare soil, rock, and water bodies were identified as the principal ground cover components (endmembers) in the upper Tekeze basin. As in the result section presented, the spectral values of each endmembers under the six bands (2-7) of Landsat 8 acquired at the wet season of 2016 were not consistently the same. Especially, the reflectance values for each of cover types were well separated in the wavelength ranges in between band 4and band 6. But, in the remaining bandsthe reflectance curves for the different ground cover types were overlapped. Similar results were found from the onsite reflectance surveyusing the spectroradiometerfor the same ground cover types (Fig. 28).

Fig.28: Photo during the field survey of reflectance from different land uses in Upper Tekeze using the Spectroradiometer. Photo in A and B were examples for bare soil and vegetation cover types respectively

This finding implied that the bands in Landsat images are not equally applicable for identifying the ground cover typeson the earth surface. In line with this finding, the investigations by Assis and Omassa (2007) inPhilippines and Song et al. (2011) in China have found the band 3- band 5 from the same Landsat image werethesensitive wavelength ranges for the same ground cover types. The slight deviation of the current study from literature may be due to reflectance values of cover types are area specific.

Based on the spectral signature profile, the spatial abundance of the principal ground cover components in the upper Tekeze basin were computed and mapped. The maps showed high spatial variability of each ground cover types. In general, the vegetation abundance in the basin is extremely diminished; even the valley bottoms and Riverbanks are highly barned. The vegetation covers in the study area were mostly limited to the cereal crops grown in the cultivated land and to the scrambled vegetation on the steeply and inaccessible lands.

Significant part of the basin was found to be under the cover of rocky which might be negative for sediment detachment rate. This was evident that unless the land is covered with rock, water, non-natural vegetation (crop), the soil is remained bare and exposed for sever soil erosion.

After identifying the cover types/endmembers in the basinand mapped their spatial distribution using the LSUA, we have computed the spatial C-factor values in the basin. The C-factor values from the LSUA on selected locations were compared with the C-factor values on the same location and evaluated if there were significant variation in between. Accordingly, the C-factor values estimated using LSUA was relatively consistent and not significantly deviated from the mean values of the field measurements suggesting that the range was reasonable. But, the C-factor values were significantly varied among and within land use-types in upper Tekeze basin. The variations were related to the spatial variability abundance of the principal ground covers in the basin. These tell us that LSUA is effective in monitoring and mapping the detail variability of C-factor of large geographic areas. Hence, LSUA can be used to determine C-factor for larger geographic area from coarser remote sensing images. Other investigators (eg. de Assis and Omasa, 2007; Meusburger et al., 2010) have also convinced the potential of such spectral unmixing (SU) in determining C-factor from coarser imageries.

5.2.2 Performance of LSUA integrated SWAT in predicting sediment yield

The finding can be evaluated based on the three-criterion recommended by Van Griensven et al. (2012). These criterions are fitness to observations, fitness to reality and fitness to purpose. Fitness to observations refers to the difference between the observed and

simulated values. Fitness to reality evaluates how well a model represents the physical process while maintaining parameters within their meaningful range and fitness to purpose accounts on how well certain watershed characteristics which the model output is needed to address are taken into consideration. Based on the model fitness to observations criteria models are considered fit if NSE >0.5 and RSR≤ 0.7, and if PBIAS is ±25% and ±55% for flow and sediment respectively (van Griensven et al., 2012). Moriasi et al. (2007) indicated NSE between 0 and 1 are generally viewed as acceptable. According to these criterias, the simulations using the conventional and modified SWAT were under acceptable range.

However, as presented in the above section, C-factor could not be consistent even within the same land use types. Not only in this research but also many findings from different areas were in line with this finding (eg. de Assis and Omasa, 2007; Song et al., 2011). But the conventional determination and assigning of C-factor has been ignored this variability and considered a homogenous C-factor map without any spatial variation that can be existed within land use unit types. Consequently, the prediction and mapping of sediment yield using SWAT and other hydrologic models which used such approach can have many uncertainties. This problem is critical especially in semi-arid areas like upper Tekeze basin where vegetation is scarce and land use plan is missed.

Hence, the C-factor estimated using LSUA from Landsat images of the study area was integrated in to HRU in SWAT which was conventionally assigned to the corresponding 'crop.dat' based on the land use/land cover type units. Such approach has advantages of widening of spatial variability and then improving the accuracy of sediment prediction using the SWAT. The estimations of sediment yield from the upper Tekeze basin at the

outlet of Tekeze hydroelectric dam using the conventional SWAT and the modified (LSUA-SWAT) were compared against the time series daily sediment yield. Not only this, the performance of the modified SWAT was compared against the performance of previous studies which used the SWAT. The NSE, RSR, PBIAS, and R^2 between the measured and the simulated sediment using the conventional SWAT were computed to be 0.72, 0.39, 34.2% and 0.68, respectively. While in between the measured and the simulation using LSUA-SWAT (modified) were 0.84, 0.23, 10% and 0.79, respectively. These values indicate the fit between the model sediment predictions using the modified SWAT and the observed sediment yield were improved compared to the predictions by the conventional SWAT.

Many studies predicting sediment yield with the conventional SWAT in Ethiopian River basins published in international journals were also reviewed (eg. Betrie et al., 2011; Steenhuis et al., 2009; Setegn et al., 2010; Ayana et al., 2012; Kositsakulchai et al., 2012; Assegahegn &Zemadim, 2013; Gebremichael et al., 2013; Mamo & Jain, 2013; Ayele et al., 2017 and …).According to these literatures, the performance of the conventional SWAT was found to be in between satisfactory and good status. A study by Yesuf et al., (2015) in the Tekeze basin was also found only a satisfactory SWAT performance.According to Yesuf et al., (2015), the model evaluation statistics suggested that SWAT was extremely under-predicted the peak sediment loads in both calibration and validationperiods.The performance of the LSUA integrated SWAT in predicting sediment yield showed an improvement over the conventional SWAT from previous related studies in Ethiopia.

In general, the modified SWAT performed well in capturing the variability of daily sediment yield compared to the conventional SWAT tested in this study and compare to the previous studies in the basin and outside the basin. This can realize that the impact of vegetation and other ground cover components on sediment transport and considering them appropriately is highly important. Similar to this finding, the critically review by Griensven et al (2012) to the studies in the Nile River basin which used SWAT for modeling hydrologic processes summarized that the critical sources of errors in SWAT is the poor parametrization of vegetation.

The LSUA integrated SWAT computed sediment yields for each sub basin and saved the results in the files of 'output.sub'. By dividing these values for the area of a computation unit and its related soil delivery ratio, it was possible to obtain the soil erosion intensity of each sub-basin in the upper Tekeze basin. The sediment yield levels in the basin were classified into lower (10–20 t ha^{-1} yr^{-1}), moderate (20–70 tha^{-1} yr^{-1}), higher (70–136 $tha^{-1}yr^{-1}$) and extremely higher (above 136 tha^{-1} yr^{-1}) categories. This classification was made according Hurni (1983 and 1985). Accordingly, the sediment yields in the upper Tekeze sub-basins werevaried from 15 to 267tha^{-1} yr^{-1}. Lower sediment yield was computed only from three sub basins while the remaining sub basins were computed to have moderate and above moderate status of sediment yield. This indicated that major part of the basin is under intensive soil erosion status. The high sediment yield production rate predicted in the sub-basins may be attributed to the presence of wider bare-land and the lack of forest cover (especially in the higher sloping lands) intensive and planned agricultural practices.

5.3 Trends and correlation between climate change and sediment yield

5.3.1 Trend of climate variables

The variability of climate in the major seasons in the study area including the summer or wet season (June–August), winter or called dry season (December– February), the autumn mostly called harvesting season (September – November), and the spring called short rainy season (March–May) were considered in this study. Results of the trend analyses (MK - test) were used to identify if the time series of annual and seasonal rainfall had a statistically significant trend during the last 50 years. Accordingly, the results from the analysis have depicted that there were no significant trends in the major climate events (rainfall, maximum and minimum temperature) of the basin both at annual and seasonal scales. The statistical indices of the test revealed a tendency of decreasing annual rainfall pattern. At the same time a decreasing of rainfall was observed in the summer, spring and winter seasons while an increasing of seasonal rainfall pattern at the autumn was observed. However, these trends have found to be nonsignificant. This findingis consistent with the finding in literatures (eg. Gebremichael et al., 2017). According to these literatures, though there is significant increasing and decreasing trend of rainfall in some stations, majority of the stations in the basin are under non-significant trend of rainfall. Due to data absence, the current and previous researches have not studied the trend of rainfall in finer time scales.

Like to the rainfall analysis in the above, the MK trend test on the average maximum and minimum temperatures (Tmax& Tmin) have shown that there are no significant trends in the basin both at annual and seasonal time scales. But, the statistical indices of the test revealed a tendency of increasing at annual and seasonal time scale. A decreasing tendency

has found on the Tmax of the summer season only. This finding is consistent with the finding in literatures (eg. Gebremichael et al., 2017). According to these literatures, though there is significant increasing and decreasing trend of temperature in some stations, majority of the stations in the basin are under non-significant trend oftemperature.

5.3.2 Changing point and Trend of sediment yield

The variability of trends of sediment concentrations in the upper Tekeze basin during the time interval 2004 – 2017 simulated using the modified SWAT at the annual and seasonal time scale were evaluated using MK test and Petit homogeneity test. This was done at monthly, seasonal and annual time scale. Hence, the statistical indices and significance level of the test revealed an abrupt and significant increasing trend of change in sediment concentration. This was true at the monthly, seasonal and annual time scale. This seems illogic if one knows the massive soil and water management mobilization in the northern Ethiopia. But there are researches in line with the current research indicating that still sediment is higher in the area (eg. Tamene et al., 2006; Guzman et al., 2013; Haregeweyn et al.,2006, 8 & 15). Consequently, this can be a base to argue for the inefficiency of the soil and water management practice on mitigating sediment yield in the area.

The Pettit test was also applied to identify if there is a changing point in the data series. Accordingly, unlike the climate variables, a significant breaking point in the data series of sediment concentration was found in the monthly, seasonal and annual simulated sediment concentration. The Petit tests have shown statistically significant breaking points. As the graphs in the result section (Fig. 25) showed the year at which a significant and abrupt

change of sediment concentration seen in the basin is after 2011.This may be related to the before and after the construction of the Tekeze hydroelectric dam (TK_5) in the basin.

5.3.3 Correlation between climate and sediment yield

The variability of the monthly, annual and seasonal average sediment concentration at the Tekezehydroelectric dam together with the rainfall and temperature in the basin were evaluated. Correlation and regression analysis between these sediment and climate variables were also made. As the discussion in the above sections indicates, even though the climate variables (rainfall and temperature) in the study area are under non-significantincreasing and decreasing trends, the sediment yields were found to be under significant increasing trends. The correlation showing the associationbetween the sediment concentrations and the rainfall at annual and seasonal scale was found to be lower. The values for coefficient of determination (R^2) of the linear regression analysis assuming the sediment concentration as dependent and rainfall as independent variable were not that much higher. These all findings assure that sediment transportation in the basin is not control only with increasing and decreasing of rainfall abundance. There are many other variables of rainfall (eg intensity) computed from finer data resolution that can contribute more for the variability of sediment transportation.

There are also factors other than the climate which control the extent of the sediment concentration in the study area. The Petit test for example has shown statistically significant breaking points on the sediment data series on 2011. As the graphs in the result section (Fig. 25) showed, the year at which a significant and abrupt change of sediment concentration seen in the basin is after 2011. This may be related to the before and after the

construction of the Tekeze hydroelectric dam (TK_5) in the basin. Due to the coming of the $Tk_5$the socioeconomic activities in the area are expected to increase. Consequently, this might be a reason for land use dynamics and then to the abrupt increasing of sediment concentration entraining to the dam. The peaks of sediment yield were not exactly confined with the peak period for water yield in the basin. It occurred early before the peak of water yield period on the basin. This shows that sediment yield is well determined by the abundance of rainfall instead of by the water yield. This finding was in line with many studies (eg. Kantoush &Sumi, 2013).

5.4 Sediment management in Upper Tekeze basin

5.4.1 Sediment yield at Tekeze hydroelectric dam

The LSUA integrated SWAT computed sediment yields for each sub basins in Upper Tekeze basin. According to the prediction using LSUA integrated SWAT, sediment yield in upper Tekeze basin varies from 15 to 267tha^{-1} yr^{-1}.This implied the Tekeze hydroelectric dam (TK 5) constructed to collect about $9*10^9m^3$of water from 30,390km^2 drainage area of upper Tekeze basin for generating 300MW has been facing and will be continued to face challenges from higher sediment entrainment. Though analyzed from inadequate data, Aforki (2006) has reported that only 25 years are enough for phasing out of the dam constructed with huge investment cost. The extreme spatiotemporal instability of climate and weather (Mengistu and Sorteberg, 2012; Michale and Semu, 2015) and human induced pressures are resulting rapid transition of naturally vegetated land into intensively cultivated land (Humphreys et al., 1997). These are the basic causes for

abundant and variable sediment yield in the basin. This evidenced that the need for more effective sediment management interventions.

5.4.2 Comparing sediment management scenarios

The simulation of sediment yield with LSUA-SWAT model under different sediment management scenarios provided different results. These variabilities were both at the sub basin outlets and at the whole basin's outlet. Due to lack of observed sediment data at sub basin level it was impossible to calibrate and validate the model at the sub basins level. So, the sediment yields at the sub basins were simply based on the simulated results.

The introduction of filter strip scenario in to the upper Tekeze basin reduced the current annual \total sediment yield ($4.25*10^5$ton ha^{-1}) by 27.20% on average. The simulation of sediment yield with assumption of strip cropping agricultural systems and stone bund/parallel terracing on nonagricultural land reduced the annual sediment yield by about 28%. This efficiency was consistent with the dominant literature values in different areas (White and Arnold, 2009). But, some deviation from some other investigations indicating that filter strip at basin scale is more efficient than the result in this study (Betrie et al., 2011; Hould-Gosselin et al., 2016).

The simulation of sediment yield with assumption of stone bund/parallel terrace in the whole basin was reduced the annual sediment yield by 38.24%. The stone bund/parallel terracing integrated with reforestation scenario that is constructing stone bund/parallel terraces on the land below 30% slope and the reforestation on the land above 30% slope was capable in reducing the current annual sediment yield by 29.44% on average. The

efficiency of stone bunds/parallel terraces on sediment yield reductions were relatively lower compared to the results in previous investigations (Herweg and Ludi, 1999; Gebremichael et al., 2005). Herweg and Ludi (1999) reported 72%–100% sediment yield reductions by stone bunds at plot scale in the Ethiopian and the Eritrean highlands. Gebremichael et al. (2005) reported 68% reductions of sediment yields by stone bunds at the field scale in the northern part of Ethiopia. But comparable results were reported at larger scales (Betrie et al., 2011). Betrie et al. (2011) reported 41% reduction of sediment yield by the same sediment management practices at basin level of the upper Blue Nile. Hence, it seems important to note that the scaling effect between a field and large scale is critical factor in selecting sediment management practices. Moreover, the targeted slope length reduction (spacing interval of the management measures) is the other factor causing efficiency variability of stone bund/parallel terracing.

Apart from these physical/integration with biological soil and water management practices, the sediment yield was simulated assuming the biological soil and water management (reforestation on none crop land) introduced to the basin and consequently 9.48% reduction from the current annual sediment yield was computed. This lower efficiency of reforestation in the upper Tekeze basin could be attributed to the size of the implementation area we assumed. We only assumed to nonagricultural land in upper Tekeze basin (15.1%). Hence, it is indicative that most of the sediment yield at the outlet of upper Tekeze basin is from cultivated land. This result agrees with the previous investigations (Hengsdijk et al., 2005; Descheemaeker et al., 2006; Betrie et al., 2011).

CHAPTER SIX:
CONCLUSIONS AND RECOMMENDATIONS

6.1 Conclusions

Recently, space, air and ground-based remote sensing has become a versatile technology to characterise, map, analyse and model sediment concentration with minimum cost and reasonable accuracy. The application of remote sensing for monitoring and modelling sediment concentrations and management mainly focused either on direct estimation of sediment loads and/or indirectly through parametrizing hydrologic models. Despite of these potentials, the spatial, temporal and spectral resolutions of most sensors are too coarse to capture sediment variabilities in River systems. The ground- and space-based sensors provide mixed reflectance values at a specific area of place (pixel), time and spectral resolution. The spatial pixel sizes of most remote sensors are often large enough that numerous disparate substances can contribute to the spectrum measured from a single pixel. Hence, the accuracy of remote sensing technology in monitoring and modelling sediment depends on the types of approaches used during the analysis. Conventionally, classification and regression/correlation analysis of the mixed spectrum in a pixel and\or reflectance values against a targeted sediment variable has been the approach commonly used with remote sensing technology for modelling and monitoring purposes. This might present general knowledge about the targeted variable, but it may not yield any further insight into the other substances that might also reside within and around the boundaries of the pixel. Consequently, the desire to extract spectrum of the materials in the mixture, as well as the proportions in which they appear, is important for numerous tactical scenarios in which sub-pixel detail is valuable.

Sediment transportation and deposition is a major river basins' problem causing irreversible impacts on socio-economic and environmental affairs. It remains the main challenge of water and energy development efforts in Ethiopia. However, the sediment transportation rate and its linkage with climate and responses to different sediment

management scenarios are inadequately studied and documented. This is mainly due to the cost ineffectiveness and inaccuracies of the conventional sediment monitoring and modelling campaigns. The decline in the number of stations, data quality and data holding policy has made sediment data less reliable for use in operational purposes. Even though Ethiopia is one of the countries with very poor in sediment data, the potential of remote sensing technology had not been exploited in sediment studies of Rivers. Hence, introducing better performing remote sensing technology to Ethiopian river systems could be of crucial importance for improving understanding and decision support systems. The main hypothesis of this dissertation was that the spectral unmixing (sub-pixel) analysis approach can enhance the accuracy of coarser remote sensing resources for monitoring the suspended sediment concentration and improve the sensitivity of hydrologic models in simulating the response of sediment transport to scenarios of climate change and management alternatives. After this research the following conclusions have drawen.

- The essential part for determining SSCs using remote sensing is the modelling approach that infers SSCs under variable conditions. Results in this study indicated that the spectral signatures of the SSCs in the Tekeze River were not consistent across the 325-1075nm wavelength ranges, grain size distribution, geological colours and level of sediment concentration. The effect of grain size distribution, geological colours and level of concentration variations in the upper Tekeze River significantly affected the relationship between SSC and reflectance. These variations together with the extreme variability of SSCs limited the accuracy and universality of empirical remote sensing model for simulating the daily sediment concentrations in the upper Tekeze Rivers. Unlike the empirical remote sensing model, the linear spectral unmixing analysis (LSUA) remote sensing model was found to be less sensitive to variation in sediment types. But the model was sensitive to the level of sediment concentration variability in the rivers. Hence, the LSUA remote sensing model was found to be relatively accurate and universal in the River system for simulating the SSCs over the extensive reaches of the upper Tekeze basin. The LSUA model has estimated SSCs of the Tekeze river from high-

resolution ground remote sensing data with an average statistical performance of R^2 = 0.92, and RMSE = ±0.75g/l in the Tekeze River. In general, this research has noted that application of remote sensing for monitoring SSCs in river systems requires detail studies of the inherent optical properties of the constituents in the turbid water and then selecting appropriate modelling approach that works for dynamic sediment transport.

- The essential part for determining SSCs using space-based remote sensing technology is managing the spatial and temporal resolution problems of the remote sensing data. To minimize the errors in estimating SSCs from direct use of spatially coarse remote sensing data like the *Moderate-Resolution Imaging Spectroradiometer (MODIS)* imagery, we have proposed a new subpixel analysis approach called *Double-stage Linear Spectral Unmixing analysis (DLSUA)*. This approach was successfully applied in estimating the daily SSCs of the Tekeze River. The DLSUA model performed better (R^2 = 0.83 and RMSE ±9.96) than the traditional empirical regression (R^2 = 0.74 and RMSE ±16.2) analysis approach in quantifying the SSCs from MODIS data. Slight differences in the performance of the DLSUA model were observed for different spectral bands. The key to properly use MODIS images for estimating SSCs at temporally heterogeneous and small Rivers such as the Tekeze River is therefore to identify and consider the inherent optical properties of the micro and macro components/endmembers.
- The direct remote sensing (LSUA and DLSUA) models estimating SSCs from ground- and space-based remote sensing data can provide general insights about the quantification of daily SSCs in the river system. This could support the design and planning of adaptation strategies for dams and reservoirs. But the models are not informative about identifying the source areas within the basin. The decision support capability of such models for mitigating the extreme sediment transport in the River basin is less powerful. Instead, remote sensing has indirect application potential to study the sediment risk areas and causing factors through paramterizing the spatially distributed and temporally continuous hydrologic models. The hydrologic models have multiple advantages over field measurements and direct

application of remote sensing techniques. At the same time, the models also have multiple potential delimitations. One of the problems is that since most of these models are developed in/ for an area that has adequate measurement data for model parameterization, it becomes challenging to use the models in data-scarce areas. Hence, these models must integrate appropriately with remote sensing technologyand field measurement programs.In the Soil and Water Assessment Tool (SWAT), the parameter recommendations for the vegetation dynamic effects of soil erosion (C-factor) included in the SWAT database are empirical values from long-term experiments that may not be applicable everywhere due to differences in vegetation systems and management practices. The spatial representation of C-factors has been considered at the land-use unit level and this result in a constant C-factor value for a large geographic area. Thus, there is an inability to reflect the effect of spatial variation of vegetation on soil losses. Despite these problems with SWAT, none of the research in Ethiopia has made internal calibration nor used other spatially distributed data sources (e.g. remote sensing data). To the best of the researcher's knowledge, none of the studies in Ethiopia has used locally adapted vegetation parameters or considered the specific vegetation dynamics of Ethiopia. Therefore, modification of the SWAT C-factor is recommended to make this factor fit observations, reality and the purposes for which the SWAT model is being applied.

- This study evaluated the suitability of the linear spectral unmixing analysis (LSUA) method to assess the spatial C-factor. The study also tested whether SWAT performance can be improved by the integration of C-factor estimates using LSUA. The study estimated minimum C-factor in the upper Tekeze basin using remote sensing data acquired at the summer season when the plants vigorously grown and then integrated it into SWAT at the HRU level, not the land use level. In comparison with the C-factor values originally determined from literatures and considered in SWAT by land use type, this method increases the spatial variation of the C-factor values within the same land use, particular in a large area, enabling it to reflect the real scenarios of heterogeneous vegetation cover in a particular

geographical area. The finding in this study implied that the C-factor value could be determined as a function of the fractional abundance of exposed soil and ground cover derived using the LSUA technique. This technique was advantageous in determining the spatial variability of C-factor values within the same land-use types. This value was successfully integrated into SWAT and then enhanced its sensitivity in capturing the spatiotemporal variability of sediment concentration in the upper Tekeze basin. The coefficients including NSE, PBIAS, RSR and R^2 for sediment yield were 0.72, 0.39, 34.2 & 0.68, respectively, when the C-factor values were for the land-use type units of SWAT. When the C-factor was for the HRUs in SWAT, the corresponding values were 0.84, 0.23, 10, & 0.89. In general, this study implied that integrating LSUA C-factors into SWAT is appropriate for minimizing costs, while enabling the computation of local detailed and time-specific C-factors that fitted observed sediment yields in large basins. The sediment yield risk map based on the LSUA integrated SWAT illustrated instructive details helpful for prioritized interventions.

- The average rainfall and temperature over the basin have shown neither significantly increasing nor decreasing trends during the dry season, short rainy season, and main rainy season and in the annual values of the last four decades. In contrast, a significant increasing trend in sediment concentration at the Tekeze hydroelectric dam observed during the last10 years. The results showed that links between the trends in climate variables considered and the sediment concentration in the basin is not very strong. This suggests that the change in sediment yield is influenced by factors other than the climate variables. A weak relationship between rainfall and sediment concentration leads to the conclusion that the significant trends in sediment yield could be due to significant changes in catchment characteristics over time, including change in land use and/or land cover in the basin. Statistical trend analyses investigated only the trend of the climate variables and sediment yield data without being able to identify the causes of those trends. Therefore, further investigations are needed to verify and quantify the sediment transport changes shown in statistical tests by identifying the physical mechanisms

behind those changes. Further investigation is also required to analyse the association between climate variables and sediment at finer time scales.

- The LSUA-SWAT model was applied to model spatially distributed soil erosion/sedimentation processes at daily time steps and to evaluate the impact of different sediment management scenarios on sediment reductions in the upper Tekeze River basin. The model showed the best fit to observed sediment yield at the outlet of the upper Tekeze basin, which is useful information for effective designing and planning. The simulation results suggested that applying filter strips, stone bunds/parallel terracing, reforestation and the integration of two of these scenarios would reduce the current sediment yield to the Tekeze hydroelectric dam. Though some part of the efficiency variation could be related to the variation of the implementation area and local topographic condition, most of the variability is related to the variability of the inherent mitigating potential of the soil and water management types. The highest efficiency in mitigating excess sediment yield for the upper Tekeze basin resulted from introducing stone bund/parallel terracing followed by reforestation. Lower mitigating potential was simulated from reforestation scenarios alone. Even though the definitive interpretation of the quantitative results may not be appropriate, this research gives insight into the variability of the effectiveness of the sediment management types in reducing sediment transport for sustainable water resources and energy development in the basin. But such research should be supported with further cost and benefit analysis of resources to use and the interests of stakeholders.

In summary, the LSUA modelling approach has found with opportunities over the conventional empirical remote sensing and enhanced the accuracy to estimate the suspended sediment concentration of the Tekeze Rivers from the ground and space reflectance data. Moreover, the model was successful in determining the spatially detailed C-factor and integrated into SWAT for improving the simulation of both the place and time specific sediment transport, as well as evaluating the impact of climate change and sediment management alternatives in the Upper Tekeze River basin.

6.2 Recommendations

Based on the findings of the research the following four recommendations were setted.

1. Most previous remote sensing-based sediment researches have relied upon empirical relationships between sediment concentration and reflectance captured by the remote sensing instrument which is potential to be hampered by the high turbidity and significant effect of sediment types existed in the Rivers. Hence there is a need of future researches to focus on understanding the effects of SSC on optical properties of surface waters so that physically based models can be developed to improve the predictability with remotely sensed data.

2. The application of remote sensing for monitoring SSCs in finer and dynamic River systems need selecting appropriate wavelength and modelling approach working under dynamic sediment transportation. To successfully apply MODIS images for estimating SSCs at temporally heterogeneous and small rivers such as Tekeze river needs first to identify the components/end-members and optical properties of each component and determining the mixing coefficient after each component.

3. This study has implied LSUA is appropriate technique of estimating C-factor that minimize costs, enable to compute spatially detailed and time specific C-factor. The C-factor computed using LSUA has successfully integrated into SWAT and then capable estimating reality fitted sediment yield in the basin. The sediment yield risk map based on the LSUA integrated SWAT illustrated instructive details helpful for prioritized interventions. Even though the definitive interpretation of the quantitative sediment results using the LSUA integrated SWAT need further detail calibration and validation analysis at finer scale and should be supported with further cost and benefit analysis of resource use of the studied sediment management types, this research gives insight to the intensity of sediment risk and variability of effectiveness of the sediment management types in reducing sediment risk for sustainable water resources and energy development in the basin. The findings in this study can be base-line information for policymakers to come up

with timely and site-specific plans and designs to mitigate and/or adapt the extreme sediment transport in the basin.

4. The time series sediment in the upper Tekeze basin were found to be under continuous and significantly increasing trends of sediment concentration though the climate variables (rainfall and temperature) are under non-significant trends. This and other indicators present that the reason for continuous and abrupt sediment transportation trend in the basin is not related to climate variables. Instead, it may be related to the before and after the construction of the Tekeze hydroelectric dam (TK5) in the basin. Due to the coming of the Tk5 the socioeconomic activities in the area are expected to increase. Consequently, this might be a reason for land use dynamics and then to the abrupt increasing of sediment concentration entraining to the dam. Therefore, it is recommendable to have environmentally sound and sustainable land use plan in the basin.

References

Abdul Aziz, O.I.A. and Burn, D.H., 2006. Trends and variability in the hydrological regime of the Mackenzie River Basin. *Journal of hydrology*, *319*(1-4): 282-294.

Adams, J.B. and Gillespie, A.R., 2006. Remote sensing of landscapes with spectral images: A physical modeling approach. Cambridge University Press.

Adams, J.B., Sabol, D.E., Kapos, V., Almeida Filho, R., Roberts, D.A., Smith, M.O. and Gillespie, A.R., 1995. Classification of multispectral images based on fractions of endmembers: Application to land-cover change in the Brazilian Amazon. *Remote sensing of Environment*, *52*(2):137-154.

Adams, J.B., Smith, M.O., and Johnson, P.E., 1986. Spectral mixture modelling: a new analysis of rock and soil types at Viking Lander 1 site. Journal of Geophysical Research, 91:8098-8812.

Adem, A.A., Tilahun, S.A., Ayana, E.K., Worqlul, A.W., Assefa, T.T., Dessu, S.B. and Melesse, A.M., 2016. Climate change impact on sediment yield in the Upper Gilgel Abay catchment, Blue Nile Basin, Ethiopia. In Landscape dynamics, soils and hydrological processes in varied climates (pp. 615-644). Springer, Cham.

Aforki, H., 2006. Sediment studies for Tekeze hydropower development. University Library (BIBSYS), Norwegian Centre for International Cooperation in Higher Education.

Alejandro, M. and Omasa, K., 2007. Estimation of vegetation parameter for modeling soil erosion using linear Spectral Mixture Analysis of Landsat ETM data. *ISPRS Journal of Photogrammetry and Remote Sensing*, *62*(4):309-324.

Altmann, Y., Dobigeon, N., McLaughlin, S. and Tourneret, J.Y., 2013. Nonlinear spectral un-mixingof hyperspectral images using Gaussian processes. *IEEE Transactions on Signal Processing*, *61*(10):2442-2453.

Amare, T., Zegeye, A.D., Yitaferu, B., Steenhuis, T.S., Hurni, H. and Zeleke, G., 2014. Combined effect of soil bund with biological soil and water conservation measures in the north western Ethiopian highlands. *Ecohydrology & Hydrobiology*, *14*(3):.192-199.

Amsalu, A., Stroosnijder, L. and de Graaff, J., 2007. Long-term dynamics in land resource use and the driving forces in the Beressa watershed, highlands of Ethiopia. *Journal of Environmental management*, *83*(4):448-459.

Arai, K., 2008. Nonlinear mixture model of mixed pixels in remote sensing satellite images based on Monte Carlo simulation. *Advances in Space Research*, *41*(11): 1715-1723.

Arnold, J.G., Allen, P.M., Muttiah, R. and Bernhardt, G., 1995. Automated base flow separation and recession analysis techniques. *Groundwater*, *33*(6):1010-1018.

Arnold, J.G., Srinivasan, R., Muttiah, R.S. and Williams, J.R., 1998. Large area hydrologic modeling and assessment part I: model development 1. *JAWRA Journal of the American Water Resources Association*, *34*(1):73-89.

Asner, G.P. and Lobell, D.B., 2000. A biogeophysical approach for automated SWIR unmixing of soils and vegetation. Remote sensing of environment, 74(1): 99-112.

Ayana, A.B., Edossa, D.C. and Kositsakulchai, E., 2012. Simulation of sediment yield using SWAT model in Fincha Watershed, Ethiopia. *Kasetsart J. (Nat. Sci.), 46* :283-297.

Ayele, G., Teshale, E., Yu, B., Rutherfurd, I. and Jeong, J., 2017. Streamflow and sediment yield prediction for watershed prioritization in the Upper Blue Nile River Basin, Ethiopia. *Water*, *9*(10):782.

Azari, M., Moradi, H.R., Saghafian, B. and Faramarzi, M., 2016. Climate change impacts on streamflow and sediment yield in the North of Iran. Hydrological Sciences Journal, 61(1): 123-133.

Babic Mladenovic Marina, Damir Bekic, Samo Groselj, Matjaz Mikos, Tarik Kupusovic, Dijana Oskorus, 2015. Establishment of the Sediment Monitoring System for the Sava River Basin, Journal of water research and management, 5/4: 3-14

Bagnold, R.A., 1977. Bed load transport by natural rivers. *Water resources research*, *13*(2): 03-312.

Balthazar, V., Vanacker, V., Girma, A., Poesen, J. and Golla, S., 2013. Human impact on sediment fluxes within the Blue Nile and Atbara River basins. *Geomorphology*, (*180)*: 231-241.

Baret, F. and Guyot, G., 1991. Potentials and limits of vegetation indices for LAI and APAR assessment. *Remote sensing of environment*, *35*(2-3):161-173.

Bateson, C.A., Asner, G.P. and Wessman, C.A., 2000. Endmember bundles: A new approach to incorporating endmember variability into spectral mixture analysis. IEEE transactions on geoscience and remote sensing, 38(2):1083-1094.

Bayabil, H. K., Tilahun, S. A., Collick, A. S., Yitaferu, B., and Steenhuis, T. S., 2010. Are runoff processes ecologically or topographically driven in the (sub) humid Ethiopian highlands? The case of the Maybar watershed. *Ecohydrology, 3*: 457–466.

Beasley, D. B., Huggins, L. F., & Monke, A., 1980. ANSWERS: A model for watershed planning. *Transactions of the ASAE*, *23*(4): 938-0944.

Belete, K., 2007. Sedimentation and Sediment Handling at Dams in Tekeze River Basin, Ethiopia. Phd Thesis, Norwegian University of Science and Technology, Faculty of Engineering Science and Technology, Department of Hydraulic and Environmental Engineering, Trondheim, Norway.

Bell, J.F., Farrand, W.H., Johnson, J.R., and Morris, R.V., 2002. Low abundance materials at the Mars Pathfinder landing site: An investigation using spectral mixture analysis and related techniques. Icarus, 158: 56-71.

Betrie, G.D., Mohamed, Y.A., Griensven, A.V. and Srinivasan, R., 2011. Sediment management modelling in the Blue Nile Basin using SWAT model. *Hydrology and Earth System Sciences*, *15*(3):807-818.

Bewket, W. and Abebe, S., 2013. Land-use and land-cover change and its environmental implications in a tropical highland watershed, Ethiopia. International journal of environmental studies, 70(1):126-139.

Beyene, K.K., 2011. Soil erosion, deforestation and rural livelihoods in the Central Rift Valley area of Ethiopia: A case study in the Denku micro-watershed Oromia region (Doctoral dissertation).

Bharrgava, D.S. and Mariam, D.W., 1992. The effect of variation in suspended sediment properties on reflectance measurements. Journal of the Indian Society of Remote Sensing, 20(2-3):139-152.

Bioucas-Dias, J. M., Plaza, A., Dobigeon, N., Parente, M., Du, Q., Gader P., and Chanussot, J., 2012. Hyperspectral un-mixingoverview: geometrical, statistical, and sparse regression-based approaches. *IEEE J. Sel. Topics Appl. Earth Observations and Remote Sens*., 5(2): 354–379.

Birhane, E., Ashfare, H., Fenta, A.A., Hishe, H., Gebremedhin, M.A. and Solomon, N., 2019. Land use land cover changes along topographic gradients in Hugumburda national forest priority area, Northern Ethiopia. Remote Sensing Applications: Society and Environment, 13:61-68.

Bonn, F., Mégier, J., Ait Fora A., 1997. Remote sensing assisted specialization of soil erosion models with a GIS for land degradation quantification: expectations, errors and beyond, in: Spiteri A. (Ed.), Remote sensing integrated applications for risk assessment and disaster prevention for the Mediterranean, Balkema, Rotterdam (1997): 191–198.

Borel, C.C. and Gerstl, S.A., 1994. Nonlinear spectral mixing models for vegetative and soil surfaces. Remote sensing of environment, 47(3):403-416.

Bracmort, K.S., Arabi, M., Frankenberger, J.R., Engel, B.A. and Arnold, J.G., 2006. Modelling long-term water quality impact of structural BMPs. Transactions of the ASABE, 49(2): 367-374.

Bryant, R.G. and Rainey, M.P. 2002. Investigation of flood inundation on playas within the Zone of Chotts, using a time-series of AVHRR. Remote Sens. Environ., 82, 360–375.

Carbonneau, P.E., Bergeron, N. And Lane, S.N., 2005. Automated Grain Size Measurements from Airborne Remote Sensing for Long Profile Measurements of Fluvial Grain Sizes. Water Resources Research, 41(11).

Chekol, D., Bernhard T., Helmut E. And Paul V., 2007. Application of swat for assessment of spatial distribution of water resources and analyzing impact of different land management practices on soil erosion in upper Awash river basin watershed, catchment research, Bon University.

Chen Zhimin, Hanson, Jim D. and Curran Paul J.,1991. The form of the relationship between suspended sediment concentration and spectral reflectance: its implications

for the use of Daedalus 1268 data. *International Journal of Remote Sensing*, *12(1*):215– 222.

Chen, X., Li Y S, Liu Z, Yin K, Li Z, Wai O, And King B., 2004. Integration of multi-source data for water quality classification in the pearl river estuary andits adjacent coastal waters of Hong Kong. *Continental Shelf Research*, 24(16): 1827-1843.

Choubey, V.K., 1994. Assessment of sediment distribution pattern in the Tungabhadra reservoir using satellite imagery. Journal of the Indian Society of Remote Sensing, 22(2):103-111.

Chu, W., Laurence C., Smith A., Rennermalm K., Richard R F., Jason E B, And Niels R., 2009. Sediment Plume Response to Surface Melting and Supraglacial Lake Drainages on the Greenland Ice Sheet. *Journal of Glaciology, 55(194):1072-1082.*

Cihlar, J., 1987. A methodology for mapping and monitoring cropland soil erosion. *Canadian journal of soil science*, *67*(3):433-444.

Combe, J.P., Le Mouélic, S., Sotin, C., Gendrin, A., Mustard, J.F., Le Deit, L., Launeau, P., Bibring, J.P., Gondet, B., Langevin, Y. and Pinet, P., 2008. Analysis of OMEGA/Mars express data hyperspectral data using a multiple-endmember linear spectral unmixing model (MELSUM): Methodology and first results. Planetary and Space Science, 56(7): 951-975.

Condé, R.D.C., Martinez, J.M., Pessotto, M.A., Villar, R., Cochonneau, G., Henry, R., Lopes, W. and Nogueira, M., 2019. Indirect Assessment of Sedimentation in Hydropower Dams Using MODIS Remote Sensing Images. Remote Sensing, 11(3):314.

Costa, L.I., Storti G., Lüscher, B., Gruber, P., Staubli, T., 2012. Influence of solid particle parameters on the sound speed and attenuation of pulses in ADM, J. of Hydrologic Eng., 17(10): 1084-1092.

CSA, 2008. Summary and Statistical Report of the 2007 Population and Housing Census of Ethiopia: Population Size by Age and Sex, Central Statistical Authority (CSA), Addis Ababa.

Curran, P J and Novo, E., 1988. The Relation between Suspended Sediment Concentra-Tion and Remotely Sensed Spectral Radiance: A Review. *Journal of Coastal Research*, 4(3):351-368.

De Asis, A. and Omasa, K., 2007. Estimation of Vegetation Parameter for Modelling Soil Erosion Using Linear Spectral Mixture Analysis of Landsat Etm Data. Isprs Journal of Photogrammetry and Remote Sensing 62(4): 309–324.

De Asis, A.M., Omasa, K., Oki, K. and Shimizu, Y., 2008. Accuracy and applicability of linear spectral un-mixingin delineating potential erosion areas in tropical watersheds. *International Journal of Remote Sensing*, *29*(14): .4151-4171.

Dedkov, A.P. and Gusarov, A.V., 2006. Suspended sediment yield from continents into the World Ocean: spatial and temporal changeability. Sediment Dynamics and the Morphology of Fluvial Systems. IAHS Publication, 396:.3-11.

Degefu G.T., 2003. The Nile: Historical, Legal and Developmental Perspective. New York Pp.413. [Online]: Http://Books.Google.Com/Books [Accessed, July 20, 2015].

Dekker, A.G., Vos, R.J., and Peters, S. W. M., 2001. Comparison of remote sensing data, model results and in situ data for total suspended matter (TSM) in the southern Frisian lakes. *Science of The Total Environment, 268(1-3)*:197–214.

Demissie, T.A., Saathoff, F., Sileshi, Y.A. and Gebissa, Y., 2013. Climate change impacts on the streamflow and simulated sediment flux to Gilgel Gibe 1 hydropower reservoir–Ethiopia. European International Journal of Science and Technology, 2(2): 63-77.

Dennison, P.E., Charoensiri, K., Roberts, D.A., Peterson, S.H. and Green, R.O., 2006. Wildfire temperature and land cover modeling using hyperspectral data. Remote Sensing of Environment, 100(2): 212-222.

Descheemaeker, K., Nyssen, J., Rossi, J., Poesen, J., Haile, M., Raes, D., Muys, B., Moeyersons, J., and Deckers, S., 2006. Sediment Deposition and Pedogenesis in Enclosures in the Tigray Highlands, Ethiopia, *Geoderma, 132: 291–314.*

Dessu, S.B. and Melesse, A. M., 2012. Modelling the Rainfall-Runoff process of the Mara River Basin using SWAT, Hydrological Processes, 26(26): 4038–4049.

Dessu, S.B. and Melesse, A. M., 2013. Impact and Uncertainties of Climate change on the Hydrology of the Mara River Basin, Hydrological Processes, 27(20): 2973–2986.

Dobigeon, N., Tourneret, J.Y., Richard, C., Bermudez, J.C.M., Mclaughlin, S. And Hero, A.O., 2014. Nonlinear Un-mixingOf Hyperspectral Images: Models and Algorithms. Ieee Signal Processing Magazine, 31(1):.82-94.

Doxaran, D, Froidefond, J M, Castaing, P et al., 2009. Dynamics of the turbidity maximum zone in a macro tidal estuary (the Gironde, France): observations from field and MODIS satellite data. Estuarine, Coastal and Shelf Science, 81(3): 321–332.

Doxaran, D., Froidefond, J. and Castaing, P., 2002. A reflectance band ratio used to estimate suspended matter concentrations in sediment-dominated coastal waters. *Int.J. Remote Sens., 23: 5079–5085.*

Doxaran, D., Froidefond, J.M. and Castaing, P., 2003. Remote-sensing reflectance of turbid sediment-dominated waters. Reduction of sediment type variations and changing illumination conditions effects by use of reflectance ratios. Applied Optics, 42(15): 2623-2634.

Durigon, V. L., Carvalho, D. F., Antunes, M. A. H., Oliveira, P. T. S., & Fernandes, M. M., 2014. NDVI time series for monitoring RUSLE cover management factor in a tropical watershed. *International journal of remote sensing*, *35*(2): 441-453.

Eckmann, T.C., Roberts, D.A. and Still, C.J., 2008. Using multiple endmember spectral mixture analysis to retrieve subpixel fire properties from MODIS. Remote Sensing of Environment, 112(10):.3773-3783.

Eleveld, M.A., Pasterkamp, R., van der Woerd, H.J. and Pietrzak, J.D., 2008. Remotely sensed seasonality in the spatial distribution of sea-surface suspended particulate matter in the southern North Sea. Estuarine, Coastal and Shelf Science, 80(1):103-113.

Elmore, A. J., J. F. Mustard, S. J. Manning, and D. B. Lobell. 2000. Quantifying vegetation change in semiarid environments: Precision and accuracy of spectral mixture analysis and the normalized difference vegetation index. Remote Sens Environ 73(1): 87–102.

El-Swaify, S. And Hurni, H.1996. Tran Boundary Effects of Soil Erosion and Conservation in the Nile Basin, *Land Husbandry,.1: 6–21.*

Escadafal, R., 1994. Soil spectral properties and their relations with environmental parameters: examples from arid regions, in: Hill, J., Mégier, J. (Eds.), Imaging Spectrometry—a Tool for Environmental Observations, Kluwer Academic Publishers, Dordrecht, The Netherlands (1994): 71–87.

Essayas, K., William P., And Tammo S., 2014. Evaluating Suitability of Modis–Terra Products for Turbidity and Tss Time Series Data Generation Over Lake Tana, Ethiopia. International Journal of Applied Earth Observation and Geo-Information, 26:286-297.

Fang, G., Chen S., Wang H., Qian J, and Zhang L., 2010. Detecting Marine Intrusion in to Rivers Using Eo-1 Ali Satellite Imagery: Modaomen Waterway, Pearl River Estuary, China. International Journal of Remote Sensing, 31(15):4125-4146.

FAO. 1995. Digital Soil Map of the World and Derived Soil Properties, Food and Agriculture Organization of the United Nations, Rome, 1995.

Felix, D., Albayrak I., Boes R.M., 2013. Laboratory investigation on measuring suspended sediment by portable laser diffractometer (LISST) focusing on particle shape. Geo-marine Letters 33(6): 485-498.

Feyisa, G.L., Meilby, H., Fensholt, R., Proud, S.R., 2014. Automated Water Extraction Index: A new technique for surface water mapping using Landsat imagery. Remote Sens. Environ. 2014, 140, 23–35.

Fiorani, L., Okladnikov, I.G. and Palucci, A., 2006. First algorithm for chlorophyll-a retrieval from MODIS-Terra imagery of Sun-induced fluorescence in the Southern Ocean. International Journal of Remote Sensing, 27(16): 3615-3622.

Forkuor, G., Hounkpatin, O.K., Welp, G. and Thiel, M., 2017. High resolution mapping of soil properties using remote sensing variables in south-western Burkina Faso: a comparison of machine learning and multiple linear regression models. PloS one, 12(1), p.e0170478.

Franke, J., Roberts, D.A., Halligan, K. and Menz, G., 2009. Hierarchical multiple endmember spectral mixture analysis (MESMA) of hyperspectral imagery for urban environments. Remote Sensing of Environment, 113(8):1712-1723.

Franke, J., Roberts, D.A., Halligan, K. and Menz, G., 2009. Hierarchical multiple endmember spectral mixture analysis (MESMA) of hyperspectral imagery for urban environments. Remote Sensing of Environment, 113(8):1712-1723.

García-Haro, F.J., Sommer, S. and Kemper, T., 2005. A new tool for variable multiple endmember spectral mixture analysis (VMESMA). International Journal of Remote Sensing, 26(10):2135-2162.

Gebremicael, T.G., Mohamed, Y.A. and Hagos, E.Y., 2017. Temporal and spatial changes of rainfall and streamflow in the Upper Tekezē–Atbara river basin, Ethiopia. *Hydrology and Earth System Sciences*, *21*(4):.2127-2142.

Gebremichael, T.G., Mohamed, Y.A., Betrie, G.D., Zaag, V., and Teferi, E., 2013. Trend Analysis of Runoff and Sediment Fluxes in the Upper Blue Nile Basin: A Combined Analysis of Statistical Tests, Physically-Based Models and Land Use Maps, *Journal of Hydrology, 482:57–68.*

Gebremichael, Y.M., Li, W., Boyle, W.J.O., Meggitt, B.T., Grattan, K.T.V., McKinley, B., Fernando, G.F., Kister, G., Winter, D., Canning, L. and Luke, S., 2005. Integration and assessment of fibre Bragg grating sensors in an all-fibre reinforced polymer composite road bridge. Sensors and Actuators A: Physical, 118(1): 78-85.

Gebrernichael, D., Nyssen, J., Poesen, J., Deckers, J., Haile, M., Govers, G. And Moeyersons, J., 2005. Effectiveness of Stone Bunds in Controlling Soil Erosion on Cropland in the Tigray Highlands, Northern Ethiopia. Soil Use and Management, 21(3):.287-297.

GEMS, 2003. Improving Global Water Quality Monitoring: Technical Advisor Paper No.1 United Nation Environment Program-Global Environment Monitoring Sys-Tem. Technical Report.

Gertner, G., Wang, G., Fang, S., & Anderson, A. B., 2002. Mapping and uncertainty of predictions based on multiple primary variables from joint co-simulation with Landsat TM image and polynomial regression. *Remote Sensing of Environment*, *83*(3): 498-510.

Getachew, H. E., & Melesse, A. M., 2012. The impact of land use change on the hydrology of the Angereb Watershed, Ethiopia. *International Journal of Water Sciences*, *1*.

Ghrefat, H.A. and Goodell, P.C., 2011. Land cover mapping at Alkali Flat and Lake Lucero, White Sands, New Mexico, USA using multi-temporal and multi-spectral remote sensing data. Int. J.Appl. EarthObs., 13, 616–625.

Gizachew, A., 2015. A Geographic Information System based soil loss and sediment estimation in Zingin Watershed for Conservation Planning, Highlands of Ethiopia. International Journal of Science, Technology and Society. 3(1): 28-35.

Gong, P. and Zhang, A., 1999. Noise effect on linear spectral unmixing. Geographic Information Sciences, 5(1): 52-57.

Goodwin, N., Coops, N. C., & Stone, C., 2005. Assessing plantation canopy condition from airborne imagery using spectral mixture analysis and fractional abundances. International Journal of Applied Earth Observation and Geoinformation, 7, 11−28.

Gottesfeld, A. S., and Tunnicliffe J., 2003. Bed load measurements with a passive magnetic induction device. IAHS Publication: 211-221.

Gray, J R, Glysson G D, and Turcios L M., 2000. Comparability and Reliability of Total Sus-Pended Solids and Suspended-Sediment Concentration Data. Usgs Water-Resources Investigations Rep. No. 00-4191.

Grey, O.P., Dale G. Webber, Setegn, S.G., and Melesse, A.M., 2013. Application of the Soil and Water Assessment Tool (SWAT Model) on a Small Tropical Island State (Great River Watershed, Jamaica) as a tool in Integrated Watershed and Coastal Zone Management, International Journal of Tropical Biology and Conservation, 62(3): 293-305.

Griensven, A. V., Ndomba, P., Yalew, S., & Kilonzo, F., 2012. Critical review of SWAT applications in the upper Nile basin countries. *Hydrology and Earth System Sciences*, *16*(9): 3371-3381.

Gruber, P., Felix, D., Storti, G., Lattuada, M., Fleckenstein, P. and Deschwanden, F., 2016, November. Acoustic measuring techniques for suspended sediment. In IOP Conference Series: Earth and Environmental Science, 49(12): 122003.

Guo, Y.L., Li, Y.M., Zhu, L. Liu, G. Wang, S. and Du, C.G., 2015. An Improved Unmixing-Based Fusion Method: Potential application to remote monitoring of inland waters. Remote Sens. 2015, 7, 1640–1666.

Guzman, C.D., Tilahun, S.A., Zegeye, A.D. and Steenhuis, T.S., 2013. Suspended sediment concentration–discharge relationships in the (sub-) humid Ethiopian highlands. *Hydrology and Earth System Sciences*, *17*(3):1067-1077.

Haboudane, D., Bonn, F., Royer, A., Sommer, S. and Mehl, W., 2002. Land degradation and erosion risk mapping by fusion of spectrally based information and digital geomorphometric attributes. International Journal of Remote Sensing, 23: 3795-3820.

Hagos, Gebreslassie., 2014. Land use-land cover dynamics of Huluka watershed, Central Rift Valley, Ethiopia. International Soil and Water Conservation Research, 2(4):25-33.

Haregeweyn, N. and Yohannes, F., 2003. Testing and evaluation of the agricultural non-point source pollution model (AGNPS) on Augucho catchment, Western Hararghe, Ethiopia. *Agr. Ecosyst. Environ. 99:* 201–212.

Haregeweyn, N., Melesse, B., Tsunekawa, A., Tsubo, M., Meshesha, D. And Balana, B.B., 2012. Reservoir Sedimentation and Its Mitigating Strategies: A Case Study of Angereb Reservoir (NW Ethiopia). *Journal of Soils and Sediments*, *12*(2):291-305.

Haregeweyn, N., Poesen, J., Nyssen, J., De Wit, J., Haile, M., Govers, G. And Deckers, S., 2006. Reservoirs in Tigray (Northern Ethiopia): Characteristics and Sediment Deposition Problems. *Land Degradation & Development*, *17*(2):211-230.

Haregeweyn, N., Poesen, J., Nyssen, J., Govers, G., Verstraeten, G., De Vente, J., Deckers, J., Moeyersons, J. And Haile, M., 2008. Sediment Yield Variability in Northern Ethiopia: A Quantitative Analysis of Its Controlling Factors. Catena, 75(1):65-76.

Haregeweyn, N., Tsunekawa, A., Poesen, J., Tsubo, M., Nyssen, J., Vanmaercke, M., Zenebe, A., Meshesha, D.T. and Adgo, E., 2015. Sediment Yield Variability at Various Spatial Scales and Its Hydrological and Geomorphological Impacts on Dam-catchments in the Ethiopian Highlands. In *Landscapes and Landforms of Ethiopia* (pp. 227-238). Springer, Dordrecht.

HEC, 1995. HEC-RAS River Analysis System. Hydraulic Reference Manual. Version 1.0. Hydrologic Engineering Center Davis CA.

Heinz, D. C., & Chang, C., 2001. Fully constrained least squares linear spectral mixture analysis method for material quantification in hyperspectral imagery. IEEE Transactions on Geoscience and Remote Sensing, 39: 529−545.

Hengsdijk, H., Meijerink, G.W. And Mosugu, M.E., 2005. Modelling the effect of three soil and water conservation practices in Tigray, Ethiopia. Agriculture, Ecosystems & Environment, 105(1-2):29-40.

Herweg, K. and Ludi, E., 1999. The performance of selected soil and water conservation measures—case studies from Ethiopia and Eritrea. *Catena*, *36*(1-2): 99-114.

Hommersom, A., Wernand, M.R., Peters, S., Eleveld, M.A., van der Woerd, H.J. and de Boer, J., 2011. Spectra of a shallow sea-unmixing for class identification and monitoring of coastal waters. Ocean. Dyn. 2011, 61, 463–480.

Hould-Gosselin, G., Rousseau, A.N., Gumiere, S.J., Hallema, D.W., Ratté-Fortin, C., Thériault, G. and Van Bochove, E., 2016. Modeling the sediment yield and the impact of vegetated filters using an event-based soil erosion model—a case study of a small Canadian watershed. Hydrological Processes, 30(16):2835-2850.

Humphreys, H., Bellier, C., Kennedy, R, Dokin, K., 1997. Tekeze medium hydropower report. Annex b—hydrology report. Ministry of water resources: Addis Ababa; pp. 264.

Hung, M.C. and Wu,Y.H., 2005. Mapping and visualizing the Great Salt Lake land scape dynamics using multi-temporal satellite images, 1972–1996. Int. J. Remote Sens., 26, 1815–1834.

Hurni, H., 1983. Degradation and Conservation of the Resources in the Ethiopian Highlands. *Mountain Research and Development, 8(2/3):123-130.*

Hurni, H., Kebede, T., and Gete, Z., 2005. The implications of changes in population, land use, and land management for surface runoff inthe upper Nile basin area of Ethiopia, *Mt. Res. Dev., 25:147–154.*

Hurni, H.1985. Erosion-Productivity-Conservation Systems in Ethiopia. Proceedings 4th International Conference on Soil Conservation, Maracay, Venezuela, 654-674.

ICOLD, 2009. Sedimentation and sustainable use of reservoirs and River systems, draft of ICOLD bulletin, CIGP-ICOLD.

Islam A., Gao J., Ahmad W., Neil D., And Bell P., 2003. Image calibration to like-values in mapping shallow water quality from multi temporal data. Photogrammetric Engineering and Remote Sensing, 69(5):567-575.

Islam M R Yamaguch Y, And Ogawa K., 2001. Suspended Sediment in the Ganges and Brahmaputra Rivers in Bangladesh: Observation from Tm and Avhrr Data. Hydrological Processes, 15(3):493-509.

Jain, S.K., Singh, R.D., Jain, M.K., Lohani, A.K., 2005. Delineation of flood-prone areas using remote sensing technique. Water Resour. Manag., 19, 337–347.

Jayakody, P. And Gamage, N., 2010. Surface runoff estimation over heterogeneous canal commands applying medium resolution remote sensing data with the scs-cn method. In Proceedings of The National Conference on water, Food Security, and Climate Change In Sri Lanka, Bmich, Colombo, June 9-11, 2009. Volume 1. Irrigation for Food Security (Vol. 1, P. 143). Iwmi.

Jiang, X.W., Tang, J.W., Zhang, M.W., Ma, R.H., Ding, J., 2009. Application of MODIS data in monitoring suspended sediment of Taihu Lake, China. Chin. J. Oceanol. Limnol. 27 (3), 614–620.

Jones, J.R., Schwartz, J.S., Ellis, K.N., Hathaway, J.M. and Jawdy, C.M., 2015. Temporal variability of precipitation in the upper Tennessee valley. *Journal of Hydrology: Regional Studies, 3:*.125-138.

Jong, S. M., 1994. Derivation of vegetative variables from a Landsat TM image for modeling soil erosion. *Earth Surface Processes and Landforms, 19*(2): 165-178.

Kantoush, S.A. and Sumi, T., 2013. Reservoir Sedimentation and Sediment Management Techniques in the Nile River Basin Countries. In *12th International Symposium on River Sedimentation, Kyoto*.Addis H K, Strohmeier S, Ziadat F, Melaku N D, Klik A 2016. modeling stream flow and sediment using swat in the Ethiopian Highlands. Int J Agric & Biol Eng, 9(5): 51－66.

Kassawmar, T., Gessesse, G.D., Zeleke, G. and Subhatu, A., 2018. Assessing the soil erosion control efficiency of land management practices implemented through free community labor mobilization in Ethiopia. *International Soil and Water Conservation Research*, 6(2): 87-98.

Kebede Wolka Olancho, 2012. Watershed Management: An option to sustain dam and reservoir function in Ethiopia. Journal of Environmental Science and Technology, 5: 262-273.

Kendall, M., 1975. Rank Correlation Methods. Charles Griffin, London.

Keshava, N. and Mustard, J. F., 2002. "Spectral unmixing," IEEE Signal Process. *Mag.*, *19(1)*:44–57.

Kilham, E., Roberts, D., and Singer, M. B., 2012. Remote sensing of suspended sediment concentration during turbid flood conditions on the Feather River, California a modelling approach, *Water Resources 48,* doi: 10.1029/2011WR010391.

Kilham, N.E., Roberts, D. and Singer, M.B., 2012. Remote sensing of suspended sediment concentration during turbid flood conditions on the Feather River, California—a modeling approach. Water Resources Research, 48(1).

Kositsakulchai, E., Ayana, A. B., & Edossa, D. C., 2012. Simulation of Sediment Yield using SWAT Model in Fincha Watershed, Ethiopia.

Krishna, P.A., Lalitha, R., Shanmugasundaram, K. and Nagarajan, M., 2019. Assessment of Topographical Factor (LS-Factor) Estimation Procedures in a Gently Sloping Terrain. Journal of the Indian Society of Remote Sensing, 47(6):1031-1039.

Kutser, T., Metsamaa, L., Vahtmae, E., Aps, R., 2007. Operative monitoring of the extent of dredging plumes in coastal ecosystems using MODIS satellite imagery. J. Coast. Res. 50:180–184.

Kwiatkowska, E.J. and McClain, C.R., 2009. Evaluation of SeaWiFS, MODIS Terra and MODIS Aqua coverage for studies of phytoplankton diurnal variability. International Journal of Remote Sensing, 30(24):6441-6459.

Lewandowski, J., Schauser, I. and Hupfer, M., 2002. The importance of sediment studies in the selection of restoration measures. *Hydrology and Water Resources Management-Germany*, *46*(1):2-13.

Li, E.H., Li, W., Liu, G.H. And Yuan, L.Y., 2008. The effect of different submerged macrophyte species and biomass on sediment resuspension in a shallow freshwater lake. Aquatic Botany, 88(2):.121-126.

Li, H. and Zhang, L., 2011. A hybrid automatic endmember extraction algorithm based on a local window. IEEE Trans. Geosci. Remote Sens., 49, 4223–4238.

Liu, Y., Islam, M.A. And Gao, J., 2003. "Quantification of Shallow Water Quality Parameters by Means of Remote Sensing", *Progress in Physical Geography, 27:24–43.*

Lodhi, M. A, Rundquist, D.C., Han L., and Kuzila, M. S. 1997. The potential for remote sensing of loess soils suspended in surface waters. *Journal of the American Water Resources Association*, 33(1):111–117.

Loisel, H. And Stramski, D., 2000. Estimation of the inherent optical properties of natural waters from the irradiance attenuation coefficient and reflectance in the presence of Raman scattering. Applied Optics, 39(18):.3001-3011.

Long, C M, Pavelsky T M, 2013. Remote sensing of suspended sediment concentration and hydrologic connectivity in a complex wetland environment. Remote Sensing of Environment, 129: 197–209.

Lu, X., 2005. Spatial variability and temporal change of water discharge and sediment flux in the lower Jinsha tributary: Impact of Environmental Changes, *River Res. Appl. 21: 229–243.*

Ma, B., Wu, L., Zhang, X., Li, X., Liu, Y. and Wang, S., 2014. Locally adaptive unmixing method for lake-water area extraction based on MODIS 250 m bands. IEEE J. Sel. Top. Appl. Earth Obs. Remote Sens., 33, 109–118.

Ma, J. W., Xue, Y., Ma, C. F., & Wang, Z. G., 2003. A data fusion approach for soil erosion monitoring in the Upper Yangtze River Basin of China based on Universal Soil Loss Eq. (USLE) model. *International Journal of Remote Sensing*, *24*(23): 4777-4789.

Ma, R.,and Dai, J., 2005. Investigation of chlorophyll and total suspended matter concentrations using land sat ETM and field spectral measurement in Taihu Lake, China. *International Journal of Remote Sensing, 26(13):* 2779-2795.

Ma, S., Zhou, Y., Gowda, P.H., Dong, J., Zhang, G., Kakani, V.G., Wagle, P., Chen, L., Flynn, K.C. and Jiang, W., 2019. Application of the water-related spectral reflectance indices: A review. Ecological indicators, 98:68-79.

Maalim, F. K., Melesse, A.M., Belmont, P., and Gran, K., 2013. Modelling the impact of land use changes on runoff and sediment yield in the Le Sueur Watershed, Minnesota using GeoWEPP, *Catena, 107*: 35–45.

Mango, L. M., Melesse, A. M., McClain, M. E., Gann, D., & Setegn, S. G., 2011a. Land use and climate change impacts on the hydrology of the upper Mara River Basin, Kenya: results of a modelling study to supporter better resource management. *Hydrology and Earth System Sciences*, *15*(7): 2245-2258.

Mango, L. M., Melesse, A. M., McClain, M. E., Gann, D., & Setegn, S. G., 2011b. Hydrometeorology and water budget of the Mara River Basin under land use change scenarios. In *Nile River Basin* (pp. 39-68). Springer, Dordrecht.

Marra, F., Morin, E., Peleg, N., Mei, Y. And Anagnostou, E.N., 2017. Intensity–Duration–Frequency Curves from Remote Sensing Rainfall Estimates: Comparing Satellite and Weather Radar over the Eastern Mediterranean. Hydrology and Earth System Sciences, 21(5):.2389-2404.

Masoumeh, R. and Mehdi, F., 2012. Estimating Suspended sediment concentration by a neural differential evolution (NDE) and comparison to ANFIS and three ANN Models. *Disaster Adv., 5:*346–359.

Melesse, A., Weng, Q., Thenkabail, P. and Senay, G., 2007. Remote sensing sensors and applications in environmental resources mapping and modelling. *Sensors*, *7*(12):.3209-3241.

Mengistu, D., And Sorteberg, A., 2012. Sensitivity of SWAT simulated streamflow to climatic changes within the Eastern Nile River Basin, Hydrology and Earth System Sciences, *Hydrol. Earth Syst. Sci., 16: 391–407.*

Merina, N.R., Sashikkumar, M.C., Rizvana, N. and Adlin, R., 2016. Sedimentation study in a reservoir using remote sensing technique. Applied Ecology and Environmental Research, 14(4):296-304.

Metternicht, G.I. and Fermont, A., 1998. Estimating erosion surface features by linear mixture modelling. Remote Sensing of Environment, 64: 254-265.

Meusburger, K, Banninger D, Alewell C. 2010. Estimating vegetation parameter for soil erosion assessment in an alpine catchment by means of quickbird imagery.

International Journal of Applied Earth Observation and Geoinformation 12(3): 201–207.

Michael, A., Schmidt, J., Enke, W., Deutschlder, T., and Malitz, G. 2005, impact of expected increase in precipitation intensities on soil loss--results of comparative model simulations. Catena, 61(2-3): 155–164.

Michael, Mamo, K. and Jain, M. K., 2013. "Runoff and sediment modeling using swat in gumera catchment, ethiopia," open journal of modern hydrology, 3(4): 2013: 196-205.

Michale, G. and Semu A., 2015. Spatial and temporal variability of rainfall at seasonal and annual time scales at Tekeze River Basin, Ethiopia. Journal of natural sciences research, 5 (19): 27-32.

Mobley, C. D., 1994. Light and Water: Radiative Transfer in Natural Waters, Volume 592. Academic Press San Diego, Ca.

Møen, K., Bogen, J., Zuta, J., Ade, P., Esbensen, K., 2010. Bedload measurement in rivers using passive acoustic sensors. US Geological Survey Scientific Investigations Report 5091: 336-351.

Moges, A., Fasikaw, A., Muluken, L., Getaneh, K., Dessalegn, C., Seifu, A., and Tammo, S., 2016. Sediment concentration rating curves for a monsoonal climate: upper Blue Nile. *SOIL, 2:* 337–349.

Mohammed, A., Yohannes, F., and Zeleke, G., 2004. Validation of agricultural non-point source (AGNPS) pollution model in Kori watershed, South Wollo, Ethiopia, *Int. J. Appl. Earth Obs.*, 6: 97–109.

Mohammed, H., Alamirew, T., Assen, M., Melesse, A.M., 2015. Modeling of sediment yield in Maybar gauged watershed using SWAT, northeast Ethiopia. *Catena*, 127:191–205.

Moore, N., Andresen, J., Lofgren, B., Pijanowski, B. and Kim, D.Y., 2015. Projected land-cover change effects on East African rainfall under climate change. *International Journal of Climatology*, *35*(8):.1772-1783.

Morgan, R. P. C., Morgan, D. D. V., & Finney, H. J., 1984. A predictive model for the assessment of soil erosion risk. *Journal of agricultural engineering research*, *30:* 245-253.

Moriasi, D. N., Arnold, J. G., Van Liew, M. W., Bingner, R. L., Harmel, R. D., & Veith, T. L. 2007. Model evaluation guidelines for systematic quantification of accuracy in watershed simulations. *Transactions of the ASABE*, *50*(3): 885-900.

MoWIE, 2008. Tekeze River Basin- Physiographic and Climate, Ministry of Water Resources, Addis Ababa, Ethiopia, (http://www.mowr.gov.et/).

Mulder, V.L., De Bruin, S., Schaepman, M.E. and Mayr, T.R., 2011. The use of remote sensing in soil and terrain mapping—A review. Geoderma, 162(1-2):1-19.

Myneni, R.B., Maggion, S., Jaquinta, J., Privette, J.L., Gordon, N., Pinty, B., Kimes, D.S., Verstraete, M.M. and Williams, D.L., 1995. Optical remote sensing of vegetation: modeling, caveats, and algorithms. Remote Sensing of Environment, 51, 169–188.

Nash J.E., Sutcliff J.V., 1970. River Flow Forecasting Through Conceptual Models. Part I: A Discussion of Principles. *Hydrology 10: 282–290.*

Nearing, M.A., Foster, G.R., Lane, L.J., & Finkner, S.C., 1989. A process-based soil erosion model for USDA – water erosion prediction project technology. Transactions ASAE 32, 1587–1593.

Nechad, B., Ruddick, K. G. and Pary, Y., 2010. Calibration and validation of a generic multisensory algorithm for mapping of total suspended matter in turbid waters. Remote Sens. Environ., 114:854-866.

NEDECO, 1997. Tekeze River basin master plan study report (TRMSR), sectorial report volume III, the Ministry of Water, irrigation and electricity of Ethiopia and Netherlands Engineering Consultants, Addis Ababa.

Neitsch, S.L., Arnold, J.G., Kiniry, J.R. & Williams, J.R. 2005. Soil and Water Assessment Tool Theoretical Documentation Version 2005. Grassland, Soil and Water Research Laboratory; Agricultural Research Service 808 East Blackland Road; Temple, Texas 76502; Blackland Research Researchcenter; Texas Agricultural Experiment Station 720 East Blackland Road; Temple, Texas 76502, Usa.

Neitsch,S.L., Arnold, J.G., Kiniry, J.R., Williams, J.R., 2011. SWAT user manual, version 2009. Texas Water Resources Institute Technical Report. A and M University, Texas, USA.

Novo Evlyn M´arcia Le˜ao Moraes, Carlos Alberto Steffen, and Cl´audia Zuccari Fernandes B., 1991. Results of a laboratory experiment relating spectral reflectance to total suspended solids. *Remote Sensing of Environment*, 36(1):67–72, 1991.

Novo, E.M.M., Hansom, J.D. and Curran, P.J., 1989. The effect of sediment type on the relationship between reflectance and suspended sediment concentration. Remote Sensing, 10(7):1283-1289.

Nyssen, J., Poesen, J., Gebremichael, D., Vancampenhout, K., D'aes, M., Yihdego, G., Govers, G., Leirs, H., Moeyersons, J., Naudts, J. And Haregeweyn, N., 2007. Interdisciplinary On-Site Evaluation of Stone Bunds to Control Soil Erosion on Cropland in Northern Ethiopia. *Soil and Tillage Research*, *94*(1):.151-163.

Ohring, G., Lord, S., Derber, J., Mitchell, K. and Ji, M., 2002. Applications of satellite remote sensing in numerical weather and climate prediction. Advances in Space Research, 30(11):2433-2439.

Ouillon, S., Durand, N., Forget, P., Fiandrino, A. and Fraunie, P., 1998, June. Remote sensing as a tool for suspended sediment transport modelling in coastal areas. In Proceeding of Third International Conference on Multiphase Flow, ICMF, (98): 8-12.

Oyama, Y., Matsushita, B., Fukushima, T., Matsushige, K., and Imai, A., 2009. Application of spectral decomposition algorithm for mapping water quality in a turbid lake (Lake Kasumigaura, Japan) from Landsat TM data. ISPRS. *Journal of Photogrammetry and Remote Sensing*, *64(1*): 73-85.

Oyama, Y., Matsushita, B., Fukushima, T., Nagai, T. and Imai, A., 2007. A new algorithm for estimating chlorophyll-a concentration from multi-spectral satellite data in case II waters: a simulation based on a controlled laboratory experiment. *International Journal of Remote Sensing*, *28*(7):1437-1453

Pan, Y., Zhang, H., Li, X. And Xie, Y., 2016. Effects of Sedimentation on Soil Physical and Chemical Properties and Vegetation Characteristics in Sand Dunes at the Southern Dongting Lake Region, China. Scientific Reports, 6:.36300.

Panagos, P., Borrelli, P., Meusburger, K., Alewell, C., Lugato, E. And Montanarella, L., 2015. Estimating the Soil Erosion Cover-Management Factor at the European Scale. Land Use Policy, 48: 38-50.

Pardo-Pascual, J.E., Almonacid-Caballer, J., Ruiz, L.A., Palomar-Vazquez, J. 2012. Automatic extraction of shorelines from Landsat TM and ETM multi-temporal images with subpixel precision. Remote Sens. Environ., 123, 1–11.

Pavelsky, T. M. and Smith, L. C., 2009. Remote sensing of suspended sediment concentration, flow velocity, and Lake Recharge in the Peace-Athabasca Delta, Canada. Water Resources Research, 45: W11417.

Pettitt, A., 1979. A Non-Parametric Approach to the Change-Point Problem. Appl. Stat. 28: 126–135.

Phinn, S.M., Stanford P., Scarth A.T. Muurray and Shyy P.T., 2002. Monitoring the composition of urban environments based on the vegetation-impervious surface-soil (VIS) model by sub-pixel analysis techniques, International Journal of remote Sensing. 23:41314153.

Pimentel, D., 2006. Soil Erosion: A Food and Environmental Threat. Environment, Development and Sustainability, 8(1):119-137.

Pimentel, D., Harvey, C., Resosudarmo, P., Sinclair, K., Kurz, D., Mcnair, M., Crist, S., Shpritz, L., Fitton, L., Saffouri, R. And Blair, R., 1995. Environmental and Economic Costs of Soil Erosion and Conservation Benefits. Science, 267(5201):1117-1123.

Plaza, A., Martínez, P., Pérez, R. and Plaza, J., 2004. A quantitative and comparative analysis of endmember extraction algorithms from hyperspectral data. IEEE transactions on geoscience and remote sensing, 42(3): 650-663.

Powell, R.L. and Roberts, D.A., 2008. Characterizing variability of the urban physical environment for a suite of cities in Rondonia, Brazil. Earth Interactions, 12(13):1-32.

Pruski, F. F. and Nearing M. A., 2002, Climate-Induced Changes in Erosion During The 21st Century for Eight U.S. Locations. Water Resources Research, 38, Doi: 10.1029/2001wr000493.

Radeloff, V.C., Mladenoff, D.J. and Boyce, M.S., 1999. Detecting jack pine budworm defoliation using spectral mixture analysis: separating effects from determinants. Remote Sensing of Environment, 69(2):156-169.

Rao, K.N., Narendra, K. And Latha, P.S., 2010. An Integrated Study of Geospatial Information Technologies for Surface Runoff Estimation in an Agricultural Watershed, India. Journal of the Indian Society of Remote Sensing, 38(2):255-267.

Riano, D., Chuvieco, E., Ustin, S., Zomer, R., Dennison, P., Roberts, D. and Salas J., 2002. Assessment of vegetation regeneration after fire through multitemporal analysis of AVIRIS images in Santa Monica Mountains. Remote Sensing of Environment, 79: 60-71.

Ritchie, J. C., Cooper C. M, and Schiebe F. R., 1990. The Relation of Mss and Tm Digital Data with Suspended Sediments, Chlorophyll, and Temperature in Moon Lake, Mississippi. *Remote Sensing of Environment, 33(2):137-148.*

Ritchie, J. C., Schiebe, F. R., and McHenry, J. R., 1976. Remote sensing of suspended sediments in surface waters. *Journal of American Society of Photogrammetry*, 42(12):1539– 1545.

Ritchie, J.C. and Cooper C.M., 1988. Comparison of measured suspended sediment concentration with suspended sediment concentrations estimated from landsat mss data. International Journal of Remote Sensing, 9 (3): 379-387.

Ritchie, J.C. and Schiebe F.R., 2000. Remote sensing in hydrology and water management, water quality, In: G.A. Schultz and E.T. Engman (Eds.) Springer-Verlag, Berlin, Germany, 351-352.

Ritchie, J.C., Zimba, P.V. and Everitt, J.H., 2003. Remote sensing techniques to assess water quality. *Photogrammetric Engineering & Remote Sensing*, *69*(6):.695-704.

Rivard, B., Feng, J., Gallie, A. and Sanchez-Azofeifa, A., 2008. Continuous wavelets for the improved use of spectral libraries and hyperspectral data. Remote Sensing of Environment, 112(6): 2850-2862.

Roberts, D. A., Smith, M. O., & Adams, J. B., 1993. Green vegetation, nonphotosynthetic vegetation, and soils in AVIRIS data. *Remote Sensing of Environment*, *44*(2-3): 255-269.

Romano, G., Abdelwahab, O.M. and Gentile, F., 2018. Modelling land use changes and their impact on sediment load in a Mediterranean watershed. *Catena*, *163*:.342-353.

Röttgers, R., Doerfer, R., McKee, D. and Schönfeld, W., 2010. Pure water spectral absorption, scattering, and real part of refractive index model Algorithm Technical Basis Document.

Santini, F., Alberotanza, L., Cavalli, R.M. and Pignatti, S., 2010. A two-step optimization procedure for assessing water constituent concentrations by hyperspectral remote sensing techniques: An application to the highly turbid Venice lagoon waters. Remote Sensing of Environment, 114(4):887-898.

Schiebe, F.R., Harrington Jr, J.A. and Ritchie, J.C., 1992. Remote sensing of suspended sediments: The Lake Chicot, Arkansas project. *International Journal of Remote Sensing*, *13*(8):.1487-1509.

Setegn, S. G., Srinivasan, R. and Dargahi, B., 2008. Hydrologic Modelling in the Lake Tana Basin, Using Swat Model. The opell hydrology journal. 2: 24-40.

Setegn, S.G., Dargahi, B., Srinivasan, R. and Melesse, A.M., 2010. Modeling of Sediment Yield from Anjeni-Gauged Watershed, Ethiopia Using SWAT Model 1. *JAWRA Journal of the American Water Resources Association*, *46*(3), pp.514-526.

Setegn, S.G., Rayner, D., Melesse, A.M., Dargahi, B. and Srinivasan, R., 2011. Impact of climate change on the hydroclimatology of Lake Tana Basin, Ethiopia. *Water Resources Research*, *47*(4).

Setegn, S.G., Srinivasan R., Dargahi1 B. and Melesse, A.M., 2009. Spatial Delineation of Soil Erosion Prone Areas: Application of SWAT and MCE Approaches in the Lake Tana Basin, Ethiopia, Hydrological Processes, 23(26): 3738-3750.

Sethre, P.R., Rundquist, B.C. and Todhunter, P.E., 2005. Remote detection of Prairie Pothole Ponds in the Devils Lake Basin, North Dakota. GISci. Remote Sens., 42, 277–296.

Shen, F, Zhou Y X, Li J F et al., 2013. Remotely sensed variability of the suspended sediment concentration and its response to decreased river discharge in the Yangtze estuary and adjacent coast. Continental Shelf Research, 69: 52–61.

Shen, Q., Liu, C., Zhou, Q., Shang, J., Zhang, L. And Fan, C., 2013. Effects of Physical and Chemical Characteristics of Surface Sediments in the Formation of Shallow Lake Algae-Induced Black Bloom. Journal of Environmental Sciences, 25(12):2353-2360.

Shi, C., and Wang, L., 2014. Incorporating spatial information in spectral un-mixing(review). *Remote Sensing of Environment, 149:* 70–87.

Shimelis, G., Bijan Dargahi, Ragahavan Srinivasan Assefa M. Melesse, 2010. Modeling of Sediment Yield from Anjeni-Gauged Watershed, Ethiopia Using Swat Model. *Journal of the American Water Resources Association (Jawra*), 46: 514–526.

Siyam, A. M., Mirghani, M., Elzein, S., Golla, S., and El-Sayed, S. M., 2005. "Assessment of the Current State of the Nile Basin Reservoir Sedimentation Problems." Group-I Rep., Nile Basin Capacity Building Network for River Engineering (Nbcbn-Re), River Morphology, Research Cluster, Sudan.

Small, C., 2002. Multitemporal analysis of urban reflectance. Remote Sensing of Environment, 81: 427-442.

Small, C., 2003. High spatial resolution spectral mixture analysis of urban reflectance. *Remote Sensing of Environment*, *88*(1-2): 170-186.

Soenen, S. A., Peddle, D. R., Hall, R. J., Coburn, C. A., & Hall, F. G., 2010. Estimating aboveground forest biomass from canopy reflectance model inversion in mountainous terrain. Remote Sensing of Environment, 114(7), 1325−1337.

Somers, B., Asner, G.P., Tits, L. and Coppin, P., 2011. Endmember variability in spectral mixture analysis: A review. Remote Sensing of Environment, 115(7), 1603-1616.

Somers, B., Delalieux, S., Verstraeten, W. W., van Aardt, J. A. N., Albrigo, G., & Coppin, P. (2010a). An automated waveband selection technique for optimized hyperspectral mixture analysis. International Journal of Remote Sensing, 31, 5549−5568.

Somers, B., Verbesselt, J., Ampe, E. M., Sims, N., Verstraeten, W. W., & Coppin, P. (2010b). Spectral mixture analysis to monitor defoliation in mixed aged Eucalyptus globules Labill plantations in southern Australia using Landsat 5TM and EO-1 Hyperion data. International Journal of Applied Earth Observation and Geoinformation, 12, 270−277.

Song, C. 2005. Spectral mixture analysis for subpixel vegetation fractions in the urban environment: How to incorporate endmember variability? Remote Sens Environ 95(2):248–63.

Song, X., Zheng, D., Yasuyuki, K and Mingyu, W., 2011. Integration of remotely sensed C factor into SWAT for modeling sediment yield, *Hydrol. Process. 25:3387–3398.*

Steenhuis, T., Collick, A., Easton, Z., Leggesse, E., Bayabil, H., White, E., Awulachew, S., Adgo, E., And Ahmed, A., 2009: Predicting Discharge and Sediment for the Abay (Blue Nile) With a Simple Model, *Hydrol. Process. 23: 3728–3737.*

Stephens, P.R., Cihlar, J. (1982). Mapping erosion in New Zealand and Canada. In: Johannsen, C.J., Sanders, J.L. (Eds.), Remote Sensing and Resource Management. Soil Conservation Society of America, Ankeny, IA, pp.232–242.

Sultana, R. and Nasrollahi, N., 2018. Evaluation of remote sensing precipitation estimates over Saudi Arabia. Journal of arid environments, 151: 90-103.

Sumi, T. and Hirose, T., 2009. Accumulation of sediment in reservoirs. Water Storage, Transport, and Distribution, Encyclopedia of Life Support Systems; Takahasi, Y., Ed, pp.224-252.

Sun, D., Yu, Y., and Goldberg,M.D., 2011. Deriving water fraction and flood maps from MODIS images using a decision tree approach. IEEE J. Sel. Top. Appl. Earth Obs. Remote Sens. 2011, 4, 814–825.

Symeonakis, E, Drake N., 2004. Monitoring Desertification and Land Degradation over Sub-Saharan Africa. *International Journal of Remote Sensing 25(3): 573–592.*

Syvitski, J. P. M., Vorosmarty C. J., Kettner A. J., And Green P., 2005, *Impact Of Humans On The Flux Of Terrestrial Sediment To The Global Coastal Ocean. Science, 308(5720): 376–380*

Syvitski, J.P., Morehead, M.D., Bahr, D.B. and Mulder, T., 2000. Estimating fluvial sediment transport: the rating parameters. *Water Resources Research, 36*(9):.2747-2760.

Tafesse, T., 2002. The Nile Question: Hydro Politics Legal Wrangling, Modus Vivendi, and Perspective, Muenster.

Takeda, I. and Fukushima, A., 2004. Phosphorus purification in a paddy field watershed using a circular irrigation system and the role of iron compounds. Water research, 38(19): 4065-4074.

Tamene, L., Park, S., Dikau, R., And Vlek, P., 2006a. Analysis of factors determining Sediment Yield Variability in the Highlands of Northern Ethiopia, *Geomorphology, 76: 76–91*.

Tamene, L., Park, S.J., Dikau, R. and Vlek, P.L.G., 2006b. Reservoir siltation in the semi-arid highlands of northern Ethiopia: sediment yield–catchment area relationship and a semi-quantitative approach for predicting sediment yield. *Earth Surface Processes and Landforms: The Journal of the British Geomorphological Research Group, 31*(11):1364-1383.

Tarek Mohamedabdel-Aziz, 2009. Water and Sediment Management for the Blue Nile Basin. Thirteenth International Water Technology Conference, Iwtc 13 2009, Hurghada, Egypt.

Theseira, M. A., G. Thomas, J. C. Taylor, F. Gemmell, and J. Varjo. 2003. Sensitivity of mixture modeling to end-member selection. Int J Remote Sens 24(7):1559–75.

Thiam, A.K., 2003. The Causes and Spatial Pattern of Land Degradation Risk in Southern Mauritania Using Multi-Temporal Avhrr-Ndvi Imagery and Field Data. Land *Degradation & Development 14: 133–142.*

Tilahun, S. A., Mukundan, R., Demisse, B. A., Engda, T. A., Guzman, C. D., Tarakegn, B. C., Easton, Z. M., Collick, A. S., Zegeye, A. D., Schneiderman, E. M., Parlange J. Y., and Steenhuis, T. S., 2013. A saturation Excess Erosion Model, T. Am. *Soc. Agr. Biol. Eng., 56:* 681–695.

Tompkins, S., J. F. Mustard, C. M. Pieters, and D. W. Forsytth. 1997. Optimization of endmembers for spectral mixture analysis. Remote Sens Environ 59(3):472–89.

Tueller, P.T. And S.G. Oleson., 1989. Diurnal Radiance and Shadow Fluctuations in a Cold Desert Shrub Plant Community. *Remote Sensing of Environment*, 29:1–14.

Tulbure, M.G. and Broich, M., 2013. Spatiotemporal dynamic of surface water bodies using Landsat time-series data from 1999 to 2011. ISPRS J. Photogramm. 79, 44–52.

Ustin, S.L., Adams, J.B., Elvidge, C.D., Rejmanek, M., Rock, B.N., Smith, M.O., Thomas, R.W. and Woodward, R.A., 1986. Thematic Mapper Studies of Semi-Arid Shrub Communities. *Bioscience*, 36:446-452.

Van Der Meer, F., 1995. Spectral un-mixing of landsat thematic mapper data. *International Journal of Remote Sensing*, *16*(16): 3189-3194.

Van Rompaey, A.J.J., Verstaeten, G., Van Oost, K., Govers, G., Poesen, J., 2001. Modelling Mean Annual Sediment Yield Using a Distributed Approach. *Earth Surface Processes and Landforms,* 26: 1221– 1236.

Vanmaercke, M., Poesena, J, Verstraeten, G., De Vente, J., Ocakoglu, F., 2011. Sediment Yield in Europe: Spatial Patterns and Scale Dependency. Geomorphology,130:142-161

Vanmaercke, M., Poesena, J., Broeck, J., Nyssenc, J.,2014. Sediment Yield in Africa, Earth-Science Reviews, 136: 350-368.

Villar, R., Martinez, J. M., Guyot, J. L., Fraizy, P., Armijos, E., Crave, A., Bazan H., Vauchel P., And Lavado W., 2012. The Integration of Eld Measurements and Satellite Observations to Determine River Solid Loads in Poorly Monitored Basins. *Journal of Hydrology*, 445:221-228.

Villar, R.E., Martinez, J.M., Le Texier, M., Guyot, J.L., Fraizy, P., Meneses, P.R. and de Oliveira, E., 2013. A study of sediment transport in the Madeira River, Brazil, using MODIS remote-sensing images. Journal of South American Earth Sciences, 44: 45-54.

Vrieling, A., 2006. Satellite remote sensing for water erosion assessment: A review. Catena, 65(1), 2-18.

Walling, D., 2008. The changing sediment loads of the world's rivers. *Annals of Warsaw University of Life Sciences-SGGW. Land Reclamation*, *39*:.3-20.

Walling, D.E and Fang, D., 2003. Recent Trends in the Suspended Sediment Loads of the World's Rivers. *Global and Planetary Change, 39:111-126.*

Walling, D.E. and Webb, B.W., 1996. Erosion and sediment yield: a global overview. *IAHS Publications-Series of Proceedings and Reports-Intern Assoc Hydrological Sciences*, *236*.3-20.

Walling, D.E., Collins, A.L. and Stroud, R.W., 2008. Tracing suspended sediment and particulate phosphorus sources in catchments. *Journal of Hydrology*, *350*(3-4):.274-289.

Wang Fan, Zhou Bin, Xingmei Liu, Gendi Zhou, and Zhao K., 2012. Remote-Sensing Inversion Model of Surface Water Suspended Sediment Concentration Based on In Situ Measured Spectrum In Hangzhou Bay, China. *Environmental Earth Sciences, 67(6):1669-1677.*

Wang J J and Lu X X., 2010. Estimation of Suspended Sediment Concentrations Using Terra Modis: An Example from the Lower Yangtze River, China. Science of the Total Environment, 408(5):1131-1138.

Wang J J., Lu X X., Liew S C., and Zhou Y., 2010. Remote Sensing of Suspended Sediment Concentrations of Large Rivers Using Multi-Temporal Modis Images: An Example in the Middle and Lower Yangtze River, China. *International Journal of Remote Sensing, 31(4).*

Wang, F, Zhou B, Xu J M et al., 2009. Application of neural network and MODIS 250m imagery for estimating suspended sediments concentration in Hangzhou Bay, China. Environmental Geology, 56(6): 1093–1101.

Wang, F., Bin, Z., Xingmei, L., Gendi Z., and Keli Z., 2012. Remote-sensing inversion model of surface water suspended sediment concentration based on in situ measured spectrum in Hangzhou Bay, China. *Environmental Earth Sciences, 67(6):* 1669-1677.

Wang, G., Gertner, G., Fang, S., & Anderson, A. B., 2003. Mapping multiple variables for predicting soil loss by geostatistical methods with TM images and a slope map. *Photogrammetric Engineering & Remote Sensing*, *69*(8):, 889-898.

Wang, G., Wente, S., Gertner, G.Z., Anderson, A., 2002. Improvement in mapping vegetation cover factor for the universal soil loss equasitionby geostatistical methods with landsat thematic mapper images. *International Journal of Remote Sensing 23*(18): 3649–3667.

Wang, J. J., Lu, X. X., Soo, C. L., and Yue. Z., 2009. Retrieval of suspended sediment concentrations in large turbid Rivers using Landsat ETM^{+}: an example from the Yangtze River, China. *Earth surface process landforms, 34(8):* 1082-1092.

Wang, J., Wang, H., Ning, S. and Hiroshi, I., 2018. Predicting future land cover change and its impact on streamflow and sediment load in a trans-boundary river

basin. *Proceedings of the International Association of Hydrological Sciences*, *379*:217-222.

Wang, M., Wei Shi, and Junwu Tang, 2011. Water property monitoring and assessment for China's inland Lake Taihu from MODIS-Aqua measurements. Remote Sensing of Environment, 115(3): 841–854.

Wang, Q., Atkinson, P.M., and Shi, W., 2015. Fast subpixel mapping algorithms forsub pixel resolution change detection. IEEE Trans. Geosci. Remote Sens., 53, 1692–1706.

Wang, S., Kang, S., Zhang, L. and Li, F., 2008a. Modelling hydrological response to different land-use and climate change scenarios in the Zamu River basin of northwest China. *Hydrological Processes: An International Journal*, *22*(14):.2502-2510.

Wang, W., Wei, J., Shao, Q., Xing, W., Yong, B., Yu, Z. and Jiao, X., 2015. Spatial and temporal variations in hydro-climatic variables and runoff in response to climate change in the Luanhe River basin, China. *Stochastic environmental research and risk assessment*, *29*(4):1117-1133.

Wang, X., Garza, J., Whitney, M., Melesse, A.M. and Yang, W., 2008b. Prediction of sediment source areas within watersheds as affected by soil data resolution. *Environmental modelling: new research*, pp.151-185.

Ward, P.J., van Balen, R.T., Verstraeten, G., Renssen, H. and Vandenberghe, J., 2009. The impact of land use and climate change on late Holocene and future suspended sediment yield of the Meuse catchment. *Geomorphology*, *103*(3):.389-400

White, M.J. and Arnold, J.G., 2009. Development of a simplistic vegetative filter strip model for sediment and nutrient retention at the field scale. Hydrological Processes: An International Journal, 23(11), pp.1602-1616.

Whitlock, C. H., L. R. Poole, J. W. Usry, W. M. Houghton, W. G. Witte, W. D. Morris, and E. A. Gurganus E.A., 1981. Comparison of reflectance with backscatter and absorption parameters for turbid waters, Appl. Opt., 20(3), 517–522.

Williams, J.R., 1975. Sediment-Yield Prediction with Universal Eq. Using Runoff Energy Factor. P. 244-252. In Present and Prospective Technology for Predicting Sediment Yield and Sources: Proceedings Of The Sediment Yield Workshop, Usda Sedimentation Lab., Oxford, Ms, November 28- 30, 1972:40.

Willis, I.C., Richards, K.S. and Sharp, M.J., 1996. Links between proglacial streams suspended sediment dynamics, glacier hydrology and glacier motion at Midtdalsbreen, Norway. Hydrological Processes, 10(4):.629-648.

Winter, M.E., 1999, October. N-FINDR: An algorithm for fast autonomous spectral end-member determination in hyperspectral data. In Imaging Spectrometry V (Vol. 3753, pp. 266-275). International Society for Optics and Photonics.

Wischmeier, W.H. and Smith, D.D., 1978. Predicting rainfall erosion losses-a guide to conservation planning. *Predicting rainfall erosion losses-a guide to conservation planning.*

WMO, 2000. WMO - Regional Association VI - Working Group on Hydrology, Sediment Transport Survey.

Wren, D. G., Barkdoll, B. D., Kuhnle, R. A., and Derrow, R.W., 2000. Field techniques for suspended-sediment measurement. Journal of Hydraulic Engineering, 126(2). 97-104.

Xie, H., Luo, X., Xu, X., Tong, X., Jin, Y., Pan, H. and Tong, X., 2014. New hyperspectral difference water index for the extraction of urban water bodies using airborne hyperspectral images. J. Appl. Remote Sen., 8, 5230–5237.

Xu, J. X., 2003. Sediment flux to the sea as influenced by changing human activities and precipitation: example of the Yellow River, China, Environ. Manage, 31: 328–341.

Xu,H., 2006. Modification of normalised difference water index (NDWI) to enhance open water features in remotely sensed imagery. Int. J. Remote Sens. 2006, 27, 3025–3033.

Yang, Y., Liu, Y., Zhou, M., Zhang, S., Zhan, W., Sun, C., and Duan, Y., 2015. Landsat 8 OLI image based terrestrial water extraction from heterogeneous backgrounds using a reflectance homogenization approach. Remote Sens. Environ., 171, 14–32.

Yesuf, H. M., Assen, M., Alamirew, T., & Melesse, A. M., 2015. Modelling of sediment yield in Maybar gauged watershed using SWAT, northeast Ethiopia. *Catena*, *127*: 191-205.

Young, R. A., Onstad, C. A., Bosch, D. D., & Anderson, W. P., 1989. AGNPS: A nonpoint-source pollution model for evaluating agricultural watersheds. *Journal of soil and water conservation*, *44*(2), 168-173.

Yue, S., Pilon, P., Phinney, B. and Cavadias, G., 2002. The influence of autocorrelation on the ability to detect trend in hydrological series. *Hydrological processes, 16*(9):.1807-1829.

Yuming, You and Min Hou 1992. Remote Sensing Analysis of the Suspended Sediment transport in Lingdingyang. *China Ocean Engineering, 6(3):331-349.*

Zaghloul, S.S., El-Moattassem, M., Rady, A.A., 2007. The Hydrological Interactions between Atbara River and the Main Nile at the Confluence Area. International Congress on River Basin Management. Antalya, Turkey, 787-799. [Online]: Http: //Www.Dsi.Gov.Tr/English/Congress2007/Chapter_2/63.Pdf. [Accessed: Sep 13, 2015].

Zare, A., Gader, P., Bchir, O. and Frigui, H., 2013. Piecewise convex multiple-model endmember detection and spectral unmixing. IEEE Trans. Geosci. Remote Sens. 51., 2853–2862.

Zeleke, G., 2000. Landscape dynamics and soil erosion process modelling in the north-western Ethiopian highlands.

Zhan, C., Yu, J., Wang, Q., Li, Y., Zhou, D., Xing, Q. and Chu, X., 2017. Remote sensing retrieval of surface suspended sediment concentration in the Yellow River Estuary. Chinese geographical science, 27(6):.934-947.

Zhang, J., Rivard, B., Sánchez-Azofeifa, A. and Castro-Esau, K., 2006. Intra-and inter-class spectral variability of tropical tree species at La Selva, Costa Rica: Implications for species identification using HYDICE imagery. Remote Sensing of Environment, 105(2), pp.129-141.

Zhang, X., Hu, L., and He, M.-X.2009. Scattering by pure seawater: Effect of salinity, Optics Express, 17, 5698–5710.

Zhang, Y., Huang, Z., Chen, C., He, Y. And Jiang, T., 2015. Particle Size Distribution Of River-Suspended Sediments Determined By In Situ Measured Remote-Sensing Reflectance. Applied Optics, 54(20):.6367-6376.

Zhou, W., Wang, S., Zhou, Y., and Troy, A., 2006. Mapping the concentrations of total suspended matter in Lake Taihu, China, using Landsat-5 TM data. International Journal of Remote Sensing, 27(6):1177–1191.

Zhu, A, Hudson B, Burt J, Lubich K, Simonson D., 2001. Soil Mapping Using Gis, Expert Knowledge, and Fuzzy Logic. *Soil Science Society of America Journa*l, 65(5): 1463–1472.

Zhu, Y.-M., Lu, X. X., and Zhou, Y., 2008. Sediment Flux Sensitivity to Climate Change: A Case Study in the Longchuanjiang Catchment of the Upper Yangtze River, China, Global Planet. Change, 60: 429–442.

APPENDICES I: SUPPORTIVE TABLES AND MAPS USED

Appendix 1: Tekeze main River sediment and reflectance monitoring in laboratory

Sampling data	Given code	Total weight	Tin weight (g)	Dry Sediment weight	volume of turbid water	SSC(g/l)	Average field reflectance at B5 (750-950nm)
2-Jul-17	Tr1	61.63	51.75	9.88	0.6	16.47	0.067
3-Jul-17	Tr2	63.31	51.75	11.6	0.6	19.27	0.074
4-Jul-17	Tr3	65.92	51.75	14.2	0.6	23.62	0.086
5-Jul-17	Tr4	63.14	51.75	11.4	0.6	18.98	0.073
6-Jul-17	Tr5	62.28	51.75	10.5	0.6	17.55	0.069
7-Jul-17	Tr6	64.34	51.75	12.6	0.6	20.98	0.082
8-Jul-17	Tr7	58.95	51.75	7.2	0.6	12	0.062
9-Jul-17	Tr8	60.44	51.75	8.69	0.6	14.49	0.069
10-Jul-17	Tr9	59.9	51.75	8.15	0.6	13.58	0.066
11-Jul-17	Tr10	56.08	51.75	4.33	0.6	7.213	0.047
12-Jul-17	Tr11	56	51.75	4.25	0.6	7.087	0.048
13-Jul-17	Tr12	56.32	51.75	4.57	0.6	7.612	0.047
14-Jul-17	Tr13	57.47	51.75	5.72	0.6	9.539	0.057
15-Jul-17	Tr14	57.57	51.75	5.82	0.6	9.708	0.054
16-Jul-17	Tr15	62.06	51.75	10.3	0.6	17.18	0.075
17-Jul-17	Tr16	66.62	51.75	14.9	0.6	24.79	0.088
18-Jul-17	Tr17	65.6	51.75	13.8	0.6	23.08	0.086
19-Jul-17	Tr18	69.06	51.75	17.3	0.6	28.85	0.093
20-Jul-17	Tr19	65.76	51.75	14	0.6	23.35	0.086
21-Jul-17	Tr20	61.1	51.75	9.35	0.6	15.59	0.072
22-Jul-17	Tr21	59.48	51.75	7.73	0.6	12.88	0.064
23-Jul-17	Tr22	59.65	51.75	7.9	0.6	13.17	0.066
24-Jul-17	Tr23	58.98	51.75	7.23	0.6	12.06	0.063
25-Jul-17	Tr24	70.85	51.75	19.1	0.6	31.84	0.097
26-Jul-17	Tr25	66.55	51.75	14.8	0.6	24.67	0.088
27-Jul-17	Tr26	69.17	51.75	17.4	0.6	29.04	0.094
28-Jul-17	Tr27	68.23	51.75	16.5	0.6	27.46	0.092
29-Jul-17	Tr28	73.18	51.75	21.4	0.6	35.72	0.101
30-Jul-17	Tr29	64.48	51.75	12.7	0.6	21.22	0.082
31-Jul-17	Tr30	56.3	51.75	4.55	0.6	7.587	0.046
1-Aug-17	Tr31	56.73	51.75	4.98	0.6	8.301	0.047
2-Aug-17	Tr32	55.97	51.75	4.22	0.6	7.041	0.045

Sampling data	Given code	Total weight	Tin weight (g)	Dry Sediment weight	volume of turbid water	SSC(g/l)	Average field reflectance at B5 (750-950nm)
3-Aug-17	Tr33	53.86	51.75	2.11	0.6	3.525	0.021
4-Aug-17	Tr34	68.63	51.75	16.9	0.6	28.14	0.094
5-Aug-17	Tr35	64.66	51.75	12.9	0.6	21.52	0.082
6-Aug-17	Tr36	59.13	51.75	7.38	0.6	12.3	0.064
7-Aug-17	Tr37	61.7	51.75	9.95	0.6	16.59	0.075
8-Aug-17	Tr38	64.31	51.75	12.6	0.6	20.93	0.081
9-Aug-17	Tr39	83.26	51.75	31.5	0.6	52.52	0.098
10-Aug-17	Tr40	66.56	51.75	14.8	0.6	24.69	0.086
11-Aug-17	Tr41	62.29	51.75	10.5	0.6	17.57	0.076
12-Aug-17	Tr42	64.3	51.75	12.6	0.6	20.92	0.082
13-Aug-17	Tr43	68.38	51.75	16.6	0.6	27.71	0.092
14-Aug-17	Tr44	66.01	51.75	14.3	0.6	23.76	0.086
15-Aug-17	Tr45	59.88	51.75	8.13	0.6	13.56	0.067
16-Aug-17	Tr46	60.6	51.75	8.85	0.6	14.75	0.068
17-Aug-17	Tr47	58.24	51.75	6.49	0.6	10.81	0.058
18-Aug-17	Tr48	58.39	51.75	6.64	0.6	11.06	0.059
19-Aug-17	Tr49	58.986	51.75	7.236	0.6	12.06	0.063
20-Aug-17	Tr50	64.41	51.75	12.66	0.6	21.1	0.083
21-Aug-17	Tr51	61.914	51.75	10.164	0.6	16.94	0.074
22-Aug-17	Tr52	63.192	51.75	11.442	0.6	19.07	0.08
23-Aug-17	Tr53	59.04	51.75	7.29	0.6	12.15	0.064
24-Aug-17	Tr54	59.334	51.75	7.584	0.6	12.64	0.065
25-Aug-17	Tr55	58.152	51.75	6.402	0.6	10.67	0.058
26-Aug-17	Tr56	59.97	51.75	8.22	0.6	13.7	0.066
27-Aug-17	Tr57	55.7874	51.75	4.0374	0.6	6.729	0.041
28-Aug-17	Tr58	56.4048	51.75	4.6548	0.6	7.758	0.044
29-Aug-17	Tr59	53.4228	51.75	1.6728	0.6	2.788	0.012
30-Aug-17	Tr60	56.886	51.75	5.136	0.6	8.56	0.051
31-Aug-17	Tr61	57.846	51.75	6.096	0.6	10.16	0.055
1-Sep-17	Tr62	54.5796	51.75	2.8296	0.6	4.716	0.023
2-Sep-17	Tr63	56.1486	51.75	4.3986	0.6	7.331	0.043
3-Sep-17	Tr64	55.632	51.75	3.882	0.6	6.47	0.041

Appendix 2:Tsirare River sediment and reflectance monitoring in laboratory

Sampling data	Given code	Total weight	Tin weight (g)	Sediment weight	volume of turbid water	SSC(g/l)	Average field reflectance atB5(750-950nm)
2-Jul-17	Ts1	60.29	51.75	8.54	0.6	14.23	0.035245
3-Jul-17	Ts2	58.94	51.75	7.19	0.6	11.98	0.027422
4-Jul-17	Ts3	60.31	51.75	8.56	0.6	14.27	0.036291
5-Jul-17	Ts4	61.91	51.75	10.2	0.6	16.93	0.040475
6-Jul-17	Ts5	56.47	51.75	4.72	0.6	7.859	0.025873
7-Jul-17	Ts6	59.08	51.75	7.33	0.6	12.22	0.027988
8-Jul-17	Ts7	59.79	51.75	8.04	0.6	13.4	0.032107
9-Jul-17	Ts8	64.23	51.75	12.5	0.6	20.8	0.04862
10-Jul-17	Ts9	64.65	51.75	12.9	0.6	21.5	0.055027
11-Jul-17	Ts10	63.83	51.75	12.1	0.6	20.13	0.046484
12-Jul-17	Ts11	66.73	51.75	15	0.6	24.97	0.069978
13-Jul-17	Ts12	69.46	51.75	17.7	0.6	29.52	0.111064
14-Jul-17	Ts13	65.26	51.75	13.5	0.6	22.51	0.059299
15-Jul-17	Ts14	57.77	51.75	6.02	0.6	10.03	0.026572
16-Jul-17	Ts15	59.37	51.75	7.62	0.6	12.7	0.028555
17-Jul-17	Ts16	60.55	51.75	8.8	0.6	14.66	0.037337
18-Jul-17	Ts17	61.05	51.75	9.3	0.6	15.5	0.038383
19-Jul-17	Ts18	85.83	51.75	34.1	0.6	56.81	0.137183
20-Jul-17	Ts19	92.91	51.75	41.2	0.6	68.6	0.15102
21-Jul-17	Ts20	88.27	51.75	36.5	0.6	60.87	0.138102
22-Jul-17	Ts21	88.7	51.75	37	0.6	61.59	0.1423
23-Jul-17	Ts22	68.99	51.75	17.2	0.6	28.74	0.105928
24-Jul-17	Ts23	69.78	51.75	18	0.6	30.05	0.121222
25-Jul-17	Ts24	70.49	51.75	18.7	0.6	31.24	0.119585
26-Jul-17	Ts25	67.67	51.75	15.9	0.6	26.54	0.095656
27-Jul-17	Ts26	67.29	51.75	15.5	0.6	25.9	0.085385
28-Jul-17	Ts27	67.08	51.75	15.3	0.6	25.55	0.080249
29-Jul-17	Ts28	64.24	51.75	12.5	0.6	20.82	0.050755
30-Jul-17	Ts29	65.32	51.75	13.6	0.6	22.62	0.059434
31-Jul-17	Ts30	64.84	51.75	13.1	0.6	21.82	0.057163
1-Aug-17	Ts31	57.88	51.75	6.13	0.6	10.21	0.026855
2-Aug-17	Ts32	54.27	51.75	2.52	0.6	24.15	0.069706
3-Aug-17	Ts33	56.22	51.75	4.47	0.6	24.45	0.064842
4-Aug-17	Ts34	53.5	51.75	1.75	0.6	18.51	0.047348
5-Aug-17	Ts35	54.35	51.75	2.6	0.6	26.25	0.090521
6-Aug-17	Ts36	54.49	51.75	2.74	0.6	28.48	0.100792
7-Aug-17	Ts37	53.67	51.75	1.92	0.6	10.43	0.027139
8-Aug-17	Ts38	53.26	51.75	1.51	0.6	13.46	0.033153
9-Aug-17	Ts39	54.91	51.75	3.16	0.6	39.83	0.116264
10-Aug-17	Ts40	54.92	51.75	3.17	0.6	18.35	0.043576

Sampling data	Given code	Total weight	Tin weight (g)	Sediment weight	volume of turbid water	SSC(g/l)	Average field reflectance atB5(750-950nm)
11-Aug-17	Ts41	53.05	51.75	1.3	0.6	18.41	0.042212
12-Aug-17	Ts42	53.52	51.75	1.77	0.6	22.96	0.06457
13-Aug-17	Ts43	54.1	51.75	2.35	0.6	21.03	0.052891
14-Aug-17	Ts44	55.01	51.75	3.26	0.6	25.1	0.075113
15-Aug-17	Ts45	54.91	51.75	3.16	0.6	15.8	0.039429
16-Aug-17	Ts46	54.67	51.75	2.92	0.6	12.64	0.028271
17-Aug-17	Ts47	55.38	51.75	3.63	0.6	13.22	0.028838
18-Aug-17	Ts48	55.25	51.75	3.5	0.6	16.94	0.041521
19-Aug-17	Ts49	54.8	51.75	3.05	0.6	18.07	0.043407
20-Aug-17	Ts50	55.47	51.75	3.72	0.6	14.15	0.034199
21-Aug-17	Ts51	55.82	51.75	4.07	0.6	12.15	0.027705
22-Aug-17	Ts52	59.742	51.75	7.992	0.6	13.32	0.035873
23-Aug-17	Ts53	54.4548	51.75	2.7048	0.6	4.508	0.025873
24-Aug-17	Ts54	55.6566	51.75	3.9066	0.6	6.511	0.025873
25-Aug-17	Ts55	53.9796	51.75	2.2296	0.6	3.716	0.024873
26-Aug-17	Ts56	54.5772	51.75	2.8272	0.6	4.712	0.025873
27-Aug-17	Ts57	54.7602	51.75	3.0102	0.6	5.017	0.026873
28-Aug-17	Ts58	55.869	51.75	4.119	0.6	6.865	0.025705
29-Aug-17	Ts59	54.129	51.75	2.379	0.6	3.965	0.020873
30-Aug-17	Ts60	56.9154	51.75	5.1654	0.6	8.609	0.026289
31-Aug-17	Ts61	54.9864	51.75	3.2364	0.6	5.394	0.024873
1-Sep-17	Ts62	53.8422	51.75	2.0922	0.6	3.487	0.01479
2-Sep-17	Ts63	53.7024	51.75	1.9524	0.6	3.254	0.013739
3-Sep-17	Ts64	53.2626	51.75	1.5126	0.6	2.521	0. 012739

Appendix 3: The reflectance values used for identification of ground cover components and their spatial abundance

Cover type	Band	Basic Stats			
		Min	Max	Mean	St. dev.
Bare soil	Band 1	0.102	0.209	0.1308	0.022
	Band 2	0.101	0.266	0.1442	0.033
	Band 3	0.096	0.31	0.1546	0.039
	Band 4	0.148	0.402	0.232	0.049
	Band 5	0.141	0.438	0.2455	0.047
	Band 6	0.104	0.327	0.183	0.035
Rocky	Band 1	0.108	0.16	0.1313	0.013
	Band 2	0.091	0.156	0.1203	0.016
	Band 3	0.078	0.154	0.1127	0.019
	Band 4	0.148	0.252	0.1964	0.023
	Band 5	0.088	0.192	0.1319	0.023
	Band 6	0.058	0.137	0.0935	0.019
Vegetation	Band 1	-0.11	0.088	0.0608	0.055
	Band 2	-0.11	0.102	0.0691	0.055
	Band 3	0.052	0.084	0.0594	0.004
	Band 4	0.216	0.517	0.3761	0.059
	Band 5	0.114	0.176	0.1383	0.012
	Band 6	0.053	0.087	0.0654	0.005
Water	Band 1	0.072	0.087	0.0832	0.003
	Band 2	0.063	0.084	0.0686	0.005
	Band 3	0.042	0.063	0.0483	0.007
	Band 4	0.025	0.184	0.0757	0.073
	Band 5	0.012	0.111	0.0438	0.045
	Band 6	0.008	0.061	0.0256	0.024

Appendix 4: C- factor values for different land uses in Tekeze basin for the year 2016 summer from field measurement

ID	Land use type	Minimum C-factor	Maximum C-factor	Mean C-factor	St. Dev.	CV (%)
1	Forest land	0.13	0.25	0.14	0.03	11.14
2	Grass land	0.14	0.71	0.43	0.02	14.65
3	Cultivated land	0.27	1.00	0.64	0.04	17.25
4	Shrub land	0.15	0.45	0.4	0.02	15.25

Appendix 5:Description of spatial model input data for the upper Tekeze basin

Input	**Resolution**	**Sources**	**Classification**	**Area (%)**
DEM	30m	SRTM	0-1o% slope	13.41
			10-15%slope	10.41
			15-30% slope	28.14
			30-45%slope	20.73
			>45%slope	27.30
Landsat images	15m	USGS	Deciduous and ever green forested area	0.10
			Agricultural Land-Close-grown:	27.87
			Pasture: naturally occurring grazing lands, a hilly slope with scattered shrub were grouped here	10.59
			Range brush: Lands characterized by xerophytic vegetative type, shrub and	4.41
			Agricultural Land-Generic	57.00
			Water bodies which include wetlands and open water	0.04
Soil type	10km	FAO and EMoWIE	Ach (Orthic acrisols)	0.38
			ARh (Cambic arenosols)	4.45
			CMd (Dystric cambisols)	1.62
			CMe (Eutric cambisol)	40.64
			CMv (Vertic cambisols)	1.89
			FLe (Eutric fluvisols)	0.11
			LPe (Leptosols)	13.22
			LVx (Cromic luvisols)	12.65
			NTr (Dystric nitosols)	13.3
			PHh (Calcic xerosols)	6.05
			RGe (Eutric regosols)	4.15
			VRe (Cromic vertisols)	1.51
			WRe (Unclassified)	0.02
Weather data	13 stations	MoWIE and CFSR	Daily precipitation, maximum and minimum temperature, relative humidity, solar radiation and wind speed	

Appendix 6: Daily sediment hydrograph at Tekeze Hydroelectric dam during the years 2004 – 2006 (Calibration of SWAT)

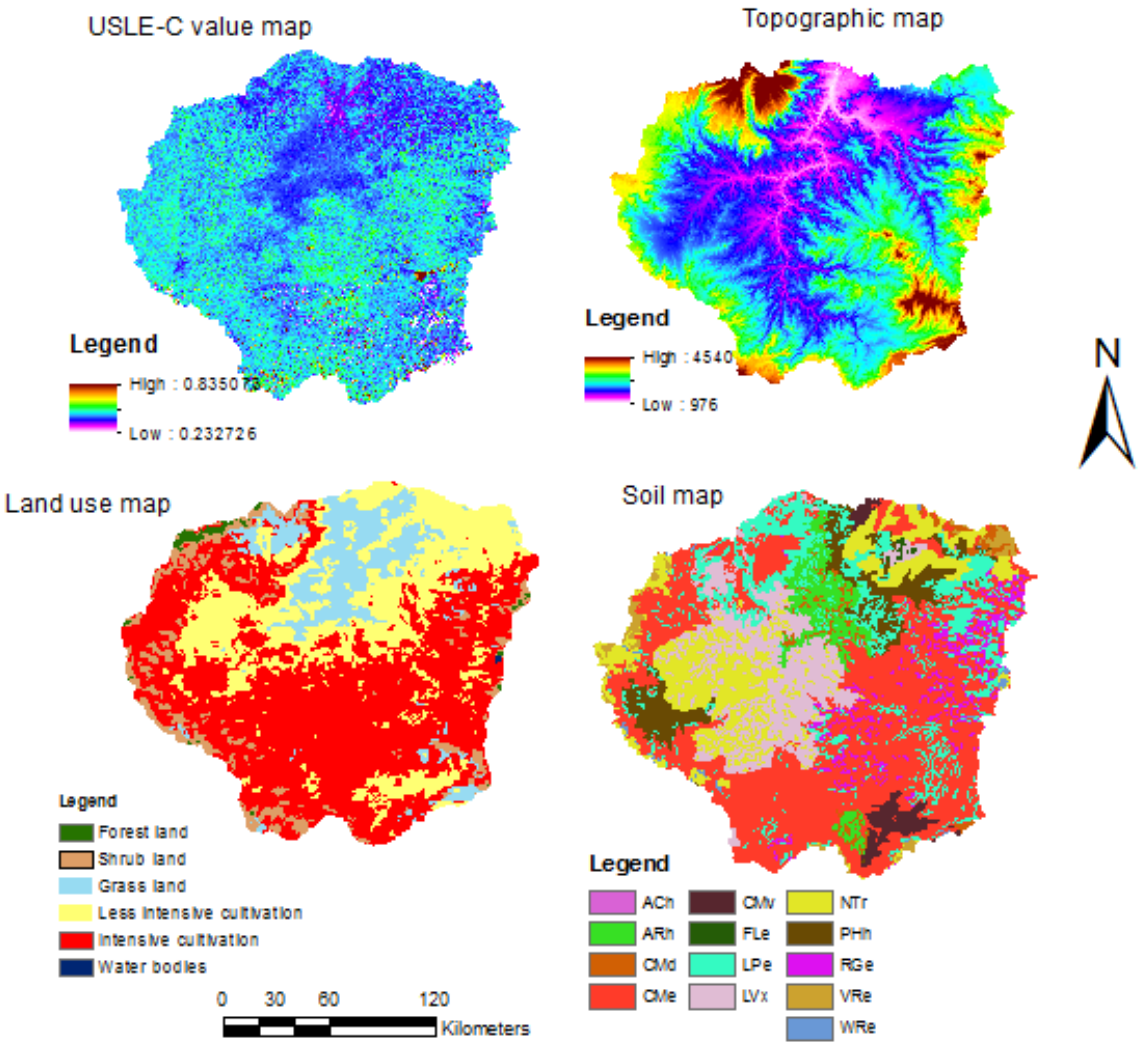

Appendix 7: Calibration and validation parameter of SWAT

Parameter Name	Description	Fitted Value
PRF	Peak rate adjustment factor for sediment routing in the main channel	2.000
ADJ_ PKR	Peak rate adjustment factor for sediment routing in the sub-basin (tributary channels)	2.000
SPCON.bsn	Linear re-entrainment parameter for channel sediment routing	0.010
SPEXP.bsn	Exponent of re-entrainment parameter for channel sediment routing	0.540
USLE_P.mgt	USLE support practice factor	0.239
PSP.bsn	Sediment routing factor in main channel	0.030
USLE_C{forested land cove}plant.dat	Minimum USLE C-factor for water erosion applicable to the land cover/plant	0.153
USLE_C{Crop land}plant.dat	Minimum USLE C-factor for water erosion applicable to the land cover/plant	0.333
USLE_C{6}plant.dat	Minimum USLE C-factor for water erosion applicable to the land cover/plant	0.140
USLE_C{12}plant.dat	Minimum USLE C-factor for water erosion applicable to the land cover/plant	0.511
USLE_C{16}plant.dat	Minimum USLE C-factor for water erosion applicable to the land cover/plant	0.405
USLE_C{water bodies}plant.dat	Minimum USLE C-factor for water erosion applicable to the land cover/plant	0.000
CH_S2.rte	Average slope of main channel	0.450
CH_N2.rte	Manning's 'n' value for main channel	0.254
CH_K2.rte	Channel effective hydraulic conductivity	274.995
CH_COV1.rte	Channel erodibility factor	0.048
CH_COV2.rte	Channel cover factor	0.650

APPENDIES II: PUBLISHED PAPERS

Appendix 8: Article 1

International Journal of Sediment Research 35 (2020) 79–90

Contents lists available at ScienceDirect

International Journal of Sediment Research

journal homepage: www.elsevier.com/locate/ijsrc

Original Research

Linear spectral unmixing algorithm for modelling suspended sediment concentration of flash floods, upper Tekeze River, Ethiopia

Hagos G. Gebreslassie [a, d, *], Assefa M. Melesse [b], Kevin Bishop [c], Azage G. Gebremariam [a]

[a] Ethiopian Institute of Water Resources, Addis Ababa University, Ethiopia
[b] Department of Earth and Environment, Florida International Universities, USA
[c] Department of Aquatic Sciences and Assessment, Swedish Universities of Agricultural Science, Sweden
[d] Department of NRM, Adigrat University, Tigray, Ethiopia

ARTICLE INFO

Article history:
Received 2 March 2018
Received in revised form
9 May 2019
Accepted 26 July 2019
Available online 2 August 2019

Keywords:
Empirical remote sensing
Flash floods
Linear spectral unmixing
Suspended sediment concentration
Tekeze River

ABSTRACT

Flash floods are the highest sediment transporting agent, but are inaccessible for in-situ sampling and have rarely been analyzed by remote sensing technology. Laboratory and field experiments were done to develop linear spectral unmixing (LSU) remote sensing model and evaluate its performance in simulating the suspended sediment concentration (SSC) in flash floods. The models were developed from continuous monitoring in the laboratory and the onsite spectral signature of river bed sediment deposits and flash floods in the Tekeze River and in its tributary, the Tsirare River. The Pearson correlation coefficient was used to determine the variability of correlations between reflectance and SSCs. The coefficient of determination (R2) and root mean square of error (RMSE) were used to evaluate the performance of the generated models. The results found that the Pearson correlation coefficient between SSCs and reflectance varied based on the level of the SSCs, geological colors, and grain sizes. The performance of the LSU model and empirical remote sensing approaches were computed to be R2 – 0.92, and RMSE – ±0.76 g/l in the Tsirare River and R2 – 0.91, and RMSE – ±0.73 g/l in the Tekeze River and R2 – 0.81, RMSE – ±2.65 g/l in the Tsirare river and R2 – 0.76, RMSE – ±10.87 g/l in the Tekeze River, respectively. Hence, the LSU approach of remote sensing was found to be relatively accurate in monitoring and modeling the variability of SSCs that could be applied to the upper Tekeze River basin.

1. Introduction

Sediment transport is the biggest challenge for operation and design of hydraulic infrastructures, and is among the environmental processes that vary spatiotemporally. The variability is related to the driving forces including climate variability (Haile & Rientjes, 2015; Wagena et al., 2016), land use change (Amsalu et al., 2007; Hurni et al., 2005), and topography (Tamene et al., 2006). Even though most Ethiopian river basins are among the international rivers with higher and variable sediment concentrations, the monitoring locations in the basins are very scarce and the cost is infeasible when using traditional sampling techniques. It is very difficult to get adequate and continuous sediment data for most rivers. Hence, researchers in Ethiopia are searching easily applicable and cost feasible techniques of monitoring sediment load. Some researchers have proposed empirical sediment rating curves developed by relating the sediment load with water discharge (Moges et al., 2016; Tamene et al., 2006). Other investigators proposed different physically based, semi-distributed, and time continuous hydrological models (Defersha et al., 2012; Haregeweyn & Yohannes, 2003; Maalim et al., 2013; Masoumeh & Mehdi, 2012; Melesse et al., 2011; Mohammed et al., 2004; Setegn et al., 2011). However, applying hydrological models is challenging and they estimate inaccurately because of two reasons. First, these models were originally developed for areas that have large amounts of data, unlike most Ethiopian river basins that have insufficient data. Second, they are designed for regions with temperate climates where the runoff mechanisms are governed by infiltration excess whereas most Ethiopian basins yield saturation excess runoff (Bayabil et al., 2010; Steenhuis et al., 2009; Tilahun et al., 2013).

* Corresponding author.
E-mail address: hagmeb@gmail.com (H.G. Gebreslassie).

https://doi.org/10.1016/j.ijsrc.2019.07.007

Appendix 9: Article 2

Double-stage linear spectral unmixing analysis for improving accuracy of sediment concentration estimation from MODIS data: the case of Tekeze River, Ethiopia

Hagos Gebreslassie Gebru, Assefa M. Melesse & Azage Gebreyohannes Gebremariam

Modeling Earth Systems and Environment

ISSN 2363-6203

Model. Earth Syst. Environ.
DOI 10.1007/s40808-019-00688-7

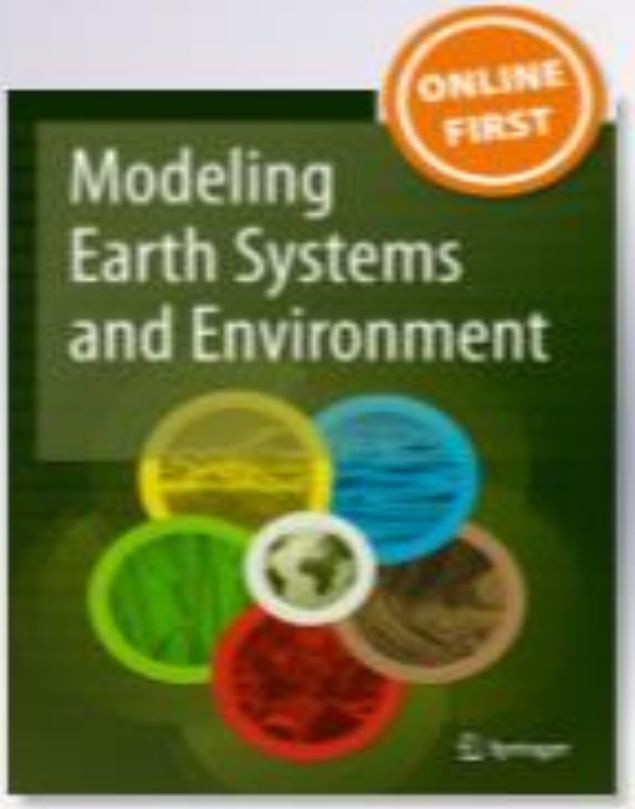

Springer

Modeling Earth Systems and Environment
https://doi.org/10.1007/s40808-019-00650-7

ORIGINAL ARTICLE

Double-stage linear spectral unmixing analysis for improving accuracy of sediment concentration estimation from MODIS data: the case of Tekeze River, Ethiopia

Hagos Gebrekiros Gebru[1,2] · Assefa M. Melesse[3] · Asrat Gebreyohannes Gebremariam[3]

Received: 23 July 2019 / Accepted: 1 November 2019

Abstract
Dynamic spectral properties of sediment types together with wide swath coverage compared to spatial resolution of pixel dimensions are the challenges for modeling suspended sediment concentration (SSC) using the conventional regression remote sensing analysis. In this study, a new subpixel unmixing approach called double-stage linear spectral unmixing analysis (DSLSUA) was proposed for modeling the variability of SSC from the moderate resolution imaging spectroradiometer (MODIS) data. In the first stage, the linear spectral unmixing analysis was used to extract the ground cover components (soil, bare land and turbid water) which contributed to the reflectance of the mixed pixels. In the next stage, the spectral mixing constituents (SMC's) of the constituents in the turbid water were determined. Finally, nonlinear regression models correlating the SSC and its SMC were generated. Furthermore, the field and laboratory based observed SSC and reflectance data were used for verifying the results. The coefficients of determination (R^2) and relative root mean square error (RMSE) were used to evaluate the performance of the models. The DSLSUA approach improved the estimations of SSC's (R^2 = 0.83 and RMSE = 9.96) compared to the estimations using the empirical regression remote sensing models (R^2 = 0.74 and RMSE = 16.2). Overall, the study showed that understanding the variability of spectral properties of primary components is important to use remote sensing for modeling and monitoring the SSC's using counter remote sensing data (MODIS).

Keywords Remote sensing · Double-stage linear spectral unmixing analysis · Suspended sediment concentration · Tekeze River · MODIS

Introduction

Spatio-temporal information of suspended sediment concentrations (SSC) is crucial to study sediment associated environmental changes such as alterations of channel morphology, degradation of water quality, and construction and operation of in-river water resources development infrastructures (Watling et al. 2008; Wang and Lo 2018). Information on the spatio-temporal dynamics of SSC is highly required for sustainable water resource management under the changing and worsening trends of climate and land use change scenarios (Lagasse et al. 2003; Mouyo et al. 2011; Deteresa and Melesse 2012b; Mustafa et al. 2015). Gathering, in situ sampling followed by laboratory analysis is the most commonly used method for sediment monitoring (Wise et al. 2008; Rienz et al. 2011) and presented base-line data for most sediment studies using hydrologic models (Setegn et al. 2009, 2010; Melesse and Melesse 2011; Melesse et al. 2011; Deteresa and Melesse 2012a; Mustafa et al. 2015; Mengistu et al. 2016; Mohammed et al. 2015; Aga et al. 2018, 2019). However, the approach (i.e., field sampling followed by laboratory analysis) is labor intensive and time consuming, and the cost of installation is very expensive. Consequently, most towns in the world especially in developing countries have either not been gauged or their sediment data are not readily available (Syvitski et al. 2003).

Unlike the field sampling, remote sensing method has the potential to provide synoptic, continuous, and wider

✉ Hagos Gebrekiros Gebru
hagosk@gmail.com

1 Ethiopian Institute of Water Resources, Addis Ababa University, Addis Ababa, Ethiopia

2 Department of Earth and Environment, Florida International University, Miami, FL, USA

3 Natural Resources Management, Adigrat University, Adigrat, Ethiopia

Published online: 14 November 2019